UNIVERSITÀ DEGLI STUDI DI PADOVA

DIPARTIMENTO DI INGEGNERIA INDUSTRIALE

CORSO DI LAUREA MAGISTRALE IN INGEGNERIA CHIMICA E DEI PROCESSI INDUSTRIALI

Tesi di Laurea Magistrale in

Ingegneria Chimica e dei Processi Industriali

Chemical-physical determinations for material and energy recovery from car fluff

Relatore: prof. Renato Bonora

Correlatore: prof. ssa. Roberta Bertani

Laureando: Rocco Leonello

ANNO ACCADEMICO 2022– 2023

INDEX

1. INTRODUCTION

1.1 The Circular Economy Context

On 11 December 2019 the European Green Deal was presented. As reported by the European commission in the press release [1]: "*The European Green Deal provides a roadmap with actions to boost the efficient use of resources by moving to a clean, circular economy and stop climate change, revert biodiversity loss and cut pollution".* The Circular Economy Action Plan (CEAP) was then adopted by the European commission in March 2020. The stated goal is to reduce the pressure and the dependence on natural resources to create a sustainable growth as prerequisite to achieve climate neutrality in 2050 [2]. Both the academic and general public interest about the circular economy have rapidly increased in the recent years, although the exact implementation of circular economy is still not clear. As reported by Lazarevic et al. [4] expectations for circular economy are the following: a perfect circle of slow material flows; a shift from consumer to user; growth through circularity and decoupling; and a solution to European renewal. Corvellec et al. [5] have collected a number of critics concluding that circular economic is far from been implemented and promising as sustained by politics. Critics reported that:

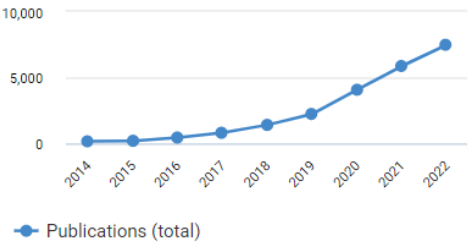

Figure 1: Published articles containing words "circular economy" per year [38]

- A circular economy future where waste no longer exists, where material loops are closed, and the place products are recycled indefinitely is, in any practical sense, impossible as every loop around the circle creates dissipation and entropy, attributed to losses in quantity (physical material losses, by-products) and quality (mixing, downgrading). New materials and energy must be injected into any circular material loop, to overcome these dissipative losses. [6]
- Limitations in material properties and the manufacturing and reprocessing technologies constitute another hindrance to closing material loops that appear to be ignored [7]
- Advocacies of the circular economy and circular business models have been found to adopt a simplified understanding of consumption reduced to purchasing and recycling [8]
- In secondary resources, it is difficult to see why anyone at the firm-level "would be interested in using waste as a resource in a circular economy instead of the well-functioning value chains with primary resources" [9]
- The circular economy has appeal to policy makers because it promises a win–win outcome, shifting attention away from "trade-offs and constraints" to "synergies and opportunities" under the guise of a suitable policy framework [10]

We believe the biggest issue to solve is the lack of reprocessing technologies. Most items are not designed for recycling and recycling itself: the approach is well investigated only for metals and glass because of the huge energy saving the recycling allows for those materials. Physical and chemical recycling of other materials such has plastic has been studied for decades, however as far as the 2018 in Europe only the 32.5% of plastic has been recycled while the 24.9% landfilled and the 42.6% was treated in waste-to-energy plants. It appears

evident that landfilling is the less desirable choice, while energy recovery plants are able to recover only a fraction of the energy used to produce the waste burned. In order to approach the concept of circular economy is then necessary to develop new processes able to produce new products from the currently landfilled and incinerated waste.

1.2 The Car Fluff problem

In Europe (EU-27) in 2019 more than 6 million vehicles reached their end of live, for a total weight of 6.9 million tons. In the period 2008-2019 the annual medium was 5.6 million vehicles (5587583) for a total of 67'051'000. [11]

European parliament directive 2000/53/EC requires EU member stated to reach a minimum rate for reuse and recycling of 85% and for reuse and recovery of 95% [12], by average weight of vehicle. In the 2019 EU-27 average were 89.6% for reuse and recycling and 95.1% reuse and recovery, while Italy reached an insufficient rate of 84.2% both for reuse and recycling and reuse and recovery.

In a 2021 parliamentary question the environmental commission reported an inadequate quality of the actual end of life car treatment facilities, where recycle and recovery is not maximized. [13] As result of that, the destination for the unrecycled fraction is landfilling.

1.3 Origin of Car Fluff

In Italy [14] the legislation related to end-of-live vehicle (ELV) is the D.Lgs. 209/2003. The car, after being cancelled from the PRA (Pubblico registro autoveicoli) is transferred to an authorized collection center where the process begins. First of all, hazardous materials are removed in order to secure the car. Battery, refrigerants, fuel, antifreeze, brake fluid, engine oil, CFC, HFC, lead containing material (display, light bulbs) and airbag are removed. Used spare parts (if any) are then disassembled. Glasses are removed, then scrap metals are divided into different fraction of different economical value. It is mandatory to remove big size plastic parts (bumbs, dashboard, tank) if they cannot be separated after shattering, which is the last final step. The remaining car body, together with other light parts not removed, is shattered and ferrous material is separated and sold for steel recycling. The remaining part is the so-called car fluff, a mixture of light, mostly plastic, heterogeneous materials. A scheme of the procedure is reported in fig.2 [14].

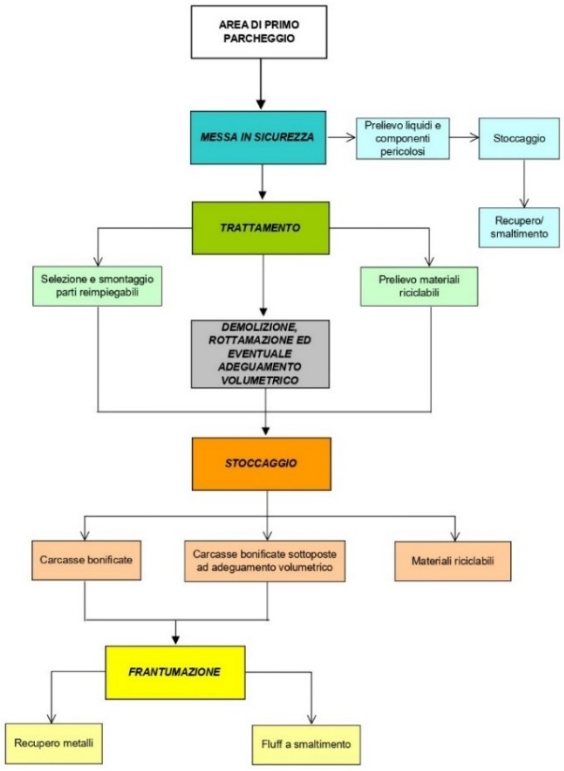

Figure 2: End of life car treatment [14]

1.4 Alternative for car fluff treatments from literature:

Aggregate for concrete:

In a paper from 2017 F. Colangelo et al. [15] suggested that non-metallic car fluff (CF) could be used together with coal fly-ash (CFA) as aggregate for sustainable concrete. The aggregates were manufactured using a cold bonding apparatus, essentially a pilot scale concrete mixer, where through cold bonding pelletization almost spherical particles are obtained. CF aggregates were then used to prepare three different concrete mixtures. Compared to a commercial concrete used as benchmark, mechanical properties where similar in one formulation out of three while slightly worst properties were shown from the other two samples. Authors concluded that about the 44% of CF could be used in the production of artificial aggregate. Authors suggest further studies.

Pyrolysis-Combustion EBARA TwinRec:

Introduced in 2000 by the Japanese EBARA corporation, the TwinRec [16] system for shredded residue is a fluidized bed gasifier combined with ash melting process. The gasifier operating temperature is of 500-600°C. EBARA claims that its process can separate metallic and large inert particles from the fine particles entrained in the gas flow leaving the gasifier. Fuel gas produced together with carbonaceous particles are then burned together in a cyclonic combustion chamber. The fine particles here are collected on the wall and due to the high temperature of 1350-1450°C can be vitrified. EBARA claims that the high temperature of combustion reduces the amount of dioxin below regulations limit and that using a compact steam generator the process is able to recover energy producing electricity with an high net efficiency. The final materials are:

- Pure metals and alloys recovered in the gasifier
- Inert material cleaned from organic matter
- Vitrified fraction containing metal oxide powder, mineral dust, volatile metal salts of Zn, Pb and Cu

EBARA claims that recovering Zn, Pb and Cu from secondary ashes the overall recycling and recovery of ELV could reach 99%, higher than the 95% required by the European normative.

Energy Recovery from Incineration

Although incineration with energy recovery is considered as a less attractive solution respect to recycling by the European commission [17], it is still considered better than landfilling and represents, as far as 2015, the principal way of managing plastic waste in (almost) zero landfill countries such as Switzerland, Germany, Austria, Luxemburg and others [18]. Mancini et al [19] have investigated the possibility of thermal valorization of car fluff using a full-scale plant developed for tyres thermo-valorization. The car fluff characterization for their waste reported a mixture of textiles material (25%), plastic (23%), sponge (17%), and sand and solids (16%). The principal hazardous materials present in the car fluff, representing a problem for incineration, are the following: sulphur, chlorine, heavy metals and contaminant oils from elastomers, PVC, metals and car fluids. These materials may lead to the emission of acidic gases, fine dusts containing heavy metals, and

organic pollutants, meaning that for being compliant with the increasingly strict regulation about gaseous emission it is necessary to use expensive gas treatment systems.

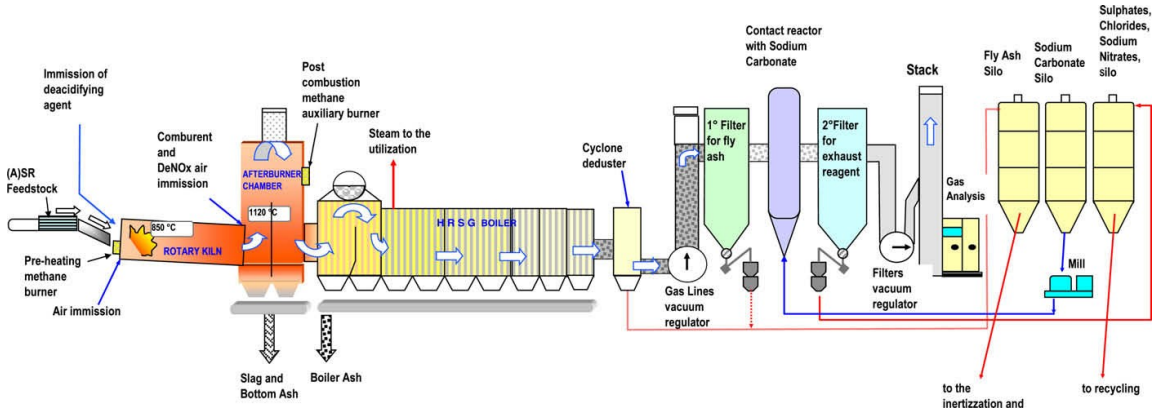

Figure 3: Operational layout of the plant. Mancini et al. [19]

The car fluff gasification–incineration experiments were carried out in the plant reported in fig. 3. The rotary kiln is operating at a temperature of 850°C with an air factor lower than 1 to allow for the conversion of solid to gas through volatilization and partial combustion reactions. The inorganic fraction melts and is removed at the bottom while the gases are burned at 1120°C eventually using methane to keep the temperature constant. The flue gas residence time is of 2 s. The heat produced is recovered producing steam at 43 bars 430 °C. Exhaust gases were continuously analyzed using FTIR and components researched were H_2O, CO_2, CO, NO, NO_2, NO_X, HCl, HF, SO_2, NH_3 and N_2O. On some exhaust gas batch samples the presence of the following contaminants was searched: Cd, Tl, Sb, As, Pb, Cr, Co, Cu, Mn, Ni, V, Hg, PCDD and IPA. All the emissions were below the limits imposed by the Italian d. lgs. 133/2005. The low calorific value of the car fluff treated was of 13'000-14'000 kJ/kg. The energy efficiency parameter calculated by the authors was of 61%. The slag produced were the 18% of the initial mass and authors believe that with metal recovery this value could be further minimized since only the 2% of produced ashes could be classified as hazardous waste. Authors claim that the drastic reduction in fluff volume may produce a considerable positive impact and that further experiments should be carried out to investigate the thermal process performance in detail.

1.5 Polyurethane

Polyurethane is produced by addition polymerization by reacting a species containing at least two isocyanates with a compound containing at least two active hydrogens, in most cases polyols. The characteristic chain link is called urethane. The reaction can be summarized as follows:

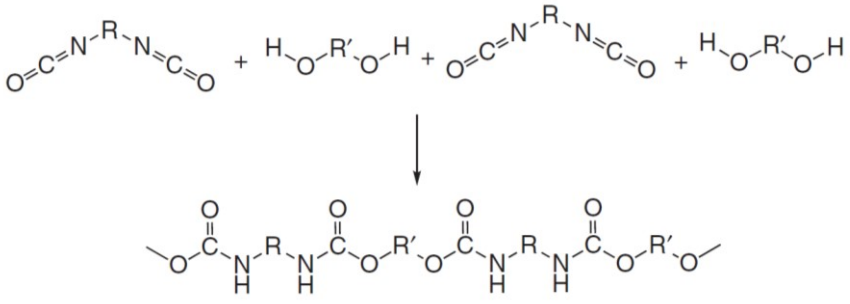

[20]

where R is usually either aliphatic or aromatic with low molecular weight while R' is usually aliphatic with a molecular weight in the order of 200 to 6000 g/mol. The urethane are therefore distributed in pairs, where the two urethane groups are near, along the polymeric chain.

Polyisocyanates

Polyisocyanates can be either bifunction or trifunctional (or more) but practically all polyisocyanates used are bifunctional. They can also be aromatic or aliphatic but industrially aromatic represent more than 90% of the market since aromatic polyisocyanates exhibit better mechanical properties due to higher reactivity and therefore higher average molecular weight of the polymer. On a theoretical base many possible aromatic polyisocyanates could be used, as for example [20]:

A. 2,4-Toluenediisocyanate (TDI)
B. 2,4-diisocyanatotoluene
C. 1,3-Bis(3-isocyanato-4-methylphenyl)-2,4-di-oxo-1,3-diazetidine
D. TDI–urea
E. 1,3,5-Tris(3-isocyanato-4-methylphenyl)-2,4,6-trioxohexahydro-1,3,5-triazine
F. Many others

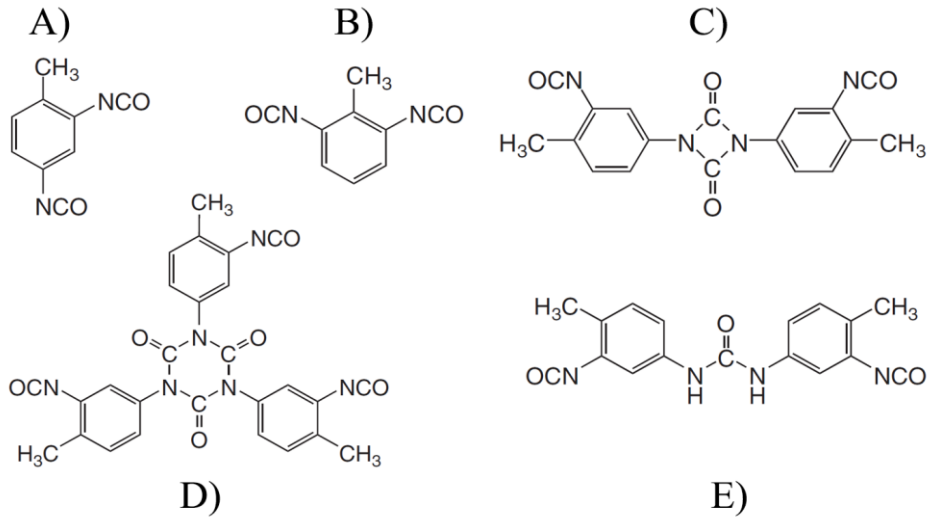

As far as 2017 [20] the two actual polyisocyanates used are MDI and TDI with a share respectively of 72% and 25%. Other polyisocyanates, either aromatic or aliphatic, represent only the 3% of the market.

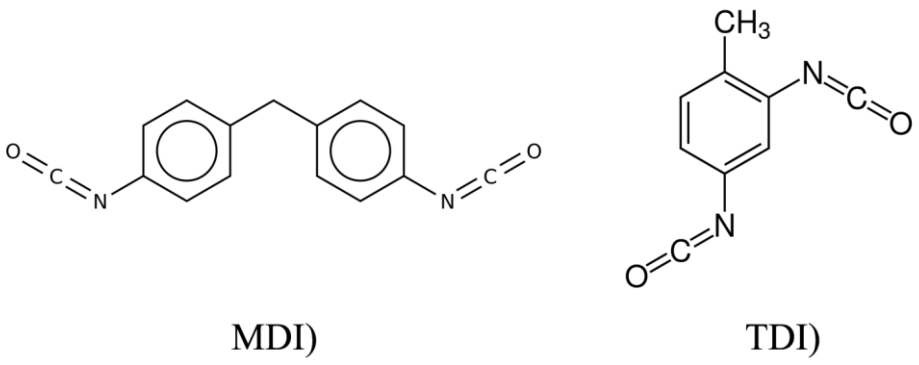

Polyols

While the polyisocyanates world is restricted to almost two compound the variety of polyols used in the PU industry is vast. This is because the relative weight of the polyol in the polyurethane polymer is much higher than polyisocyanates due to higher molecular weight, resulting in polyols determining the physical properties of the PU obtained. The two main type of polyols used are polyether polyols and polyester polyols with, commonly, functionality between 2 and 4. They represent respectively 34% and 10% of total polyurethane mass produced in 2017 [20].

Additives and catalyst

Catalyst used in PU production are used to balance the two reactions occurring in the industrial production of polyurethane, namely the reaction between isocyanate and water reaction (*blowing reaction*) and the reaction between isocyanate and polyol reaction (*gel reaction*). The blowing reaction leads to the formation of CO_2 which is responsible for the foamy aspect while the gel reaction is responsible for the creation of the actual polyurethane links. Three different kinds of additives are used: Lewis bases, Lewis acids and insertion catalyst. Examples are respectively triethylamine, tin dioctanoate and organotin alkoxides.

Additives are largely used, and they are cataloged as: foam stabilizers, hydrolysis stabilizers, oxidation stabilizer, UV stabilizers, blowing agent, colorants and flame retardants.

As far as 2017 the raw material consumption for PU is 22.8 million tons and could be summarized as follows:

Figure 4: Raw material consumption [2017]

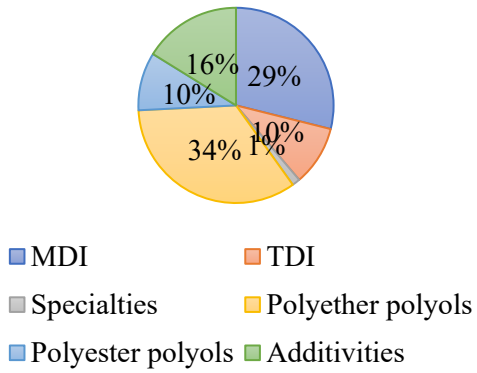

In the car industry PU foam is largely used to reduce noise, to protect from vibration, to make armrests, cushioned dashboard parts, headliners and pillar covers. A schematic representation of PU made component in a car is reported in fig.5:

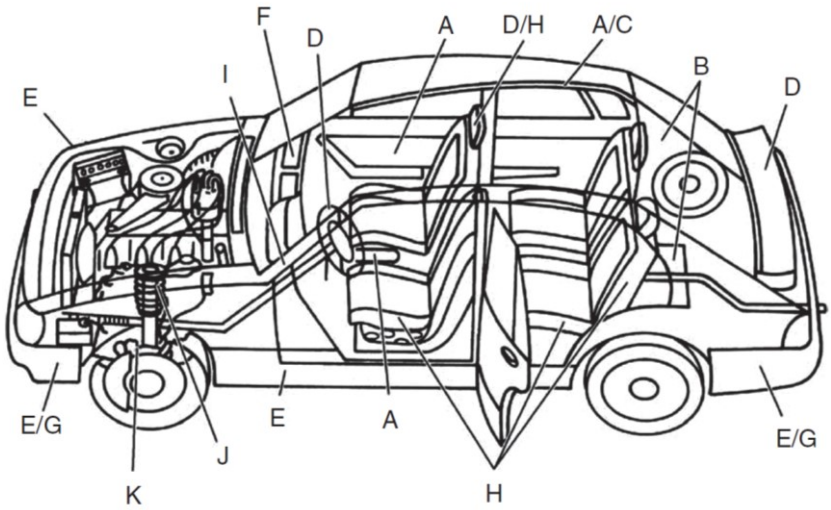

Figure 5: Polyurethane in cars [20]

1.6 Possible processes to investigate for car fluff treatment

Dealing with car fluff two possible alternatives are possible: treating all the material together or differentiate it. While having a solution for the undifferentiated waste seems attractive, it results in likely to be impossible to overcome difficulties in find a process different from thermal valorization. For this reason we identified polyurethane foam to constitute a high fraction of the car fluff in volume terms and for its low density it's also likely to be easier to separate using mechanical processes. Three possible processes have been investigated based on the literature: *hydrothermal carbonization, chemical recycling and pyrolysis*.

1.6.1 *HTC: hydrothermal carbonization*

Hydrothermal carbonization (HTC) is a thermochemical process which can convert organic material such as biomass and plastic into hydrochar. Differently from other thermochemical such as pyrolysis and gasification, HTC reactions occur under wet conditions where water acts both as reagent, medium and catalyst. HTC was initially investigated as treatment for biomass aiming to obtain soil conditioner and an alternative solid fuel to coal [21]. Hydrochar has in fact comparable heating value to lignite although the chemical structure is different. However, hydrochar is not stable in the soil and may present phytotoxicity while hydrochar production cost is too high compared to the cheap coal. For this reason, currently hydrochar for biomass is investigated as:

- Treatment for sewage sludge which are burned or disposed in landfilling. Since reducing the amount of water is a priority for cost reduction, HTC is a cost-effective treatment.
- Phosphate recovery from sewage sludges. Phosphate is a non-renewable fertilizer whose reserves are running out. HTC enables 80% of phosphate recovery.
- Activated hydrochar could be used for different purposes such as water cleaning, CO_2 sequestration, hydrogen storage and as electrode material.

HTC is part of the broader field of hydrothermal processing (HTP) which is commonly classified in three main parts:

- HTC: Hydrothermal carbonization. Temperature: 180-260°C. Pressure: 20-60 atm. Main product is a carbon-rich solid. Time required for biomass is 5-240 min. The pressure at which the process is performed is the saturation pressure of water.
- HTL: Hydrothermal liquefaction. Temperature: 200-370°C. Pressure: 40-200 atm. Main product are hydrocarbons.
- HTG/SCWG: Hydrothermal gasification or Supercritical water gasification. Temperature: >374°C. Pressure: >220 atm. Main product: Syngas ($CO+H_2$).

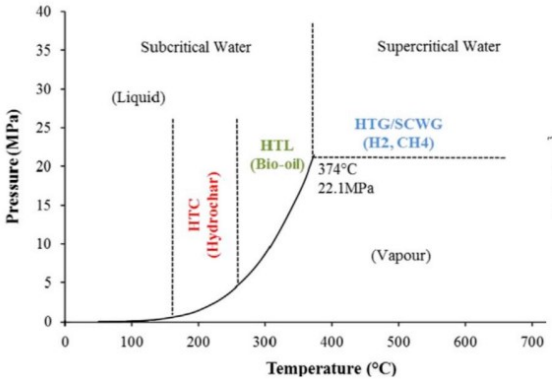

Figure 6: Subcritical and supercritical water

Currently there is a lack in process understanding and reaction kinetic even for long-term studied material such as lignocellulosic biomass and reactor design is based on empirical laboratory studies. In HTC main reaction occurring for biomass are dehydration, polymerization and carbonization.

Plastic wastes are commonly dry or almost dry, so classical thermochemical process such as gasification or pyrolysis are the most used, however a few research have been conducted on HTC mainly of brominated/chlorinated plastics [22][23][24][25]16]. The direct combustion of halogenated plastic leads to the formation of environmentally dangerous compounds so incinerator do not accept PVC or other halogenated plastics. The HTC of PC, HIPS, ABS, PP and PA6 from electronic devices and end-of-life vehicles have been investigated by Zhao et al. [24]. Each sample of plastic waste weighted 10g and was treated in an autoclave for 1h with 300 mL of water at 250-300-350°C. At 250°C the solid residual yield was of about 20-30% for PC and PA6 while for PP, ABS and HIPS was higher than 90%. The organic component in the liquid phase was extracted using dichloromethane and analyzed through GC-MS reporting the following composition:

- Oil from PC: BPA (8.24%), phenol (29.98%), 3-(1-methylethyl)-phenol (43.41%)
- Oil from HIPS: styrene monomer (5.14%), toluene (1.62%), ethylbenzene (6.71%), 1-methylethyl-benzene (1.45%), amethystyrene (2.10%), 1,3-Diphenylpropane (18.98%), 1,3-Diphenylbutane (6.28%), phenylnaphthalene (2.58%), phenyl-terphenyl (5.02%), quaterphenyl (3.46%), polycyclic aromatic products (11.06%)
- Oil from ABS: Ethylbenzene 13.52%, diphenylpropane (11.92%), toluene (5.39%), styrene (5%), methylnaphthalene (1.42%), m-terphenyl (0.77%)
- Oil from PP: hexylcyclohexane (1.20%), n-Nonylcyclohexane (8.64%), 1,2-diethyl-1-methylcyclohexane (1.72%)
- Oil from PA6: caprolactam (42.39%)

Authors concluded that organic liquid oil produced may be reused as chemical feedstock. The solid fraction was visually analyzed concluding that at least for PP at 300°C and 350°C the surface presents interesting

porosity. Finally, enthalpy of combustion was determined using DSC, concluding that for all plastics, except PA6, the heating value was hugely increased.

1.6.2 *Polyurethane chemical recycling*

The production of polyurethane is done by reacting a diisocyanate and a polyol:

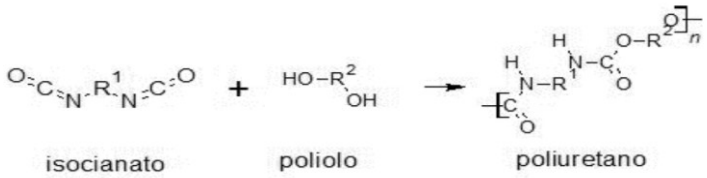

Chemical recycling of polyurethane aims to obtain starting polyol that could be used as feedstock for the synthesis of new polyurethanes. Currently the following reactions have been tested:

- *Hydrolysis*: it was the first attempt to recover valuable products by depolymerization. According to Mishra et al. [27] the mechanism is the following:

$$\mathrm{NCO---R'\text{-}R'NHCOOR''---R''\text{-}OH + nH_2O}$$
$$\downarrow$$
$$\mathrm{NH_2\text{-}R'\text{-}NH_2 + HO\text{-}R''\text{-}OH + HO\text{-}R'\text{-}NH_2 + HO\text{-}R''\text{-}NH_2 + ---}$$

Here, R′ is polyisocynate monomer and R″ polyhydroxy monomer.

  - The expected products are polyamines and polyols. According to Mishra et al. [27] hydrolysis reaction of PU starts at 130° and reach a maximum at 220°C. Pressure is needed just to keep water in liquid state. According to Dai et al. [28], minimum temperature is 200°C and maximum recovery of product is at 300°C. The polyols obtained have to be separated and could be used as reagent for the production of new PU. The amines obtained could not be used directly and have to be separated from the mixture, resulting in a process overall not economically competitive.
- *Methanolysis*: decomposition of PU using methanol in sub-critical and super-critical conditions was investigated by Asahi et al. [29] without catalyst. Operating condition tested were: temperature between 160°C and 300°C, pressure up to 150 atm and 2 hours. The identified products of the reaction were polyol and carbamates.
- *Amynolysis:* decomposition of PU can be performed using ethanolamine, diamines, and polyamines. The presence of many side reaction and the difficulty in separating the useful products make this process uneconomical.
- *Acidolysis:* organic or inorganic acids are used to decompose PU. Polyols, ammine salt and CO_2 are produced using inorganic acid while main products using dicarboxylic acids are oligomers with urea, amide, amine and hydroxyl groups.
- *Glycolysis:* decomposition of PU is obtained using diethylene glycol (DEG), dipropylene glycol (DPG), glycerol and other glycols. Even if it could be performed without the use of a catalyst, commonly a catalyst is used. Alkaline hydroxides, amines, inorganic salts, inorganic acids,

phosphorous compounds, potassium acetate and sodium acetate are used as catalysts [30][31][45]. Glycolysis is generally recognized as the most promising route for chemical recycle and has been investigated since 1980s. The principal reaction is the following [15]:

Polyols produced could lead to the formation of a second layer making easier and economical the separation from the other products of the reaction. Temperature of the reaction is between 160 and 200°C [30].

- *Hydroglicolysis:* it's the combination of hydrolysis and glycolysis, the reaction is catalyzed by sodium hydroxide and potassium hydroxide. Compared to hydrolysis, it allows for a phase splitting where the polyols produced are recovered in the upper phase. Amines by-products make the purification of the polyols difficult [31].

A schematization of main reactions occurring using diethylene glycol, ethanol, water and glycerol for a PU based on 4,4'-MDI is reported. The ROH is the wanted product to recover to produce new PU [44].

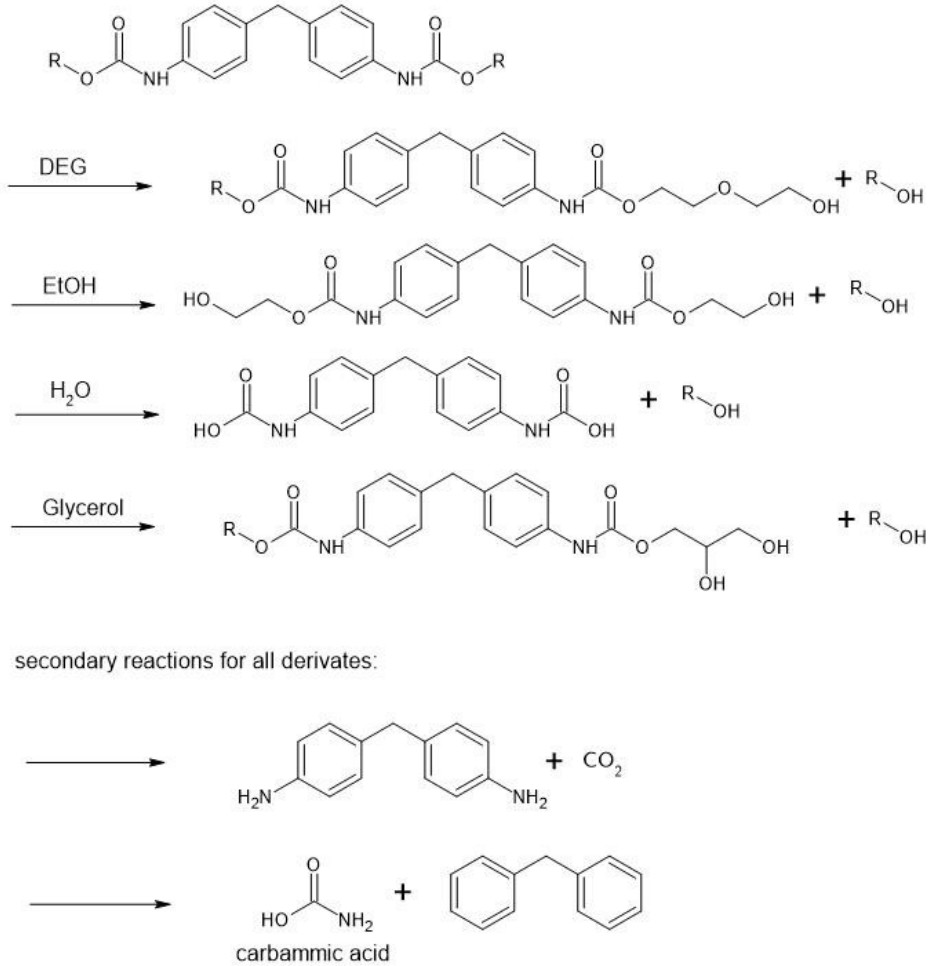

From a chemical point of view we can describe this reaction as a transesterification where different catalyst could be used. In this thesis we will use NaOH under microwave activation as catalyst while products have been characterized using NMR, FTIR spectroscopy and HPLC/GCMS.

1.6.3 *Pyrolysis: N-doped carbon synthesis*

In recent years the research about metal-free catalysts has increased as they are supposed to be more environmentally friendly. Briefly speaking, metal-free compounds based on carbon and possibly other elements such as nitrogen, phosphorus, oxygen and sulfur (among the others) are suitable since those elements are available in large amounts and are easily accessible, are renewable and they could eventually be incinerated once not anymore suitable for their service, since products of combustion are considered to be easily treatable. On the contrary metals, differently, require the environmental damaging operation of milling, produce hazardous liquid/solid wastes in their treatment and, if not correctly recycled, dispersion, in the environment may cause a problem in case of toxic metal such as As, Co, Cr, and others.

Carbon, for its peculiar characteristics, is considered to be a suitable compound for preparing metal-free catalysts. It has different allotropic forms such as graphite and nanotubes resulting in compounds with different characteristics in terms of surface area and electrical conductivity. Surface area as well as the tridimensional geometry is of huge interest for the catalytic properties while the conductivity is important for the production of innovative capacitors. In the literature many papers are dealing with N or P doped carbon as catalyst and supercapacitors production: we briefly describe two of them.

Zong et al. [32] have reported the production of N/O self-doped hierarchical porous carbons for the production of high-performance supercapacitors. Coal tar pitch is graphitized and co-activated using KOH/Ni. The supercapacitor produced reported a maximum energy density of 27.45 Wh/kg in 1 M Na_2SO_4. The operating temperature for calcination and operation, under N_2 atmosphere, was of 400°C. Authors concluded that the compound produced could be used as electrode materials with excellent electrochemical performance and that this route is a viable way for adding value to the inexpensive coal tar pitch.

Wang, Sun et al. [33] have reported the production of N-doped graphene as metal-free catalyst for oxidation of phenol through peroxymonosulfate. They used glucose as a precursor for carbon, urea for nitrogen and hexahydrate ferric chloride as catalyst and template. The solid was calcinated at 700°C under nitrogen atmosphere for 6h. The product has concentrations of oxygen and nitrogen respectively of 2-4% and 0.5-1.8%. Authors concluded that they have found an efficient green catalyst with excellent performance in catalytic activation of peroxymonosulfate for phenol oxidation.

Dealing with polyurethane we think it could be an interesting reagent for pyrolysis, it has in fact already present nitrogen in its composition. Dealing with pyrolysis the heating time is of crucial importance [34]. While in fact slow pyrolysis is meant to produce charcoal, the fast pyrolysis is intended for converting the solid reagent to a liquid. If the intention is to recover chemicals for the production of new polymers the fast pyrolysis is the right choice. But, since it needs equipment not available for us, we investigated the possibility to recover a nitrogen doped coal using the home-made slow pyrolizer.

2. OBJECTIVE OF THE THESIS

The objective of the thesis is to evaluate some different approaches to carry on for the valorization through recycling/recovery of car fluff, of which the most abundant component from a volumetric point of view resulted to be polyurethane. After a detailed characterization on a real sample the processes we decided to investigate can be summarized as follows:

a) Energy recovery: determination of gross calorific value.

b) Pyrolysis processes: even if a lot of environmental problems do not allow to perform it at industrial level in Italy, these processes are extensively tested abroad with the aim to recover fuels from suitable pyrolytic conditions. It is known that ratios between the gaseous, liquid and solid products are depending on the experimental conditions in particular heating rate.
   Our attention has been devoted to the solid residue with the objective to evaluate if nitrogen would remain within the carbonaceous final material to achieve N-doped active carbons.

c) Chemical recycling: one of the most investigated processes concerning polyurethane is glycolysis. We studied the process under microwave activation in the presence of glycerol, diethylene glycol and ethanol (NaOH as catalyst) with the aim to identify the most abundant reactions products.

d) Hydrothermal processes. With the objective to achieve the hydrothermal carbonization, which is known to convert biomass into hydrochar, we planned to study the effect of water, water and H_2O_2 and Fenton conditions on either polyurethane or car fluff. This last study was part of a project concerning the treatment of car fluff under supercritical water conditions to achieve oxidation: owing to the fact that no equipment available in our laboratories was able to realize nor subcritical or supercritical water conditions, the information achieved have been considered in any case useful for the project. Despite this, based on the literature some consideration on this aspect have been made.

3. MATERIALS AND METHODS

3.1 Equipment

- Microwave Ethos 1600 Milestone
- Microwave Anthon Paar Monowave 400
- ATR-FTIR PerkinElmer Spectrum 100
- NMR-Bruker 600 MHz
- ESEM FEI Quanta 200
- Pyrolizer

3.1.1 Microwave Ethos 1600 Milestone

Ethos 1600 produced by Milestone is a lab-scale microwave reactor designed for acid digestion. It contains up to 10 vessels where 9 are suitable for reactions and one is a reference for pressure and temperature. In the configuration we used only 2 vessels were available and no reference vessel for pressure and temperature was usable. The vessel material is Teflon, suitable for its high resistance to acid corrosion. The volume of the vial is of 100 mL and each vessel is claimed to be usable up to 300°C and 100° bars. The rotor in which the vessel is put is schematized in the Figure 7. The compressor screw is tightened up to 25 N*m using a torque wrench in order to assure the pressure tightness of the vessel. The Ethos 1600 microwave reactor used has a programmable power controller without control on temperature and pressure. Milestone Cookbook for acid digestion (1 January 1996) was given in dotation with the Ethos 1600 and was used according to the programs used for the experiments to carry out on different materials.

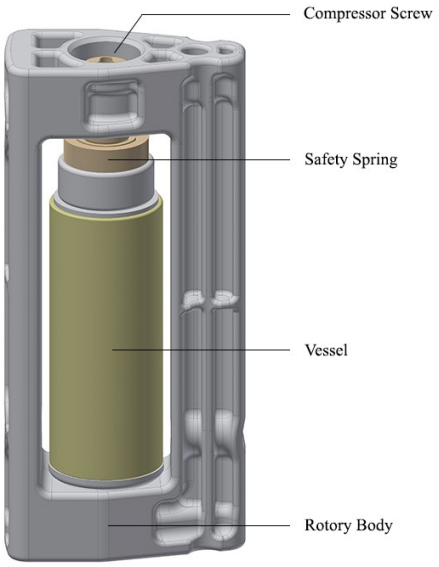

Figure 7: Ethos 1600 vessel

3.1.2 Microwave Anton Paar Monowave 400

Monowave 400 is a microwave reactor produced by Anton Paar. It's a small lab scale reactor designed for synthesis. It has space for 1 vial containing a volume from 2 to 20 mL of solution. Temperature is measured using an IR thermometer while pressure is obtained by measuring the deformation of the cap. Maximum operating temperature and pressure are 300°C and 30 bars. Vials are made of borosilicate glass while the maximum power is 850 W. The Monowave 400 reactor has an incorporated controller for setting predefined temperature and time. Temperature, time, pressure and power are recorded by the system and plotted, giving the possibility to easily spot exothermic or endothermic reactions.

3.1.3 PerkinElmer Spectrum 100

Infrared spectrophotometry is based on the absorption by molecules bonds of photons with wavelength between 0.78 and 100 μm. This range is divided into three categories:

- Near IR (NIR): from 0.78 to 2.5 μm (or from 13000 to 4000 cm^{-1})
- Mid IR (MIR): from 2.5 to 50 μm (or from 4000 to 200 cm^{-1})
- Far IR (FIR): from 50 to 1000 μm (or from 200 to 10 cm^{-1})

The MIR region is the most interesting one since most of bond absorb photons in this range and a lot of data and experience has been achieved during decades in interpreting the diagrams obtained. NIR and FIR regions have lower interest since correlation of peaks with bonds is much more difficult, though both could be used in same very specific application.

The principle behind IR spectroscopy could be explained by the classical model based on the harmonic oscillator for which the Hooke rule holds. The bond behaves like a spring and atoms swing around the equilibrium position. The frequency at which the atoms swing is evaluated as $\nu = \frac{1}{2\pi c}\sqrt{\frac{k}{\mu}}$, where μ is the reduced mass of the harmonic oscillator system and k is the bond force constant. The vibrational energy associated to this movement is $E_{vibr} = h\nu$ where h is the Plank constant. For the classical model this system can enter in resonance with a photon only if the wavelength of the photon is equal or a multiple of this energy E_{vibr}. Moreover, this oscillation must cause a variation of the dipole moment, thus not all vibrational movements lead to a peak in the diagram. Other movement, over symmetric and asymmetric stretching, that could lead to a variation of the dipole moment and to an absorption in the IR range are scissoring, rocking, twisting and wagging.

The basic parts of an IR spectrophotometer are:

- Light source: it is necessary to have a source of photons which emits in the full IR range. The most common sources are the Nerst lamp, the chrome–nickel alloy coil and the Globar (usually made of silicon carbide)
- Detector: it detects the photons after the sample. Common detectors are the pyroelectric detectors, which are made of pyroelectric crystals like gallium nitride, caesium nitrate, polyvinyl fluorides and cobalt phthalocyanines
- Interferometer: the light generated by the source is divided into two streams through a semitransparent mirror. One half is then reflected back through a fixed mirror while the other half is reflected back from a moving mirror. The two halves are then gathered and the final light stream is sent to the sample. Using the property of interference and the mathematical Fourier transform all the IR range is simultaneously investigated.

The IR spectrometer used in this thesis is a ATR-FTIR meaning that works using the property of total internal reflection. The light beam passes through a crystal and penetrates inside the sample for a length of 0.5-2 μm, where it interacts with matter and in then reflected back to the detector. This accessory gives the possibility to catch the interaction of infrared radiation with solids other than liquids.

Commercial software have the possibility to compare the IR spectrum obtained with big databases in order to suggest a possible matching component. This increases by a lot the usefulness of IR spectroscopy since the only correlation with general absorption bond tables is often difficult.

3.1.4 NMR spectroscopy

Nuclear magnetic resonance (NMR) is a spectroscopic technique based on the absorption of photons in the range of radio waves by nuclei with spin. Necessary condition to have NMR active nuclei is that the nuclear spin number I is different from zero. If both the number of protons and neutrons are even then I=0 and the nucleon has not NMR activity, in all other case nuclei are NMR active. Example of NMR active isotopes are: ^{1}H, ^{13}C, ^{14}N,^{15}N, ^{19}F, ^{31}P. Example of inactive isotopes are: ^{12}C, ^{16}O. For isotopes ^{1}H and ^{13}C I=1/2, $m_I=\pm 1/2$ then 2 quantic states (α and β) are associated: $\mu_z = \pm\frac{1}{2}\gamma\frac{h}{2\pi}$. If the external magnetic field B_0 is equal to zero than the energy associated to state α and β are equal, while if $B_0 \neq 0$ then $E_\alpha \neq E_\beta$ where $E_\alpha = -\frac{1}{2}\gamma B_0\frac{h}{2\pi}$ and $E_\beta = +\frac{1}{2}\gamma B_0\frac{h}{2\pi}$. Then the difference of energy between the two quantic states depends on the external magnetic field B and the gyromagnetic ratio γ. While γ depends on the isotope, B_0 is the actual magnetic field applied by the machine, then in order to increase the difference ΔE and increase the resolution it is necessary to work with high magnetic field, up to $20\ Tesla = 2 * 10^5\ Gauss$ where, for reference, the surface terrestrial magnetic field is of about $0.4\ Gauss$. The frequency of the photons needed to cause the transition from the low energetic quantic state to the high energetic quantic state is the Larmor frequency where: $\nu = \frac{1}{2\pi}\gamma B_0$. The Larmor frequency is the actual frequency needed for an isolated nucleon but in a molecule the frequency depends on the chemical environment resulting in very small but still measurable differences. This difference between the standard proton and the standard ^{13}C present in tetramethylsilane is known as chemical shift and is used to get information about the chemical structure of the molecule since the nucleon returning to the low energy quantic states generates a transient signal which can be detected. The chemical shift δ is evaluated as: $\delta = \frac{\nu - \nu_{ref}}{\nu_{ref}} * 10^6$. The chemical shift is non-dimensional and does not depend on B_0 while ν does. Increasing the frequency of the magnetic field results in a higher difference easier to detect between the nucleon and the standard resulting in an higher resolution of the instrument. Two NMR instruments have been used, both made by Bruker, one capable of working at 200 MHz and one at 600 MHz (for protons), where the one working at 600 MHz has an higher resolution and the possibility to make 2D analysis, where both ^{1}H and ^{13}C are simultaneously analyzed. In order to analyze the samples, deuterated water and deuterated acetone have been used as solvents since deuterium has different physical properties from protium. Analyzing an organic molecule, the backbone is made of carbon for which the non NMR active isotope ^{12}C has about the 99% of abundance. ^{13}C is still a stable isotope but on earth has an abundancy equal only to the 1%, resulting in high concentration of sample needed in order to be able to measure the signal in an NMR analysis.

3.1.5 ESEM FEI Quanta 200

ESEM is the acronymous of Environmental Scanning Electron Microscope. Similarly to SEM, a beam of electrons is used to scan the surface of a sample for creating an image. Differently from the SEM, ESEM works with different and specialized electron detectors which enable the possibility to work at low vacuum instead of the high vacuum needed by the SEM. This is important since gives the possibility to work with uncoated wet sample, which is an interesting feature since samples can be analyzed as they are without damaging or modify them. In scanning electron microscope electrons are used instead of light to scan the surface of a sample. This is because white light has wavelength in the range 400-700 nm, resulting in a theoretical limit of resolution of 200-250 nm. Electrons instead have a much lower associated wavelength, resulting in better resolution. For example, an electron with 100 keV of energy is associated to a wavelength of only 3.70 pm [35]. However, practically the resolution is limited by other factors and is in the order of 0.1 nm. A conventional electron gun could be used as source of the electron beam used in a SEM microscope. It has a cathode made in tungsten or LaB_6 where thermal energy produced through joule effect cause electrons to jump into the Fermi level. Those electrons are emitted from the surface of the cathode and, in vacuum, travel towards the anode being accelerated through the very high electromagnetic field. Electrons acquire kinetic energy and, depending on the system, the associated energy is between 0.2 to 40 keV.

Electron beam interacts with the surface of the sample in three ways: some are reflected, some penetrate the surface, and some are absorbed, producing excited ions. These ions returning to their fundamental states emit photons, Auger electrons or secondary electrons. By analyzing the emitted photons, it's possible to obtain information about the surface morphology creating an image of the sample. By analyzing the X-ray emitted by the sample it is furthermore possible to determine the elemental composition of the sample. Since electrons have to be absorbed in order to create the ion which will emit the X-ray photons, the elemental composition determined is not the exact composition of the point in the surface of the sample analyzed but it the composition of a pear-shaped portion of material. A schematization of a SEM microscope is reported in fig.8.

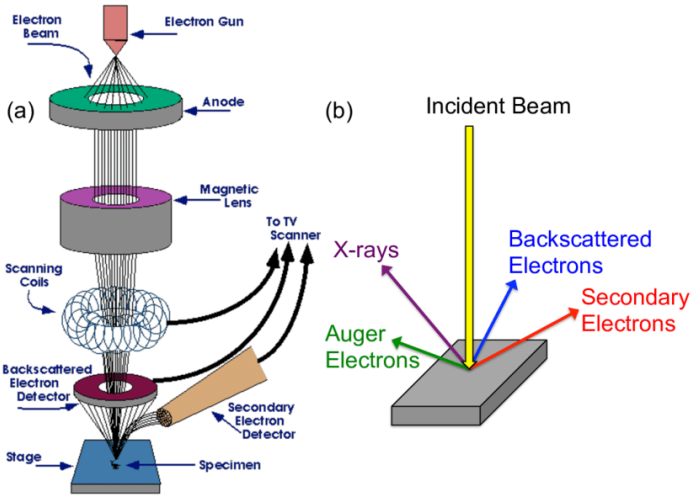

Figure 8: SEM schematization [36]

3.1.6 Pyrolizer

A schematization of the home-made pyrolizer used in this thesis has been reported in Figure 9a. It uses a resistance coil which is heated through joule effect and by radiation heat up the chamber, where a crucible is inserted. In order to achieve pyrolysis condition it is necessary to work in absence of oxygen, so for this reason a continuous flow of nitrogen is present. Temperature is monitored using a thermocouple inside the chamber and a PID controller is used to keep the temperature constant. Insulation is used to avoid heat dispersion but anyway due to the coil power the heating rate is of about 40 °C/min, meaning that fast pyrolysis is not achievable using this equipment. In this configuration fumes passes through a copper chimney and due to the length of the chimney, the copper heat conductivity, the relative low fume flowrate the outlet temperature is about equal to room temperature meaning that some fumes condense on the chimney wall. In order to analyze the non-condensed fumes two different configurations, named A and B have been used. In the A configuration two paper filters are bent to form a cap anchored to the top of the chimney by rubber bands, while in the B configuration, reported in Figure 9b, liquid nitrogen is used together with a Schlenk tube to condense all the condensable gases. Since the nitrogen flow is continuous it is necessary to keep the outlet line of the Schlenk tube open.

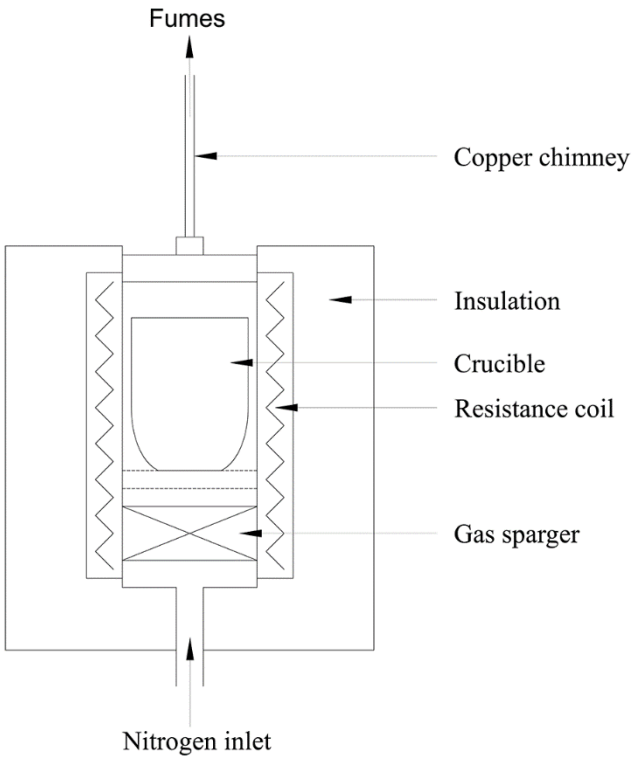

Figure 9a: Home-made pyrolizer

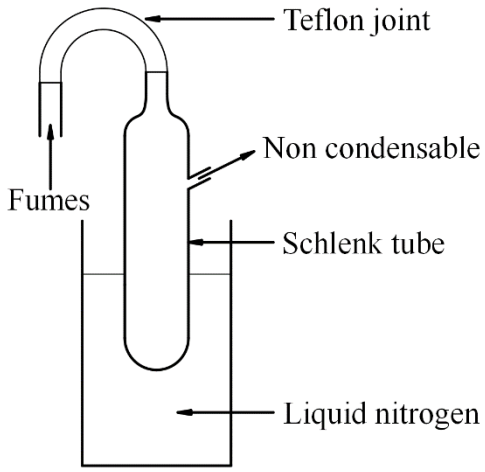

Figure 9b: Configuration B of pyrolizer chimney

4 CAR FLUFF CHARACTERIZATION

The car fluff sample has been divided in multiple batches called CFX according to their macroscopic appearance. Each batch has been investigated using ESEM analysis, EDX analysis and ATR-FT-IR.
The result composition is:

NAME	WEIGHT [G]	DESCRIPTION
CF1	32.35	Polymeric filaments
CF2	196.70	Various rigid polymers
CF3	49.68	Flexible polyurethane foam
CF4	1.52	Wood
CF5	0.35	Glass
CF6	1.55	Rigid polyurethane foam
CF7	19.40	Flexible polymers
CF8	11.45	Sheets of polymers
CF9	20.13	Electric wire
CF10	27.27	Textile material
CF11	253.14	Undifferentiated (polyurethane, textile, polymers)
CF13	1.75	Electronic material
CF14	44.24	> 2 mm particles
CF15	99.40	< 2 mm particles

The total mass is 759 g. Looking at the sample, we could estimate that about 60% of batch 11 mass is polyurethane. Assuming that composition on CF14 and CF15 are the same of the complete sample, we could estimate that the mass fraction of polyurethane is about the 25-30%. From a volumetric point of view, since polyurethane density is very low compared to other plastics like PP or PET, the volumetric fraction of PU is higher, in the order of 50-70% assuming a density of about 0.1-0.3 g/cm^3 for PU and 0.9 g/cm^3 for all other materials.

4.1 Analysis of batch CF1

Figure 10: Photo of a sample from batch CF1

Batch number 1 is a mixture of polymeric filaments which were probably part of the padding.

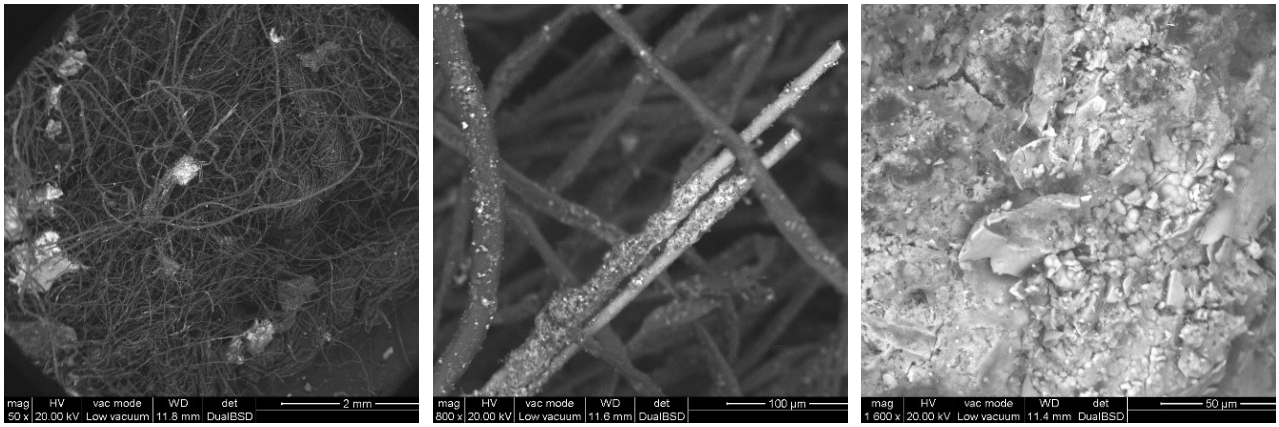

Figure 11: ESEM images

From ESEM analysis the batch shows a mixture of polymeric filaments (1) with the presence of glass fibers (3) and other plastic elements (4).

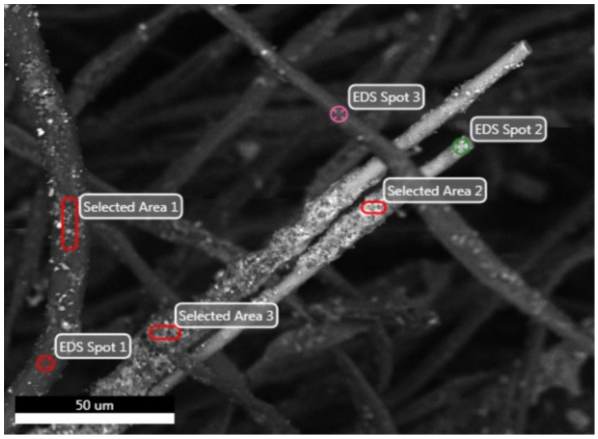

Figure 12: ESEM images

Spectrum	% C	% O	% Zn	% Al	% Si	% Ca	% Fe	% Na	% Mg	% Ti
Area 1	53.66	40.64	1.67	0.60	0.92	1.27	1.24	-	-	-
Spot 2	20.82	43.22	0.95	4.53	15.34	9.92	2.76	1.72	0.59	0.13
Area 2	24.91	38.26	3.11	0.91	1.79	4.75	24.55	1.04	0.67	-

From EDX analysis the highlighted area 1 shows the presence of mainly carbon and oxygen. Since hydrogen presence is not visible through EDX, the analysis suggests us the filaments is a polymer containing oxygen.
For spot 2, EDX confirms that it is a glass fiber due to the presence of O, Si and Al. Carbon presence in the analysis results is due to EDX technique which is not able to analyze the composition of a point but it is disturbed by the close region.
The selected area 2 shows the presence of other contaminants in the sample, in this case mainly made of iron oxide.

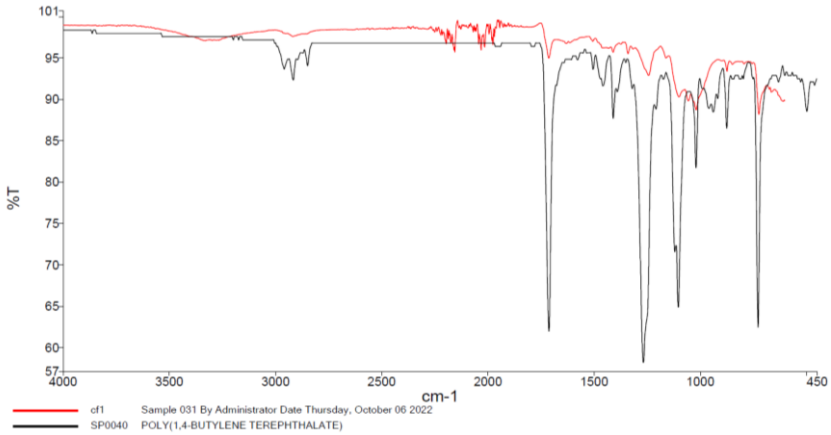

Figure 13: FTIR analysis of a sample from batch CF1

ATR-FT-IR analysis suggests that the polymer could mainly made of polybutilenterephtalate (65% correspondence), which is a polymer made of carbon hydrogen and oxygen, in agreement with EDX analysis.

4.2 Analysis of batch CF2

Figure 14: Photo of a sample from batch CF1

Figure 15: Photo of a sample from batch CF1

Batch 2 is made of rigid plastic, 2 pieces with different color have been analyzed.

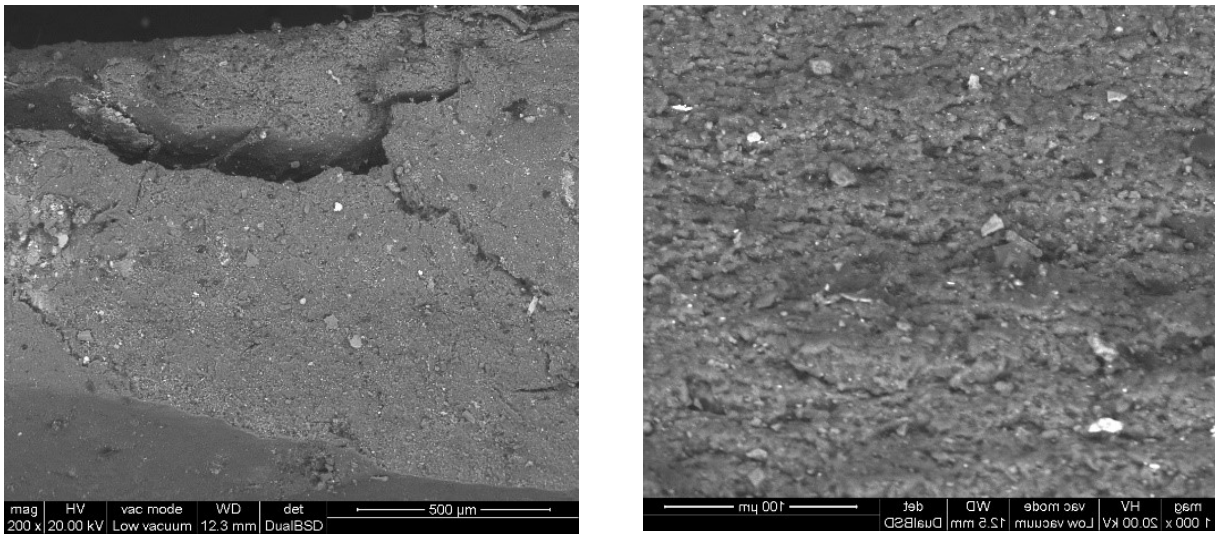

Figure 16: ESEM of the sample from figure 14

Spectrum	% C	% O	% Al	% Si	% S	%Cl	% Ca	% Ti	% Fe	% Zn
Area	40,08	26,29	0,76	1,13	0,45	23,88	4,96	0,13	1,45	0,87

Dark plastic is a filled polymer with a high presence of chlorine, suggesting that it could be PVC. EDX analysis shows also the presence of other elements in small traces such as Ca, Fe and even Ti, used probably as additives.

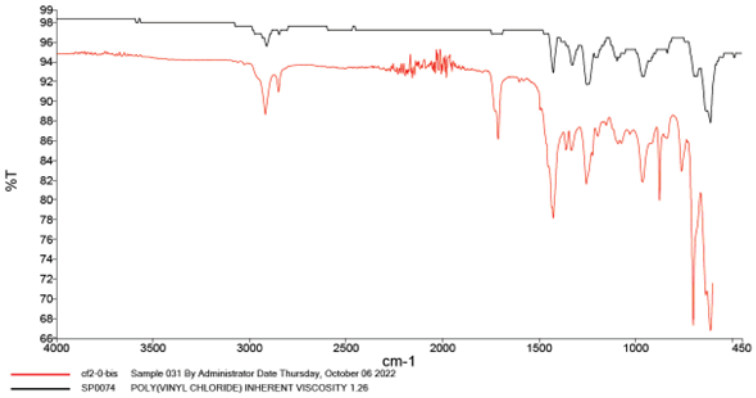

IR analysis confirms it is PVC (76% correlation).

Figure 17: FTIR analysis of the sample of figure 14

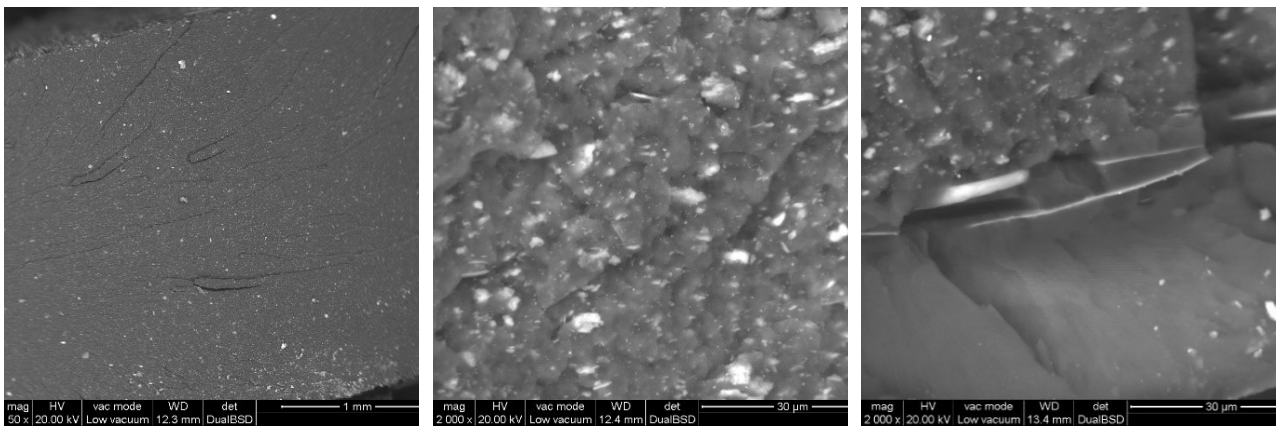

Figure 18: ESEM of the sample of figure 15

Light colored plastic (fig.15) is a filled polymer with a shining coating, well visible in fig 18. In this case the presence of a filler is more abundant than in the darker plastic piece.

Spectrum	% C	% N	% O	% Mg	% Al	% Si	% K	%Ti	% Fe
Area 200x	58,54	12,2	23,79	0,17	2,36	2,36	0,12	0,39	0,07

An EDX analysis performed on a large area shows the presence of C, O, Al and Si. EDX analysis shows also the presence of Nitrogen, element which is often difficult to detect.

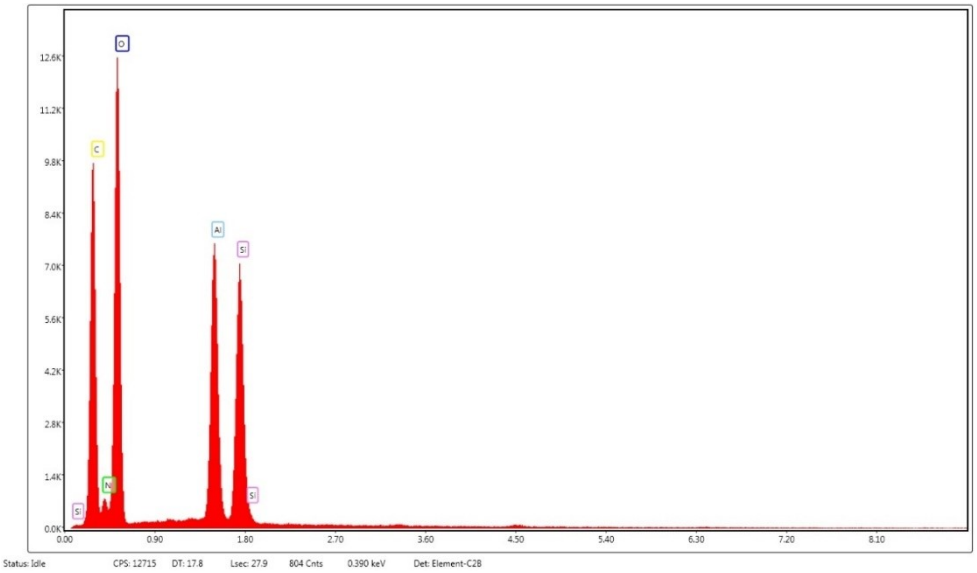

Figure 19: EDX analysis of the sample of figure 15

The EDX analysis performed on a small part of filler shows it is made of Al, Si and O. The presence of C and N and the abundance of O is because EDX is not able to perform an analysis on a point but it analyze a small pear shaped volume.

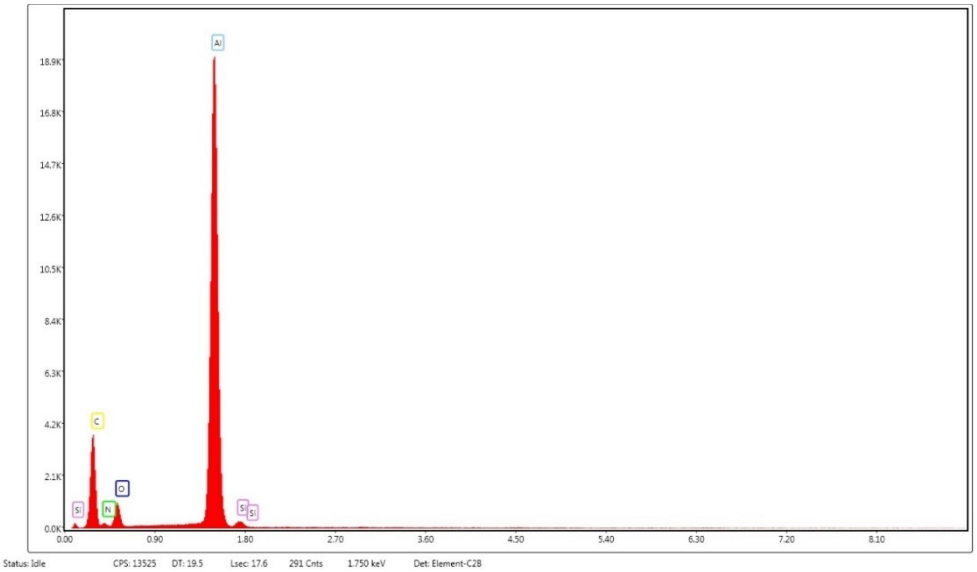

Figure 20: EDX analysis of the sample of figure 15

The coating is made of a small layer of Aluminum.

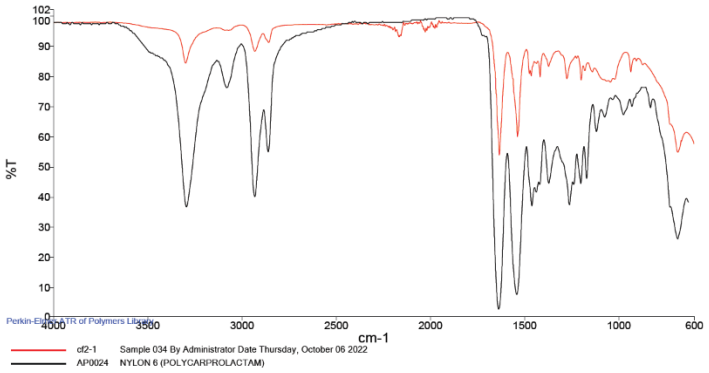

Figure 21: FTIR analysis of the sample of figure 15

IR analysis suggests that the polymer is nylon, with a 95% correlation with nylon 6.

4.3 Analysis of batch CF3

Figure 22: A sample from batch CF3

Batch number 3 is made of soft foam which could probably be part of some padding.

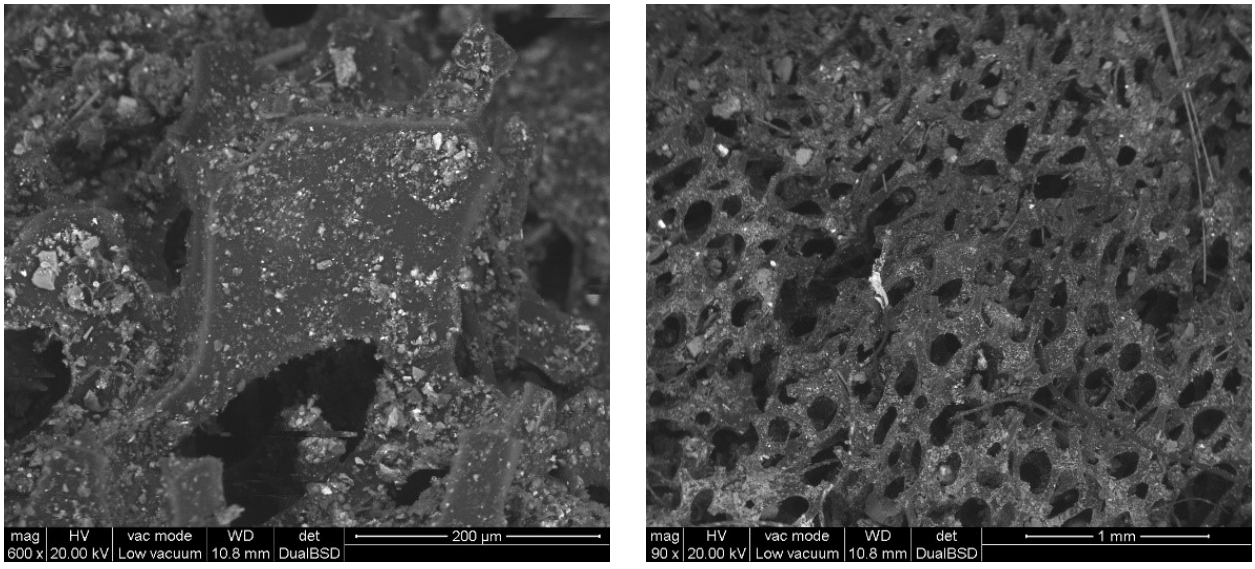

Figure 23: ESEM of the sample from figure 22

ESEM analysis highlights the foam structure and the presence of contaminants inside the sample.

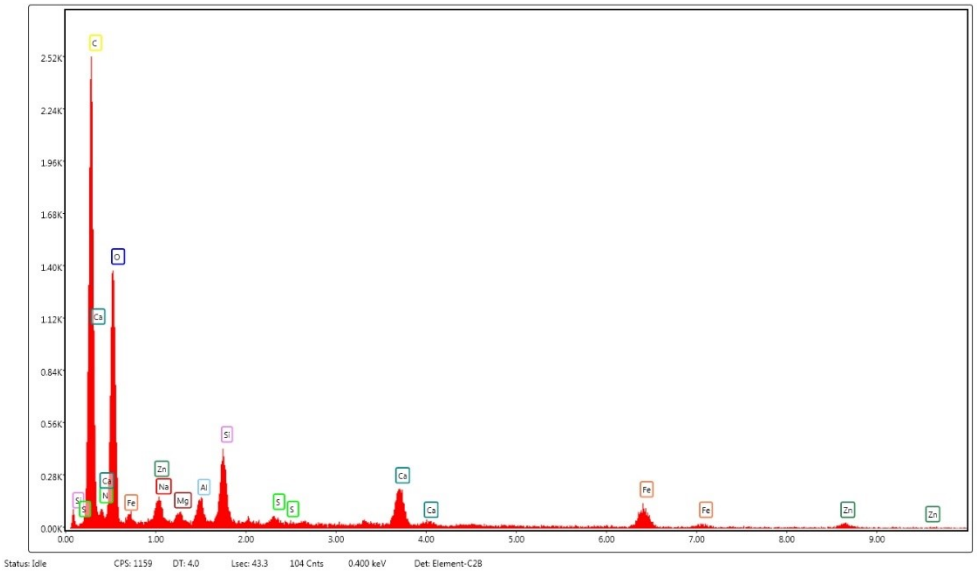

Figure 24: EDX analysis of sample from batch CF3

EDX analysis detects the presence of C, N and O which are probably part of the polymer and the presence of other element such as Si, S, Ca, Fe and Zn which contaminate the polymer

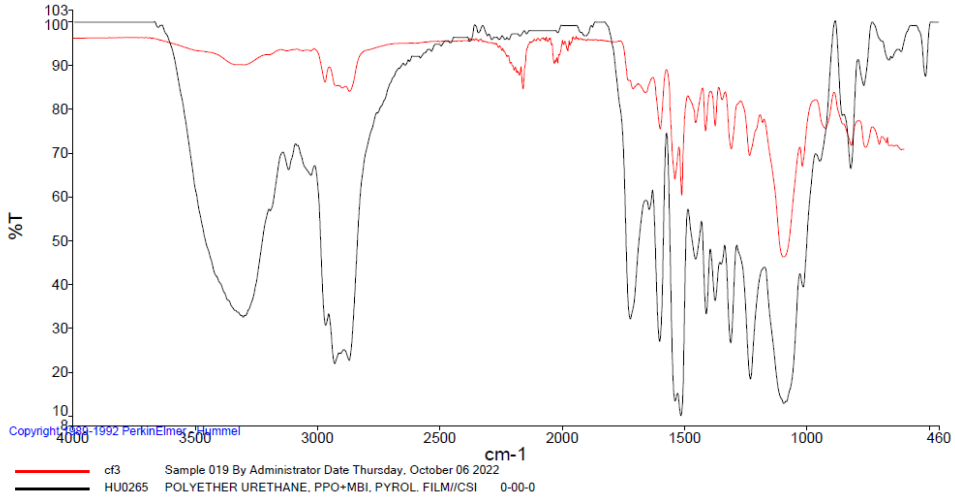

Figure 25: FTIR analysis of the sample of figure 22

IR analysis suggests a possible correlation (81%) with polyurethane which agrees with the presence of C, N, O and the macroscopic structure.

4.4 Analysis of batch CF4

Figure 26: Photo of batch CF4

Batch number 4 is made of wood. No further analysis has been considered necessary.

4.5 Analysis of batch CF5

Figure 27: Photo of batch CF5

Batch number 5 is made of small pieces of glass. From a visual inspection two different type of glass are present, thus two different analyses have been performed.

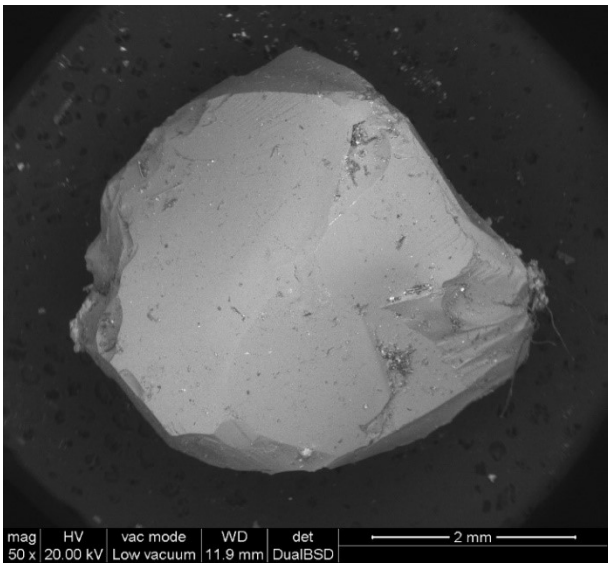

Clear piece of glass shows the presence of some small impurities on the surface.

Figure 28: ESEM photo of a clear piece of glass

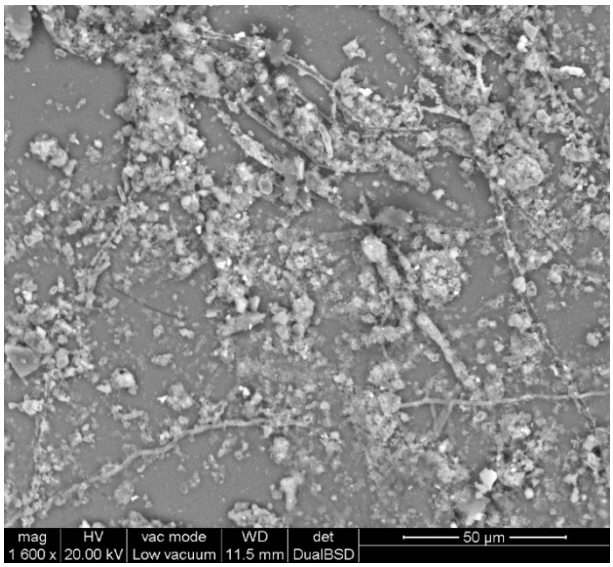

Figure 29: ESEM photo of a yellow piece of glass

Yellow piece of glass presents some inclusion which are the source of yellow color.

Spectrum	% O	% Na	% Mg	% Al	% Si	% Ca	% Fe	% K
Transparent Glass (fig28)	46.17	12.15	2.41	0.36	31.64	6.59	0.67	-
Yellow Glass (fig29)	45.8	12.04	2.15	0.15	31.23	7.12	1.18	0.45

Clear glass and yellow glass show a very similar EDX spectrum.

Yellow glass has only a bit more of Fe and K.

IR analysis has not been performed on the sample as not considered necessary.

4.6 Analysis of batch CF6

Figure 30: photo of a sample from batch CF6

Batch number 6 is made of rigid foam with some impurities on the surface.

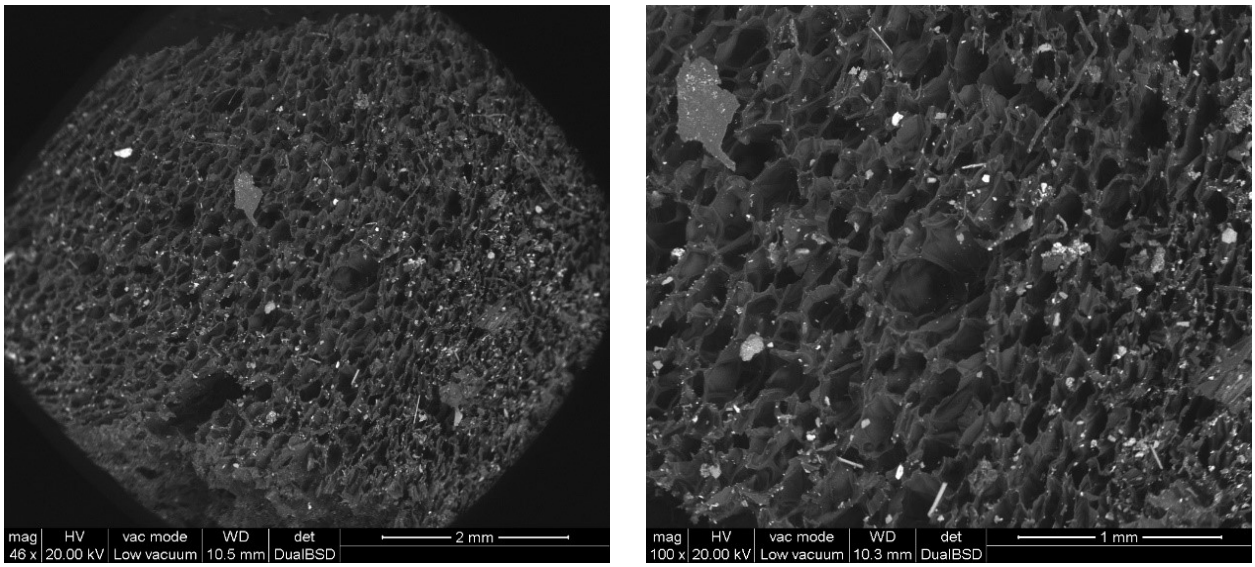

Figure 31: ESEM photo of a piece from batch CF6

ESEM analyses shows the structure of the foam and the presence of some small particles of contaminants.

Spectrum	% C	% N	% O	% Na	% Al	% Si	% P	% Cl	% Ca	% Fe
CF6 Area	63.25	5.67	27.31	0.28	0.3	0.77	0.6	0.19	0.75	0.88

EDX analysis show the presence of C, O and N, together with some elements in traces.

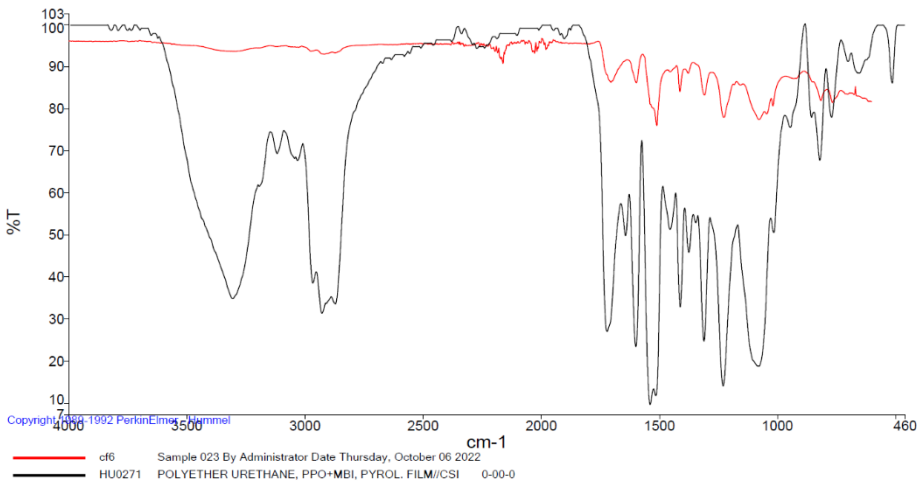

IR analysis suggests a correspondence with polyurethane with 83% of correlation, in agreement with EDX elementary analysis.

Figure 32: FTIR analysis of the sample of fig.31

4.7 Analysis of batch CF7

Figure 33: Photo of a sample from batch CF7

Batch number 7 is made of flexible plastic.

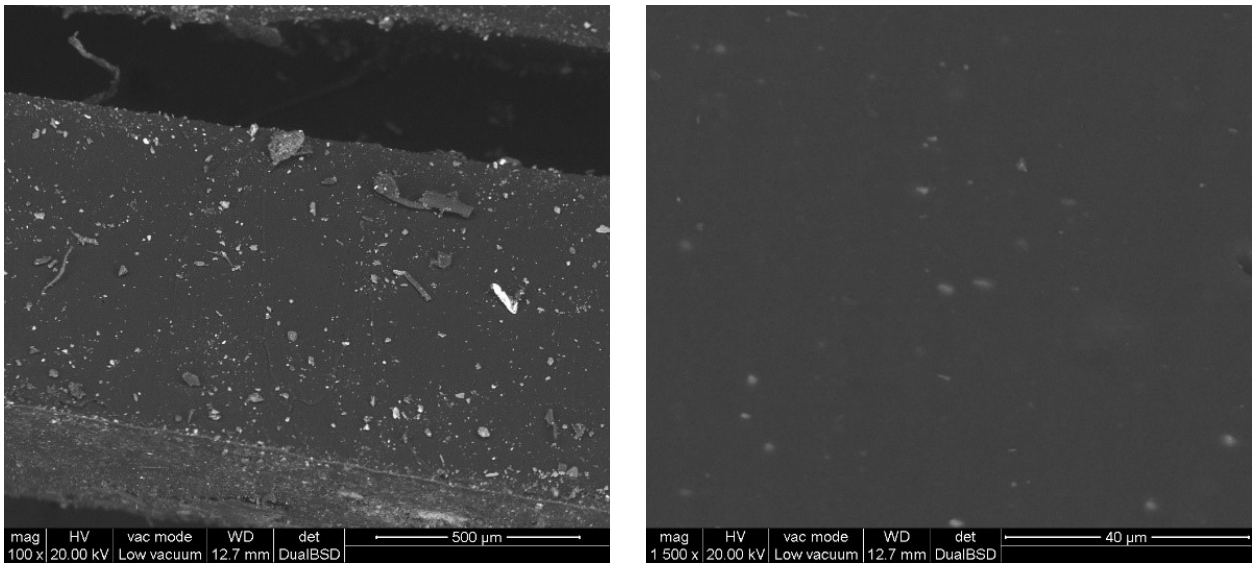

Figure 34: ESEM of the sample from figure 33

ESEM analysis shows the polymer is lightly loaded with some very small particles.

Spectrum	% C	% O	% S
CF7 Point	91.97	7.96	0.07

EDX analysis shows the presence of C and a very low presence of O and S, probably part of the inclusion.

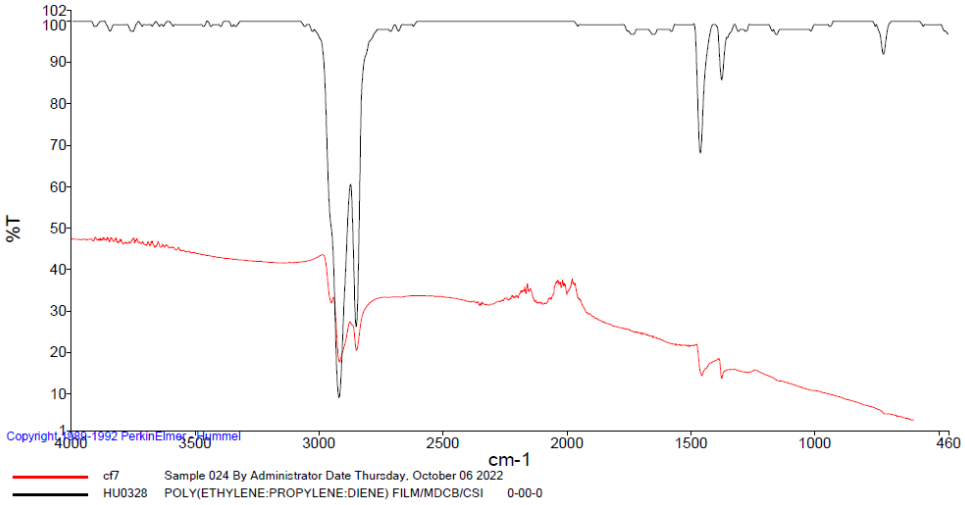

Figure 35: FTIR analysis of the sample of figure 33

IR analysis suggests a correspondence (75%) with polyethylene, in agreement with EDX analysis.

4.8 Analysis of batch CF8

Figure 36: Photo of two samples from batch CF7

Batch number 8 is made of polymers in sheets. Two visibly different types of polymers are identified and analyzed.

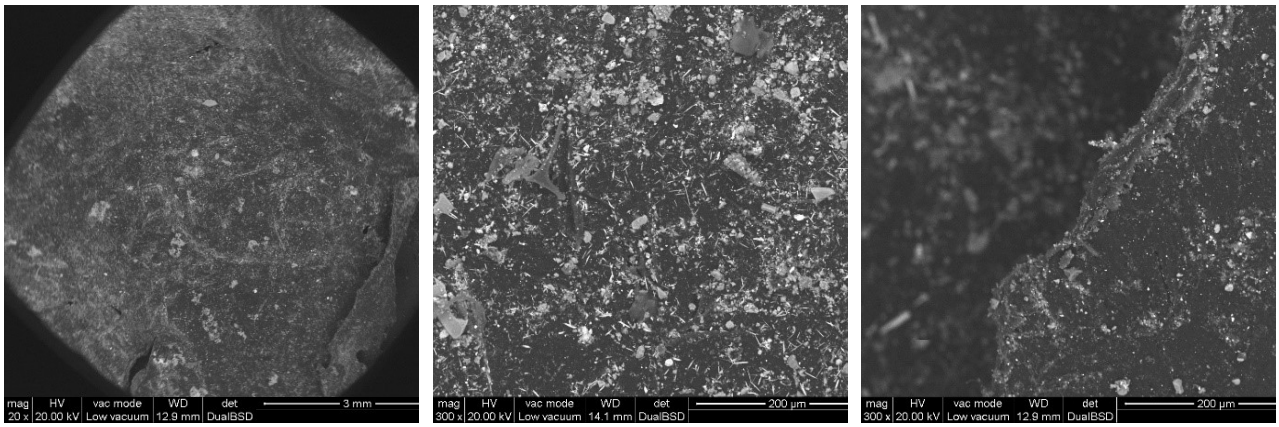

Figure 37: ESEM of sample white from fig.36

Spectrum	% C	% O	% Na	% Al	% Si	% Ca	% Fe	% Ti	% Br
Point on polymer	99.75			0.03	0.08	0.11		0.05	
Area	67.06	24,97	1,01	1,88	1,39	2,11	1,58		
Loading particle	67.47	18.83			1.03	1.96	1.98		8.73

ESEM analysis shows the polymer is highly loaded with different type of particles. The polymer structure appears to be compact.

EDX analysis on the polymer matrix shows it is made only of carbon, suggesting it possibly is a polyolefin.

EDX analysis on a large area shows the presence of many different loading particles such as aluminum silicate and calcium and iron oxides.

Another EDX analysis on a different loading particle shows the presence of bromine, probably used in a flame-retardant agent.

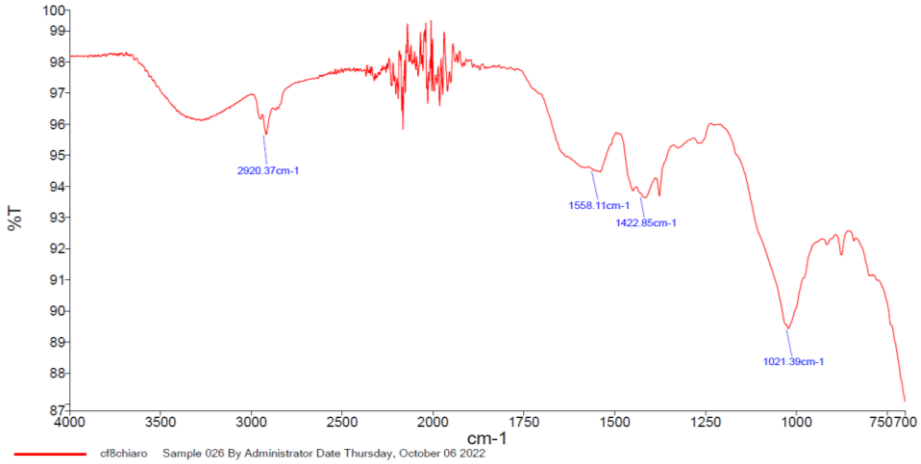

Figure 38: FTIR of sample from fig.37

IR analysis suggests possibly the presence of an alcoholic group and that the presence of C-H bonds, anyway due to the presence of many pollutants no correspondence has been found in the database of the software.

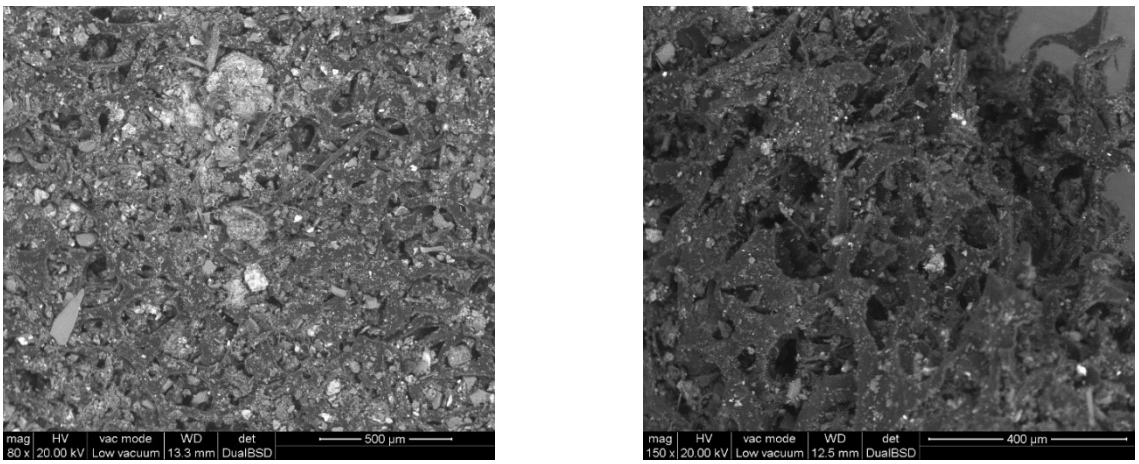

Figure 39: ESEM of sample black from fig.36

ESEM analysis shows a grid structure lightly loaded. The holes present in the structure entrap many small particles of different nature.

Spectrum	% C	% O	% Al	% Si	% Ca	% Ti	% Fe	% Zn	% Na	% Mg	% S
Polymer point	63.57	27.04	1.4	1.71	2.25	0.45	2.16	1.42	-	-	-
Area	37.29	37.91	2.11	4.61	4.77	-	7.16	3.67	1.65	0.48	0.3

The EDX analysis on the matrix shows it is manly made of carbon. The oxygen is probably present as oxide of Al, Fe, Ca, Zn, Ti, Si since, as already said a small pear-shaped volume around the point is analyzed.
An EDX analysis over an area shows how the content of oxygen increases as well as the content of other elements, suggesting that the oxygen is present as oxide of metals and not in the polymer chain.

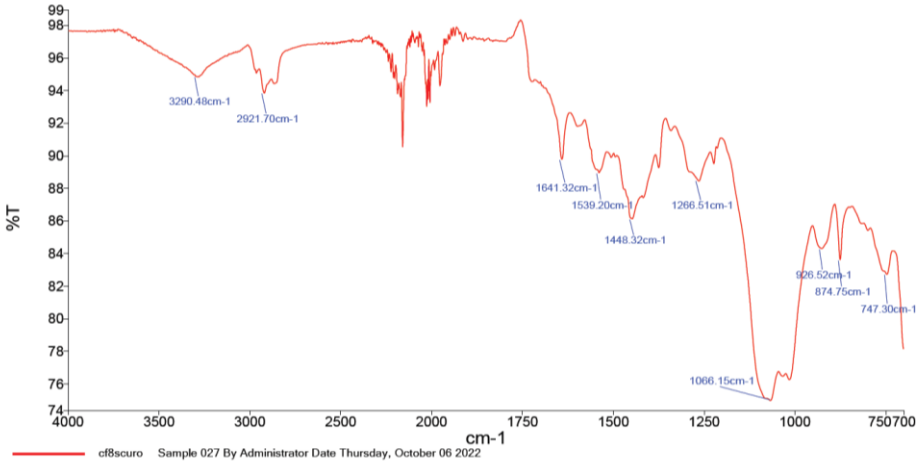

Figure 40: FTIR of sample from fig.39

Since the sample contains many different pollutants, it was not possible to get reliable information through the IR analysis.

4.9 Analysis of batch CF9

Figure 41: Photo of sample from batch CF9

This batch is made of electric wires. No further analyses are done.

4.10 Analysis of batch CF10

Figure 42: Photo of sample from batch CF10

This batch is made of textile material. No further analyses are done.

4.11 Analysis of batch CF11

Figure 43: Photo of sample from batch CF11

Batch 11 is a mixture of undifferentiated macroscopic pieces of plastic and textile materials. From a visual inspection it seems to be mainly made of the same material as the batch number 3. It has been left undifferentiated since it would need a significant amount of work to differentiate material from that batch.

4.13 Analysis of batch CF13

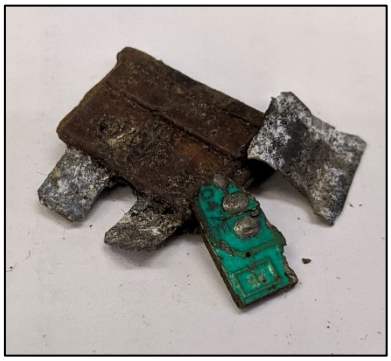

Figure 43: Photo of sample from batch CF11

Batch 13 is made of electronic material. In this case it is a fuse with small pieces of PCB.

4.14 Analysis of batch CF14

Batch 14 is made of small particles with dimension higher than 2 mm. 5 different pieces are analyzed as examples.

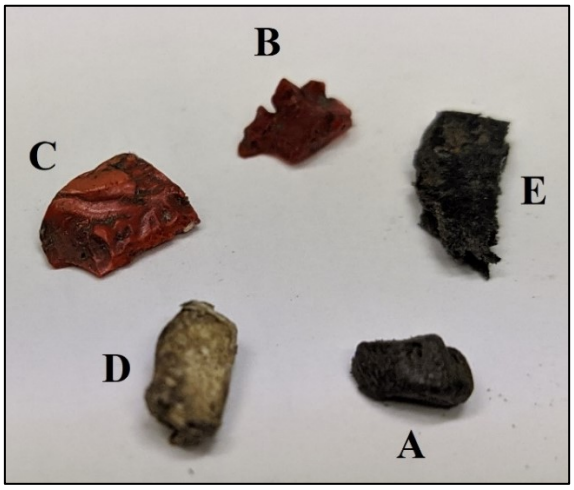

Figure 43: photo of pieces analyzed from batch CF14

4.14A

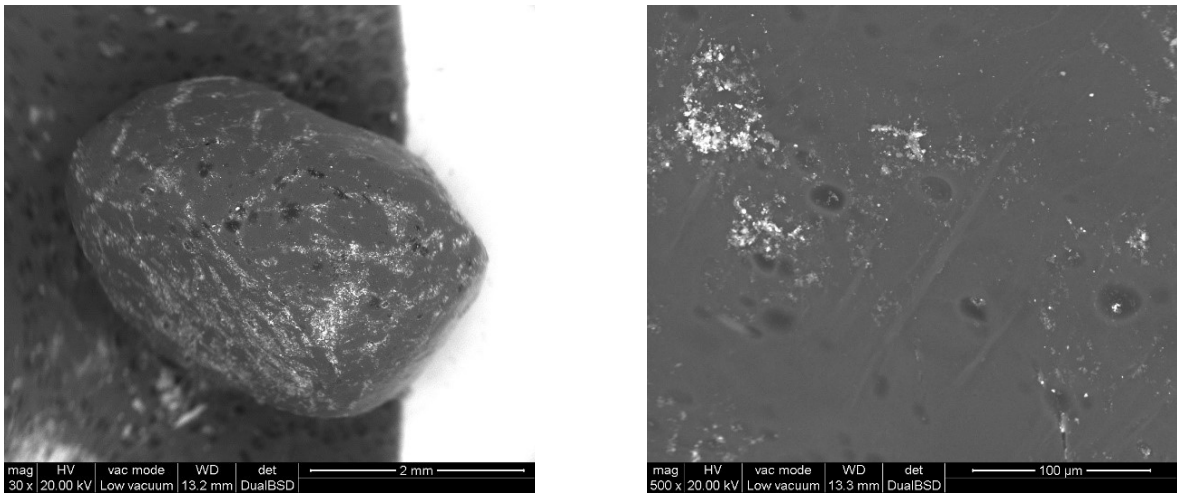

Figure 44: ESEM of piece A from fig.43

ESEM analysis highlights a compact structure, without loading and with the presence of some small particles on the surface.

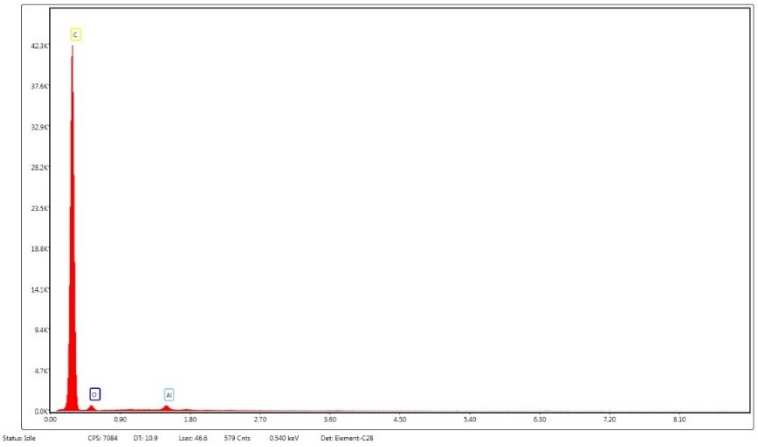

EDX analysis on an area shows the presence of only C and that the particles on the surface are made of aluminum oxide.

Figure 45: EDX of piece A from fig.43

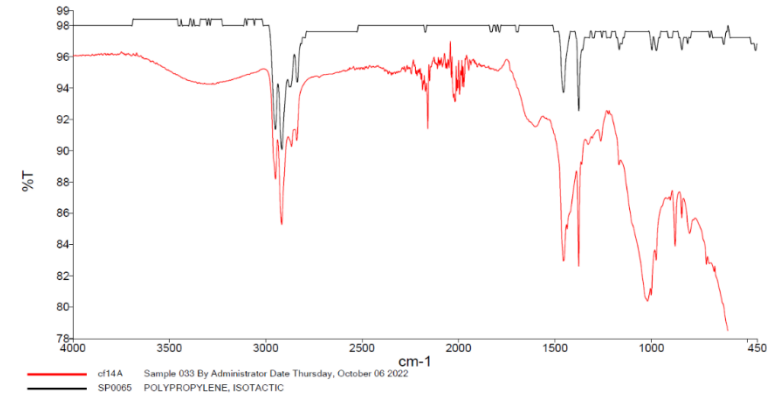

IR analysis suggests a weak (68%) correspondence with polypropylene, which is in agreement with EDX analysis.

Figure 46: FTIR of piece A from fig.43

4.14B

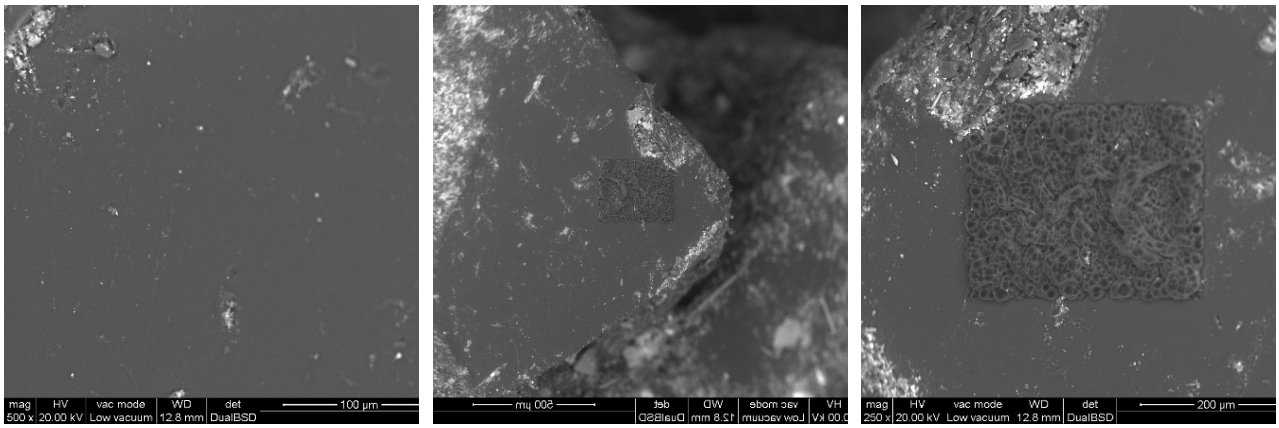

Figure 47: ESEM of piece B from fig.43

Sample B shows a compact structure with low loading. Although EDX analysis is generally considered safe for the sample and not destructive, in this case it is possible to see how the analysis damaged the surface of the sample.

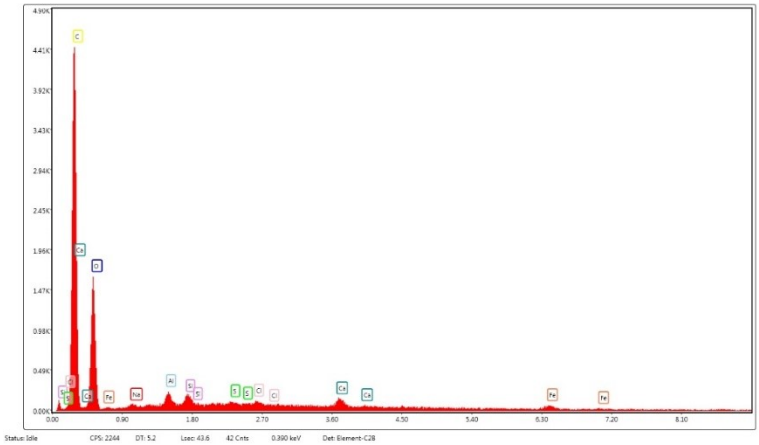

The EDX analysis, on the well visible area reported above, shows the presence of C and O, as well as other element present on the surface as contaminants and loading particles.

Figure 48: EDX of piece B from fig.43

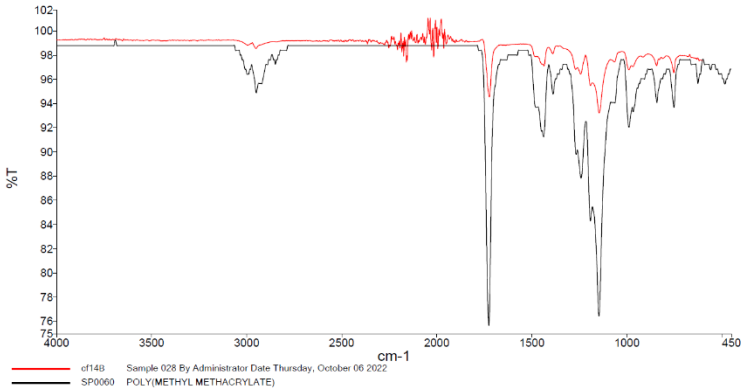

IR analysis suggests the polymer could be polymethylmethacrylate (92% correspondence) in agreement with the elemental EDX analysis.

Figure 49: FTIR of piece B from fig.43

4.14C

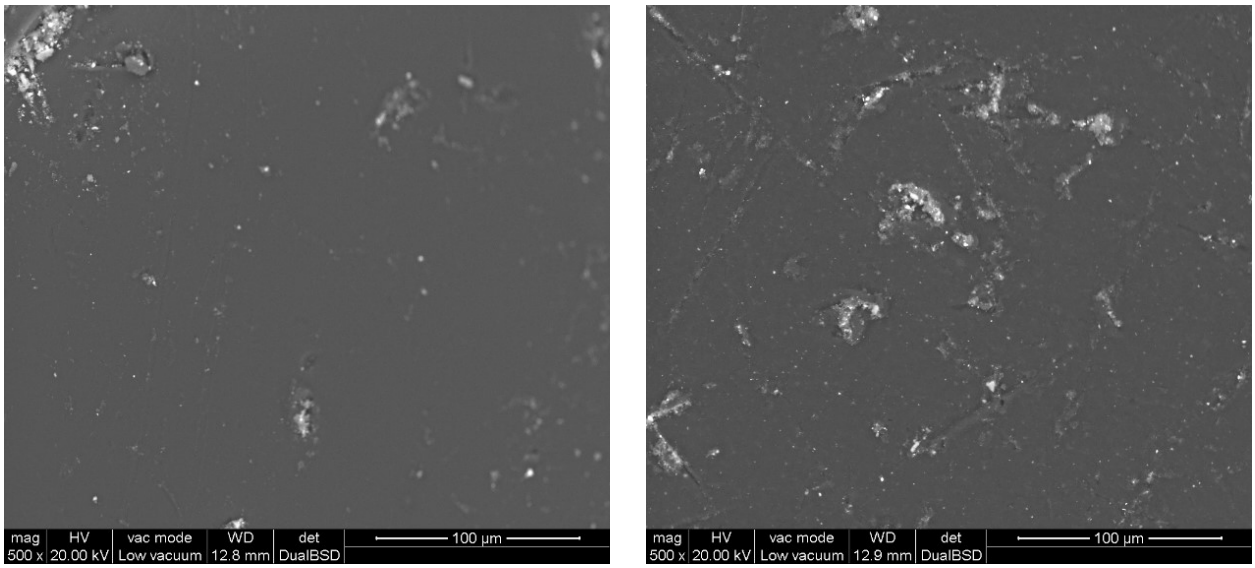

Figure 50: ESEM of piece C from fig.43

ESEM analysis of sample C is similar to sample B, showing a low level of charge and some contaminants on the surface.

EDX analysis shows how the polymer is almost made of C.

Figure 51: EDX of piece C from fig.43

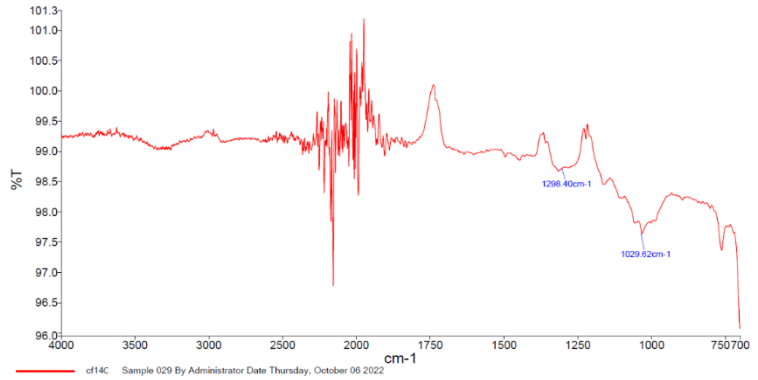

IR analysis was not able to determine the nature of the polymer. The noise in the band around 2000 cm^{-1} is due to the instrument.

Figure 52: FTIR of piece C from fig.43

4.14D

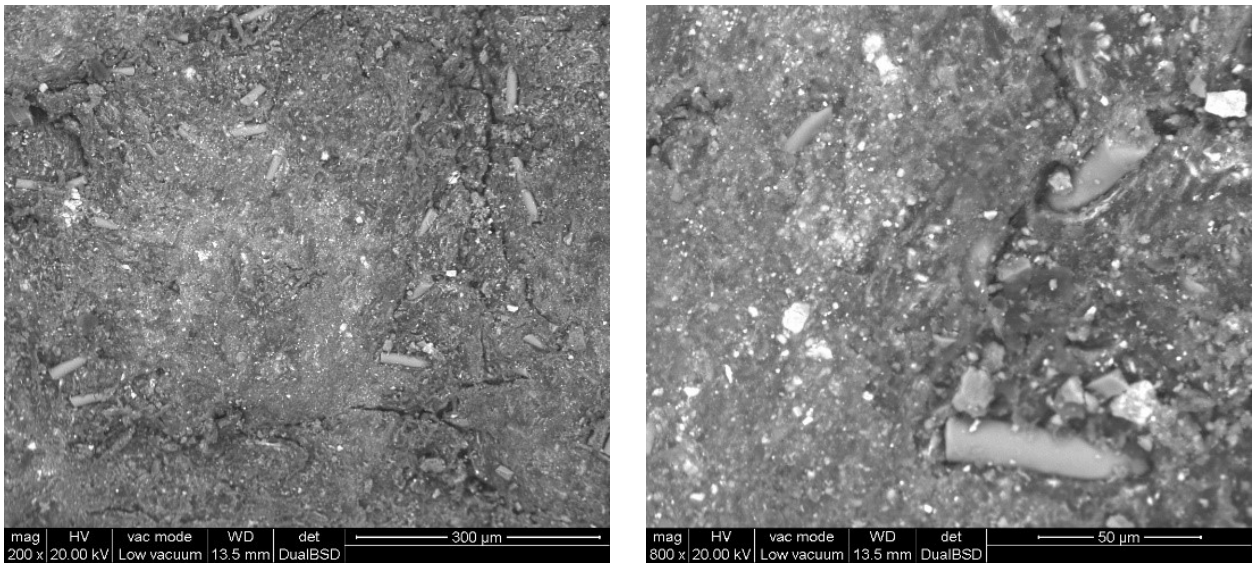

Figure 53: ESEM of piece D from fig.43

ESEM analysis shows a rich and complex matrix full of different charging particles and filaments.

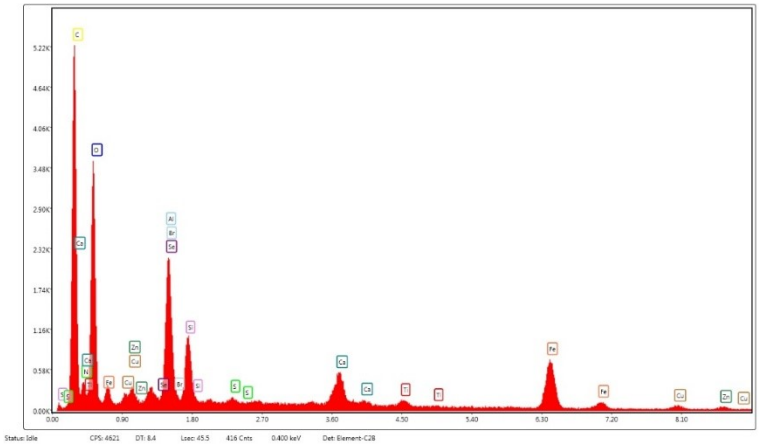

EDX analysis confirms a complex structure full of different elements. The polymer matrix may probably made of C, O and N.

Figure 54: EDX of piece D from fig.43

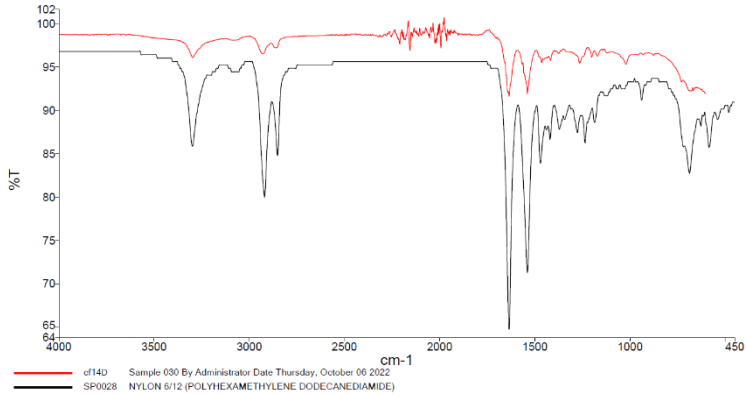

IR analysis is able to determine with a 93% correspondence the nature of the polymer, which is nylon.

Figure 55: FTIR of piece D from fig.43

4.14E

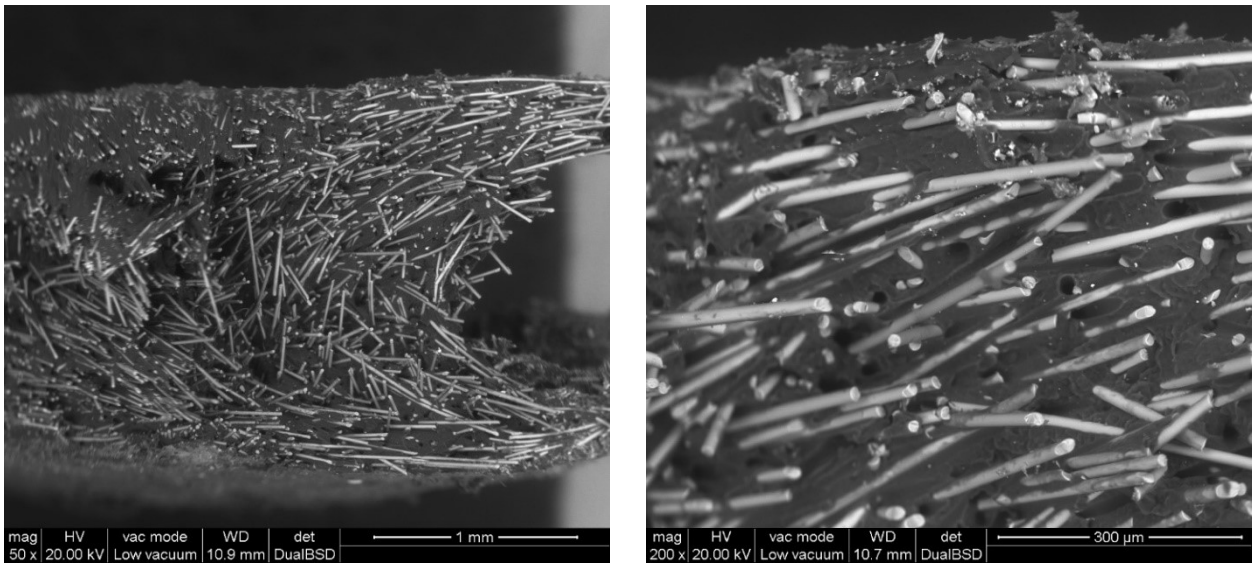

Figure 56: ESEM of piece E from fig.43

This sample is made of a polymer heavily charged with glass fibers.

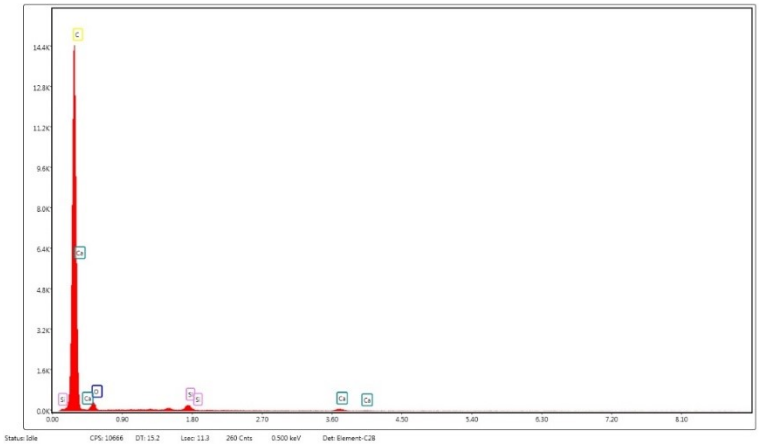

The EDX analysis on the matrix highlights the presence of only C.

Figure 57: EDX of piece E from fig.43

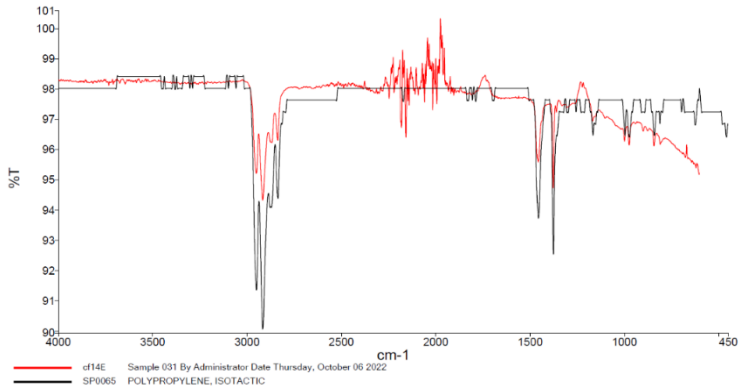

IR analysis suggests, with a good correspondence (82%), that the polymer could be polypropylene, in agreement with the EDX elemental analysis.

Figure 58: FTIR of piece E from fig.43

4.15 Analysis of batch CF15

Batch 15 is made of small particle with diameter lower than 2 mm.

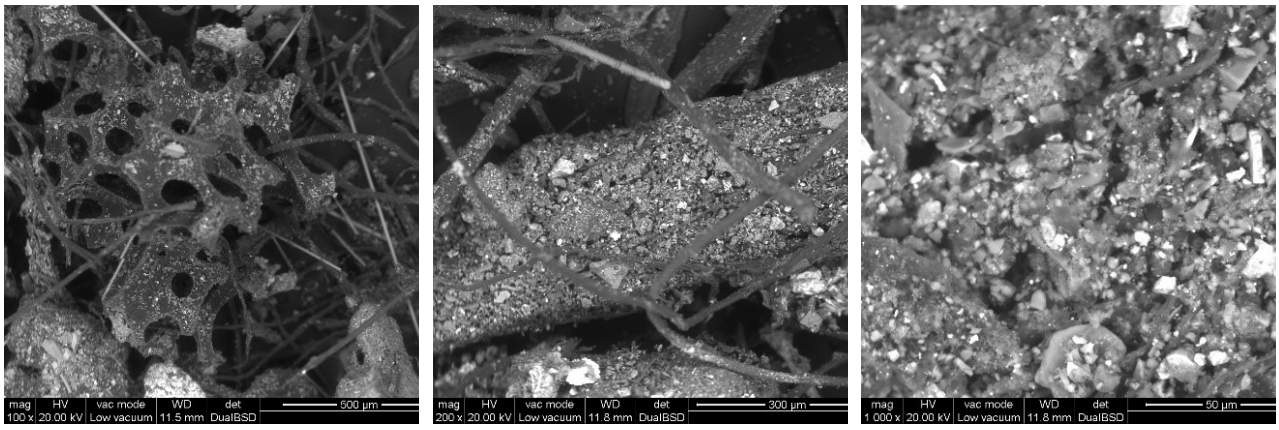

Figure 59: ESEM of a sample from batch CF15

ESEM shows that, as predictable, small size particle are essential fragments of larger pieces. Polymers, glass fibers and minerals are identifiable. EDX analysis on a large area shows a large variety of elements, confirming the inhomogeneity of the sample, identifying C, O, N, P, Cl, Si, Ca, Ti, Zn, Fe, K, Al and Mg.

5. ENERGY RECOVERY

As introduced in chapter 1, energy recovery is the last option for materials where recycling is unfeasible. In order to assess the thermal properties of the car fluff sample in our possession a sample has been reconstituted according to the composition found in chapter 3.

5.1 Gross calorific value

The gross calorific value has been assessed using a calorimeter and following ISO 1928:2020. A sample has been reconstituted from different batches following the ratio found in chapter 4. The sample has been hashed in small pieces using an appropriate multiblade hasher obtaining particular with diameter lower than 212 μm as requested by the norm. The combustion has been performed using a calibrated calorimeter in a certified laboratory. Three combustions have been performed obtaining the following result:

- 18742 kJ/kg
- 17969 kJ/kg
- 18186 kJ/kg

The average value is 18299 ± 368.377 kJ/kg (95% confidence).

Equipment to measure the fumes of a combustion was not available but we expect the production of NO_x, HCl, polycyclic aromatic, heterocyclic compounds, polychlorinated dibenzodioxins and dibenzofurans and other compounds containing chlorine due to the presence of PVC.

The hashes of a sample of 6.8362 g burned in muffle at 800°C for 2 hours have been analyzed using ESEM. The final mass of hashes was of 1.6446 g, the 24% of the initial mass.

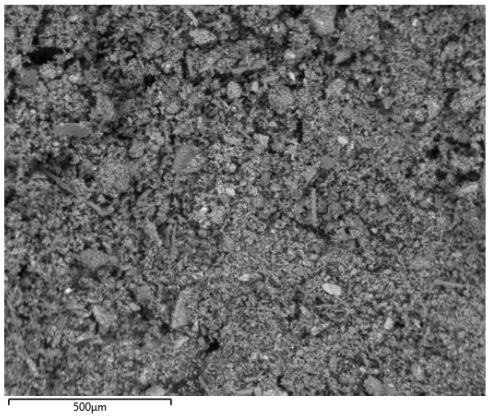

Figure 60: ESEM of combustion ashes

Spectrum	% O	% Fe	% Ca	% Si	% C	% Mg	% Zn	% Al	% Cu	% Cl	% Na	% Ba	% Ti
Area	34.9	14.9	12.1	9.8	7.3	4.7	4.1	3.0	2.9	1.5	1.4	0.9	0.9

From this elemental analysis we conclude that all the hashes are made of oxides, mainly iron oxide, calcium oxide, silica and carbonates. No hazardous material is present.

Concerning the energy recovery we analyzed the possibility of using combustion in supercritical water as an alternative to incineration.

5.2 Supercritical water

The critical point of water is at $P = 217.8\ atm, T = 373.946\ °C$ where at those condition density is $\rho = 322 \pm 3\ kg/m^3$. Initially water above those conditions was considered to be just steam at very high pressure useful for electricity generation. However starting from 70s the unique properties of supercritical water (SCW) are investigated, finding that at those conditions nonpolar fluids are completely miscible with SCW, dissolved ions have very high mobility and water conductivity increases. While initially SCW was just considered to be a reaction medium useful for the destruction of dangerous materials through supercritical water oxidation (in presence of O_2), in recent years the possibility of using SCW as a reagent for hydration and dehydration reactions have been investigated [37]. These two approaches may be an alternative solution for the car fluff problem. Some consideration based on the literature have been here reported.

5.3 Supercritical water oxidation

Water is by far the most used solvent by industries. It's cheap, harmless, available almost everywhere and abundant. Following green chemistry principles it is also considered to be the best option wherever a solvent has to be used. Many industries chose water for this reasons, resulting in a huge production have wastewater to be treated containing, depending on the processes where it is used, harmful materials of organic and inorganic nature. Wastewater treatment, in brief, consists in a series of chemical-physical processes where the concentration of contaminants is gradually increased resulting ultimately in a sludge containing about 80% of water. If this sludge contains dangerous materials, it has to be treated as a hazardous waste and has to be landfilled. To reduce the volume and the cost of the disposal of this material the sewage sludges are dried using turbo dryers and methane reaching about 10% of final water concentration. The powder finally obtained usually contains carbon derived products and some metals with a high calorific value, however for environmental problems they cannot be incinerated.

Supercritical water oxidation aims to completely bypass the problems above discussed. The idea is that, while water cannot be incinerated, the organic species dissolved can. Reaching supercritical conditions allows for a serious of gasification reaction and ultimately in-water combustion if oxygen is present. In a work from 2020 Wang et al. [38] proposed a serious of reaction pathways for different species such as hydrocarbons, N-containing compounds and Cl-containing compounds.

The mechanism proposed is a radical mechanism which can be summarized as follows

Initiation		
1	Hydrogen Abstraction	$RH+O_2 \rightarrow R\bullet+HO_2\bullet$
Propagation		
2	Oxygen Addition	$R\bullet+O_2 \rightarrow RO_2\bullet$
3	H-abstraction	$RO_2\bullet+RH \rightarrow ROOH$
4	Isomerization	$RO_2\bullet \rightarrow HOOR\bullet$
5	β-Scission	$R\bullet \rightarrow R\bullet+C{=}RH$
Chain Transfer		
6	Disproportionation	$2RO_2\bullet \rightarrow O_2 + 2RO\bullet$
Branching		
7	Decomposition	$ROOH \rightarrow RO\bullet + HO\bullet$
Termination		
8	Radical Recombination	$RO_2\bullet+RO_2\bullet \rightarrow Products$

Figure 61: SCW oxidation suggested mechanism [38]

The overall reaction considering the 3 types of species previously mentioned lead to the production of $CO_2 + CO + NO_X + HCl + NH_3$. Hydrochloric acid represents a problem for the material but can be efficiently removed from the final fume gases using the already present technologies. Nitrogen oxides can be reduced as well using already know technologies, while ammonia represents a dangerous product since it can further react producing HCN and carbamate that are dangerous products for the environment and for the materials of the plant.

While supercritical water oxidation (SWO) of sewage sludges has been investigated by different authors, SWO of solids is less researched manly because dry materials can be easily incinerated directly. This leads however for some materials to the production of dioxins and dioxin-like compounds that must be reduced before the emissions of fumes in atmosphere, resulting in higher cost. SWO is claimed to be greener since production of this dangerous materials is minimized due to different conditions from incineration.

Incineration is conducted at atmospheric pressure at 850°C for at least 2 seconds for waste while for hazardous waste containing chlorine temperature is increased to 1100°C for at least 2 seconds [39]. The process is sustained by itself using due to the calorific value of the waste and additional natural gas burners are used only if it is necessary to increase the temperature in the furnace. Heat is recovered to produce steam and electricity. *Overall the process produces more energy (as electricity and heat) than required by the plant, resulting in a net energy production.*

SWO differently is conducted at pressure higher than 220 atm and temperature in the range 400-600°C. Compression of gases is an extremely expensive operation so in order to reach a process which is able to auto-sustain by itself it is necessary to operate an effective energy integration. Cocero et al. [40] in 2001 proposed an energy integration for a possible SWO process:

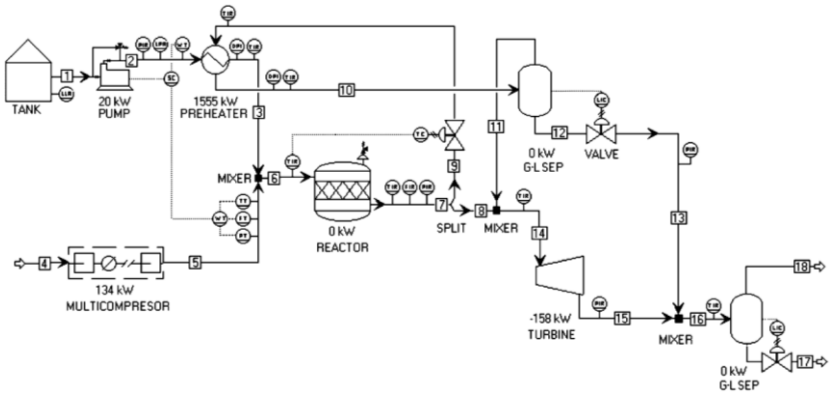

Figure 62: SCW oxidation plant. Cocero et al. [40]

Using ASPEN PLUS simulation software they found that a minimum heating value of 930 kJ/kg in the feed stream is enough to reach self-sufficient operation.

In 2017 Zhang et al. [41] proposed a power generation system using coal in surface water gasification coupled with CO_2 capture. The process proposed consists in a gasifier operating at 650°C and 250 bar in SCW and absence of oxygen producing syngas burned in a successive step using pure O_2 in SCW. Aspen Plus 11.1 was used to simulate the process using Soave Redlich-Kwong EOS with modified Huron-Vidal mixing rule. Pure

oxygen is used for allowing the separation of CO_2 avoiding the presence of N_2. The model proposed achieves an overall thermal efficiency of 38% with complete CO_2 capture. A critic we would make about this model is that pure oxygen is not available for free and air distillation is an energy expensive process which will likely reduce if not make negative the overall efficiency of the process if O_2 production is considered.

Based on the gross calorific value of the car fluff in our possession (18'000 kJ/kg) a scheme of a possible gasification-combustion in SCW is reported. A mixture of car fluff, water and stoichiometric air has gross calorific value higher than the minimum value suggested by Cocero et al. if car fluff represent more than 1/18 of the mixture in ponderal fraction, value which appear to be conservative. Car fluff calorific value is moreover lonely slightly different than coal, for which calorific value is assumed to be in the range 16'000 – 30'000 kJ/kg based on the humidity and on the type of coal (lower for lignite, higher for anthracite), so we assume that if a self-sustainable process is developable for coal, it should also be for car fluff. Energy integration has been skipped in this base case BFD. Critical part to model is the gasifier, operating at high temperature high pressure (about 250 atm 600°C base on literature) for which a model based on experimental values has to be developed.

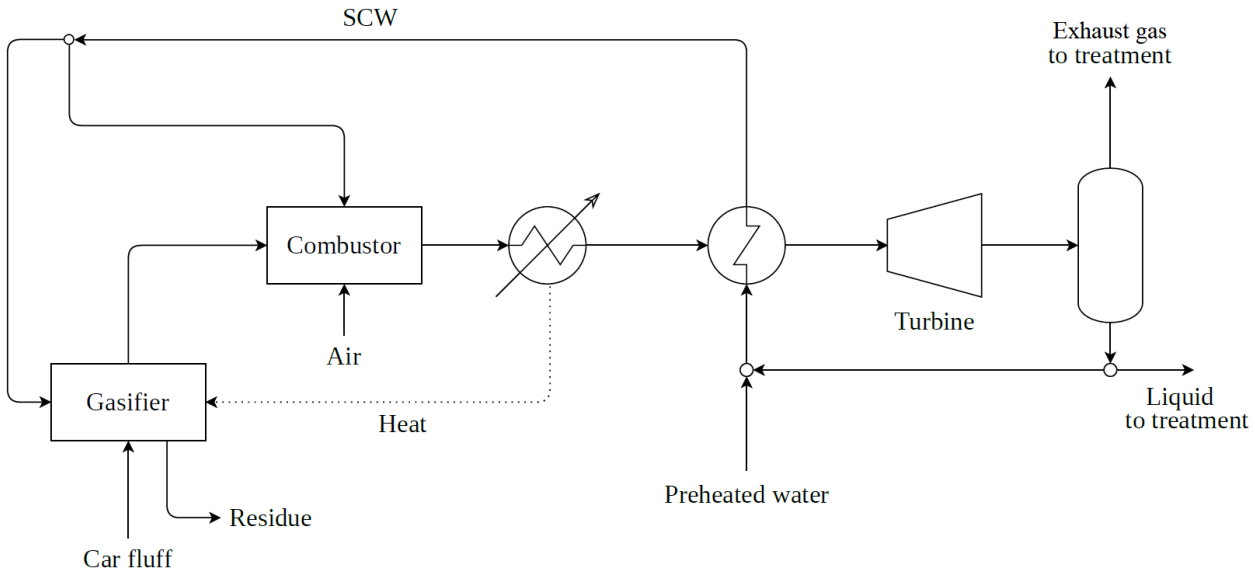

Figure 63: BFD of a Gasification-Combustion in SCW plant

6 PYROLYSIS

Pyrolysis is a thermal unit operation conducted in absence of oxygen, or any other comburent, at temperature between 350 and 900°C. Pyrolysis of carbon derivatives always leads to the formation of three products: gas, oil and solid. The gas produced are hydrocarbons with low molecular weight, hydrogen and in general other products from the polymer chain rupture. Oils produced have higher molecular weight and therefore higher boiling temperature, while the solid produced is a carbon in one of is allotropic form (graphite or amorphous) englobing other heteroatoms. Modulating temperature, heating rate, residence time, pressure and use of catalyst it is possible to obtain different products in different ratios. One of the major downside of pyrolysis is that it always gives a wide range of products for which a separation process would be necessary in order to use pyrolysis products as chemical feedstock.

Concerning the pyrolysis of polyurethane, different decomposition reactions have been proposed [42]:

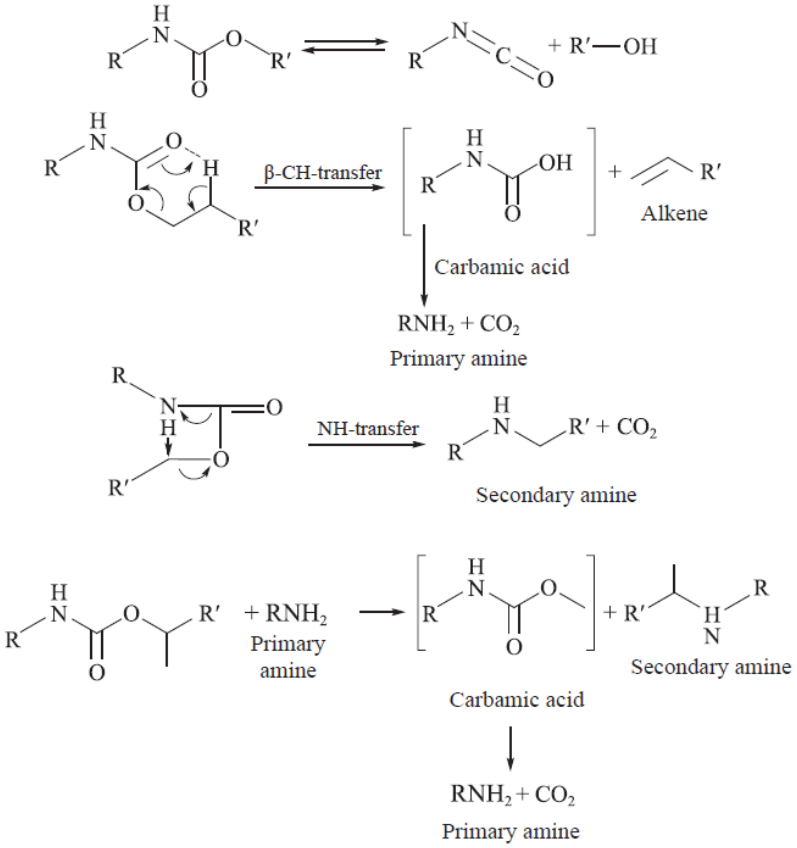

Decomposition leads to formation of starting reagents and other products such as primary and secondary amines, carbon dioxide and alkenes.

Another possible thermal reaction occurring is the breaking of the diphenyl methane structure following the reaction [42]:

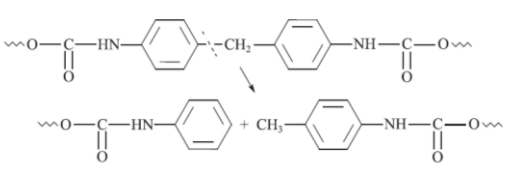

Concerning polyols thermal degradation, it leads to break of the long backbone as suggested by Allan et al. [43] producing low molecular weight molecules:

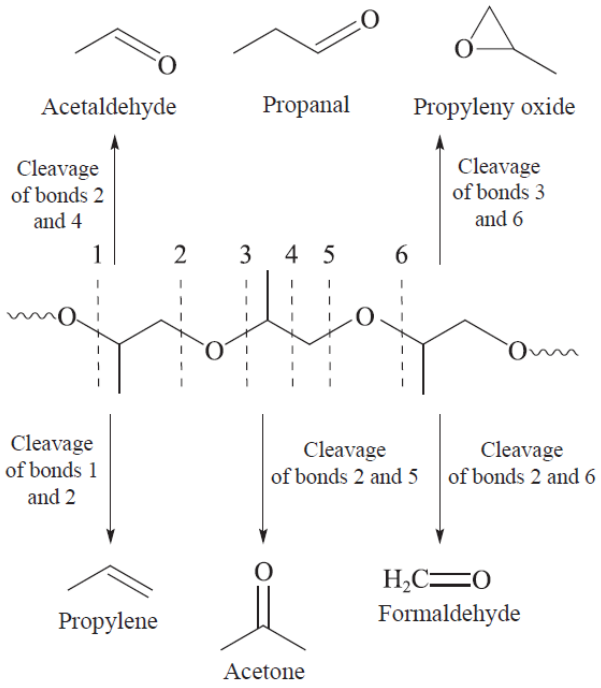

As introduced in chapter 2 we made a series of experiment to investigate the pyrolysis of PU. This topic is not strictly correlated to car fluff and four first experiments were done on a clean polyurethane produced using 4,4′-Methylene diphenyl isocyanate and a mixture of two different polyols, namely a trifunctional polyether and a bifunctional polyester.

6.1 Polyurethane pyrolysis at 400°C for 2h

1.9050 g of clean polyurethane of known composition has been pyrolyzed at 400°C for 2 hours. The pyrolizer reported in Figure 9 has been used. The heating ramp was of 33°C/min. After 10 minutes at 350°C white/gray fumes have been observed exiting from the chimney. White fumes flowrate reached a maximum 4 minutes later at 400°C and ended 16 minutes later. After 2 hours at 400°C heating has been stopped and the pyrolizer has been left cooling. Nitrogen flow in the heating chamber has been stopped once room temperature has been reached. The paper filters recovered showed yellow spots. The pyrolyzed residue was scraped from the crucible and weighted: 0.2583 g are recovered (13.56% of initial weight).

The black solid residue was analyzed through ESEM, EDX and FTIR.

The chimney has been washed using acetone to recover gas/liquid residue condensed; the acetone solution was dried in fume hood and the residue has been analyzed through IR, NMR, and mass spectrometry. The paper filters have been washed using acetone, the liquid was evaporated in fume hood and the residue has been analyzed through IR.

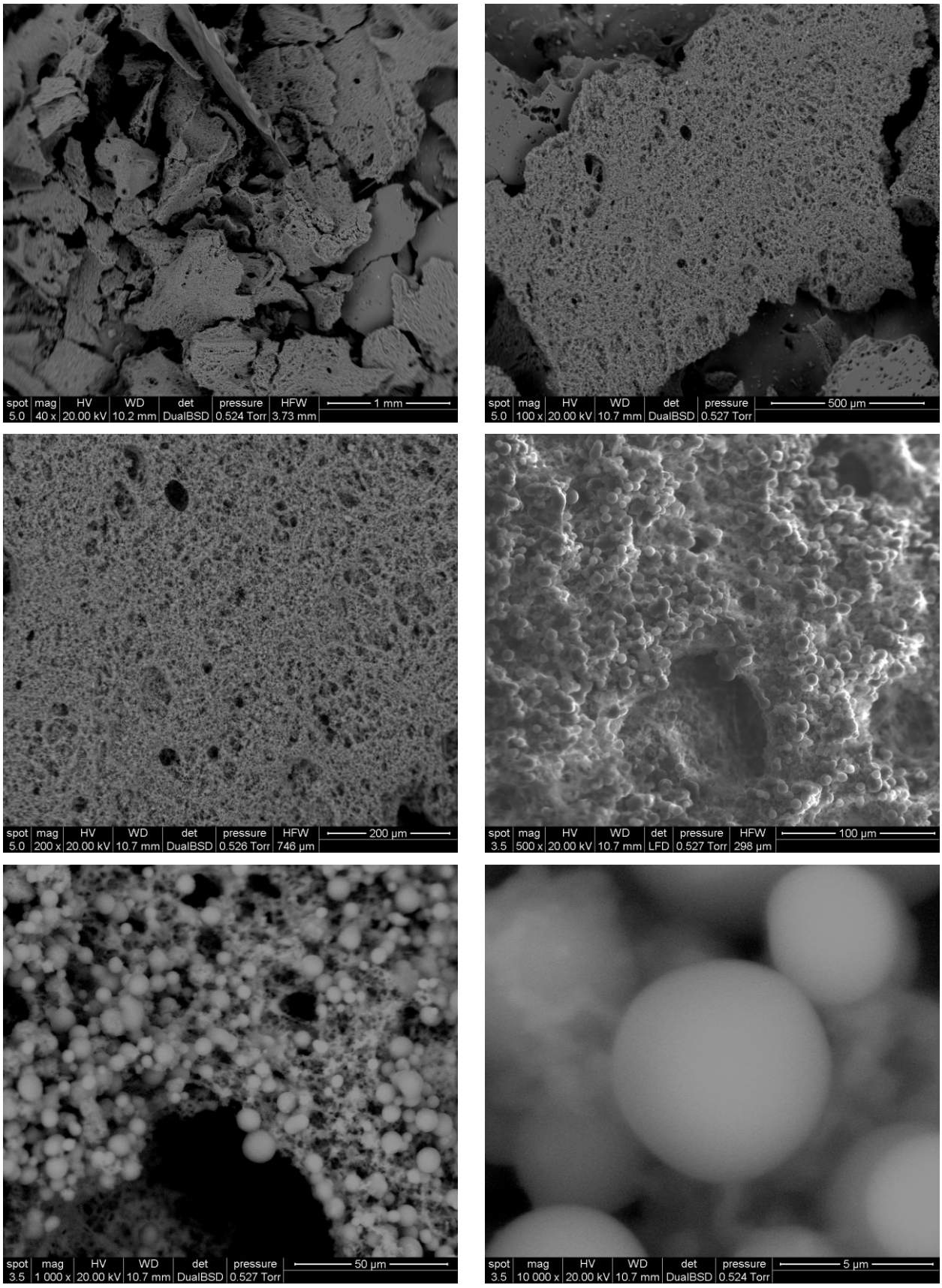

Figure 64: ESEM of solid residue from pyrolysis at 400°C

ESEM photos of the solid black residue obtained outlines the presence of a backbone structure directly derived from the original PU and the formation of spheres with a diameter approximately of 5 µm correlated to a highly porous structure.

EDX

Spectrum	% C	% N	% O	% Si	%Al
Area 3rd image	86.9	9.1	3.6	0.3	0.2
Point sphere 6th image	86.6	8.1	5.3	-	-

Compared to original PU, for which EDX analysis showed a concentration of N of 3.5-4.1%, the pyrolyzed PU contain un higher concentration of N, reasonably in aromatic rings.

For the liquid recovered from the chimney:

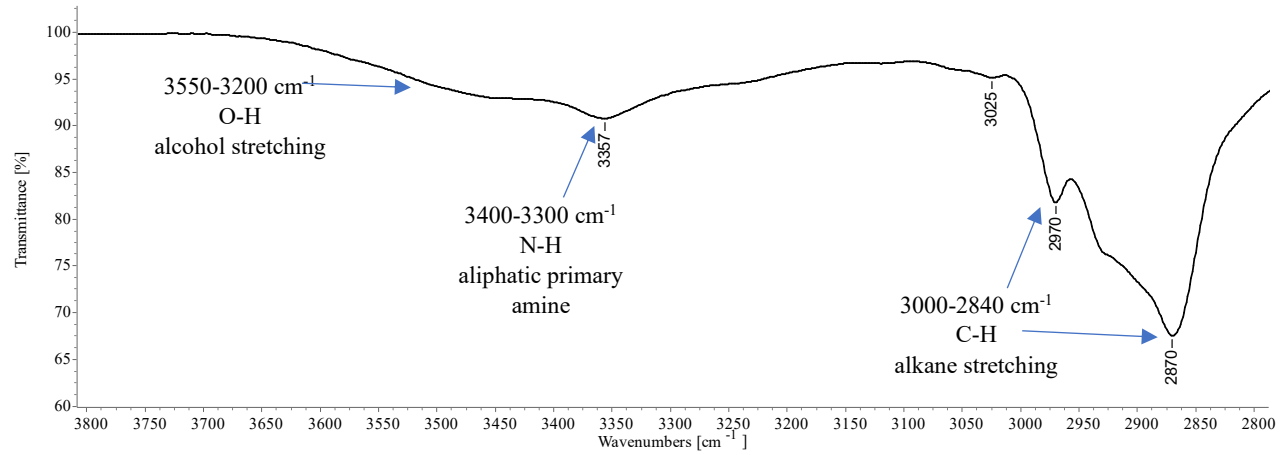

Figure 65: FTIR of liquid condensed in the chimney. Range 3800-2800 cm^{-1}. Pyrolysis at 400°C

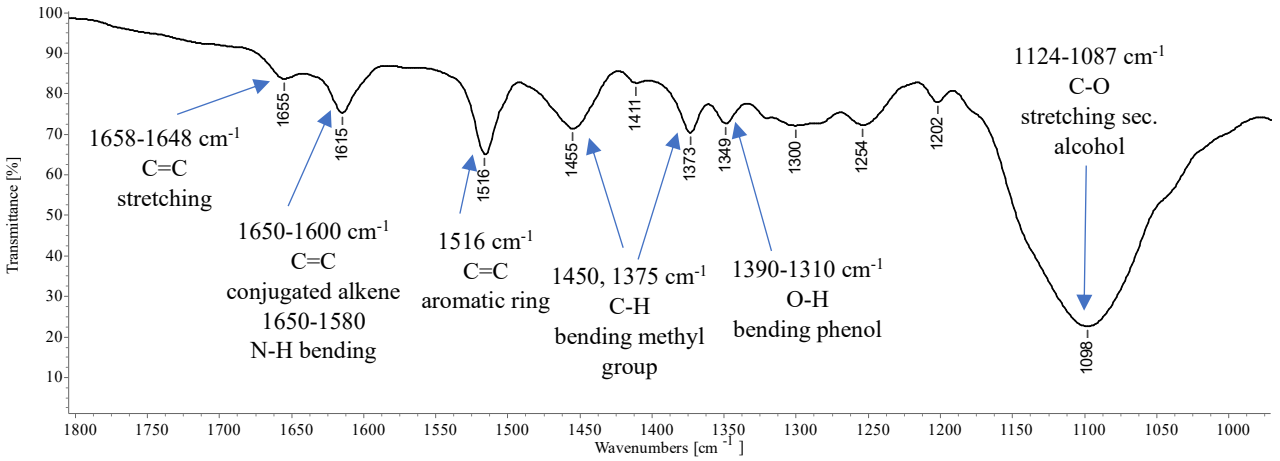

Figure 66: FTIR of liquid condensed in the chimney. Range 1800-1000 cm^{-1}. Pyrolysis at 400°C

FTIR analysis highlights the presence of some functional group. Using NMR, GC and HPLC a suggestion of some of the possible molecules will be presented at the end of the chapter.

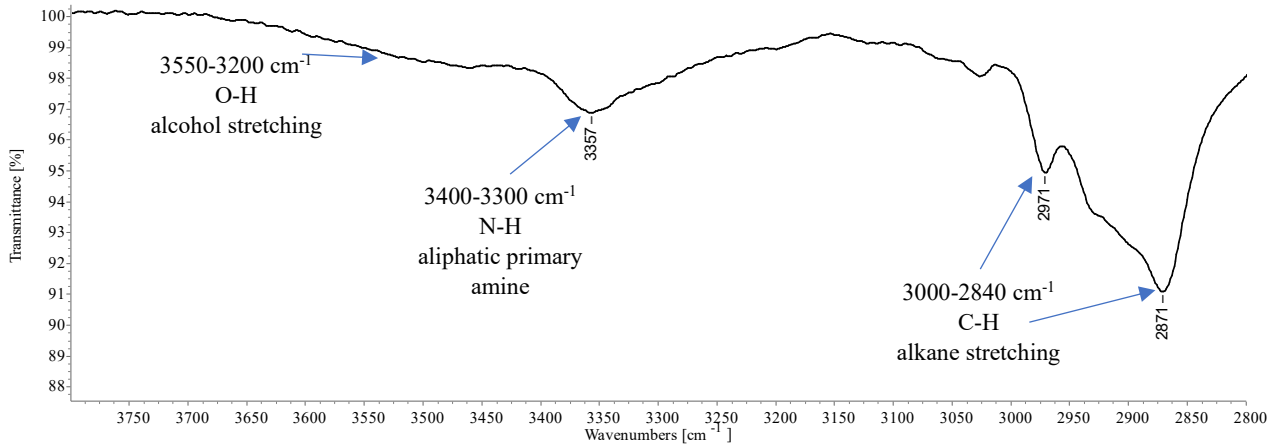

Figure 67: FTIR of liquid recovered from filter. Range 3800-2800 cm-1. Pyrolysis at 400°C

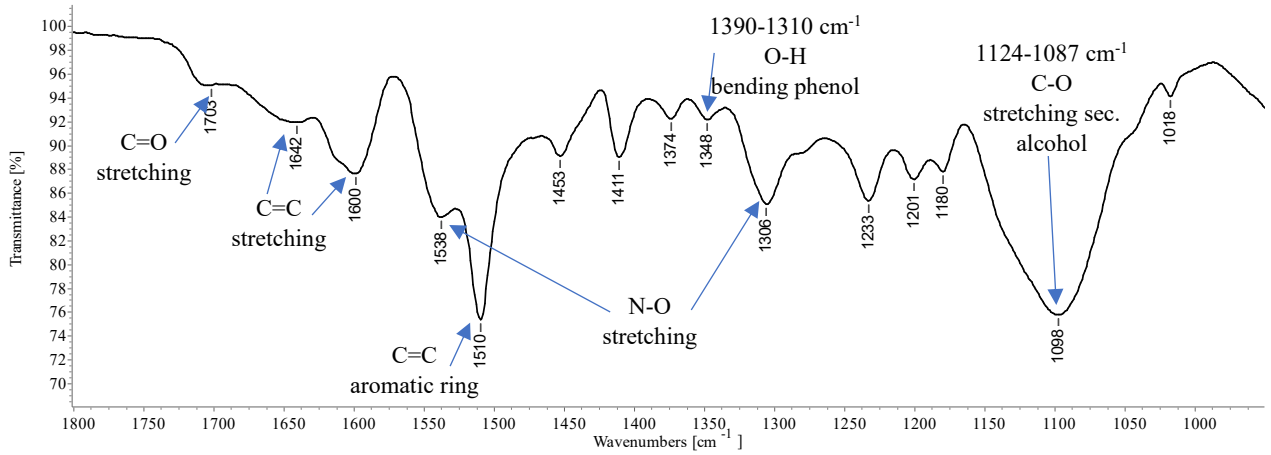

Figure 68: FTIR of liquid recovered from filter. Range 1800-1000 cm-1. Pyrolysis at 400°C

FTIR analysis highlights a higher presence of aromatic groups respect to the liquid condensed in the chimney. This is in agreement with the hypothesis for which polyol have higher molecular weight and lower volatility respect to aromatic diisocyanates.

6.2 Polyurethane pyrolysis at 600°C for 2h

1.9768 g of clean polyurethane of known composition has been pyrolyzed at 600°C for 2 hours. The pyrolizer reported in Figure 9 has been used. The heating ramp was of 33°C/min. After 10 minutes at 350°C white/gray fumes have been observed exiting from the chimney. White fumes flowrate was overall less significant respect to previous experiment at 400°C. After 2 hours at 600°C heating has been stopped and the pyrolizer has been left cooling. Nitrogen flow in the heating chamber has been stopped once room temperature has been reached. The paper filters was almost clean as result of less fumes. The pyrolyzed residue was scraped from the crucible and weighted: 0.2332 g are recovered (11.80% of initial weight). The black solid residue is analyzed through ESEM, EDX and RAMAN. The chimney has been washed using acetone to recover liquid residue condensed, the liquid was evaporated in fume hood and the residue has been analyzed through IR, NMR, GC.

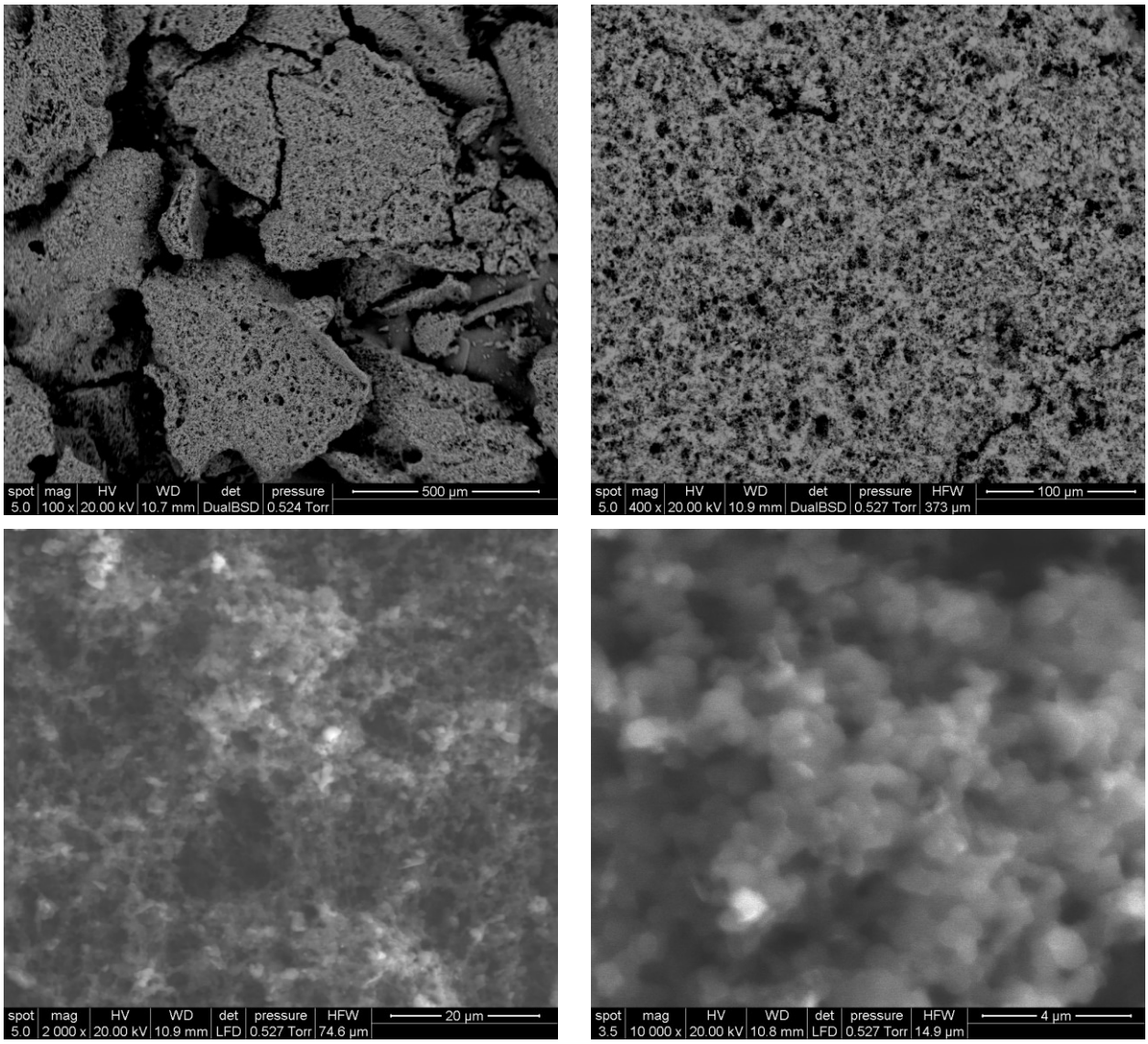

Figure 69: ESEM of solid residue from pyrolysis at 600°C

ESEM photos of the solid residue outline again the presence of a backbone structure which could also in this case be directly derived from the original PU. There's still the presence of spherical particles but in this case they have a significant lower dimension, about 0.5 µm, compared to those from experiment at 400°C.

Spectrum	% C	% N	% O
Area 2nd	89.9	6.9	3.2

Compared to original PU, for which EDX analysis showed a concentration of N of 3.5-4.1%, the pyrolyzed PU contain un higher concentration of N. The concentration of nitrogen is lower compared to experiment at 400°C for which nitrogen concentration was 8.1-9.1%.

To achieve deeper information concerning the carbonization degree and the microstructure of the ACs, a detailed analysis of the Raman spectra has been carried out.

It shows the two principal absorptions at 1591 cm^{-1} (G-Band) and at 1354 cm^{-1} (D-band) indicating that an activated carbon has been achieved.

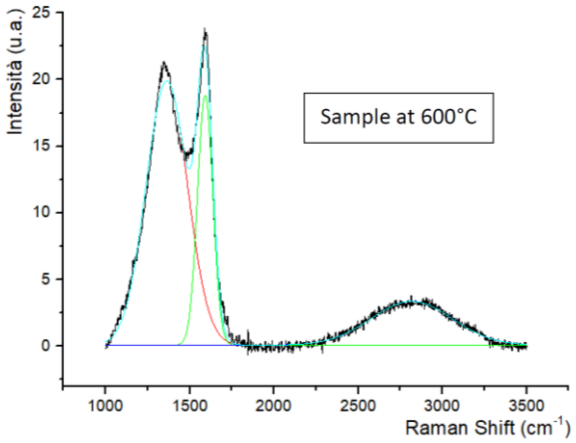

Figure 70: RAMAN of solid residue of pyrolysis performed at 600°C

The Raman spectra show signals in two distinct regions: (a) the defect-derived peak centered at about 1350 cm^{-1} related to a disordered (amorphous) carbon structure (the D-band, related to the K-point phonons of A1g symmetry, indicating the disorder in the breathing mode of the 6-fold aromatic ring near the basal edge) and the graphite structure-derived (G-band, related to the zone center phonons of E2g symmetry) peak centered at about 1570 cm^{-1} indicative of a hexagonal carbon structure; and (b) a broad absorption centered at about 2800 cm^{-1}, the 2D or G' band, related to the interactions between the stacked graphitic layers.

For the liquid recovered from the chimney:

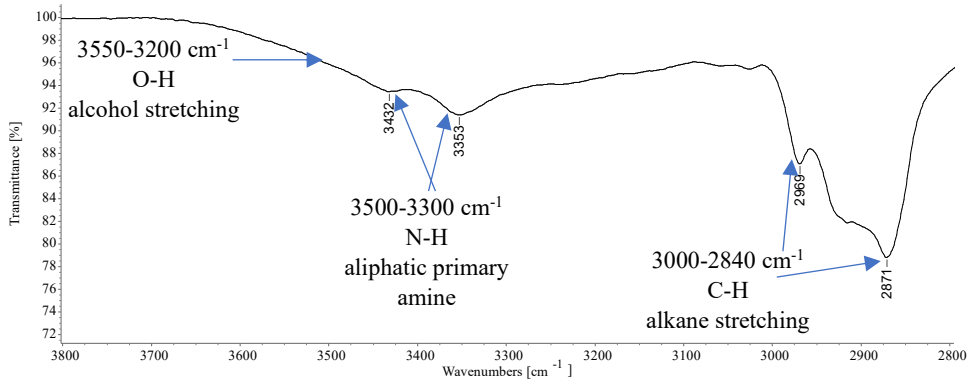

Figure 71: FTIR of liquid condensed in the chimney. Range 3800-2800 cm^{-1}. Pyrolysis at 600°C

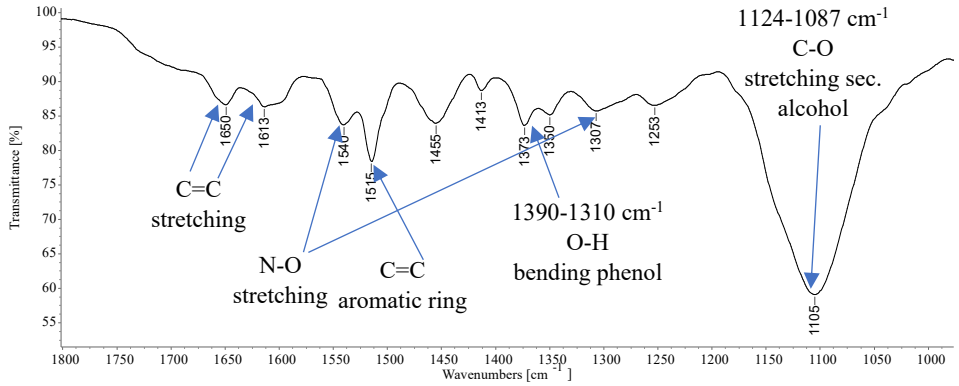

Figure 72: FTIR of liquid condensed in the chimney. Range 1800-1000 cm^{-1}. Pyrolysis at 600°C

Functional group identified are the same of pyrolysis at 400°C

6.3 Polyurethane pyrolysis at 580°C for 2h

2.2734 g of clean polyurethane of known composition has been pyrolyzed at 580°C for 2 hours. The pyrolizer set point was set at 800°C but due to insufficient thermal power the temperature reached was of 580°C. Since the value of the temperature is almost equal to 600°C, this experiment is used to test the repeatability of the process. The pyrolizer reported in Figure 9 has been used. The heating rate was initially of 50°C min, at 420°C slowed down to 33°C/min and at 520°C slowed down to 20°C. At 420°C white/gray fumes have been observed exiting from the chimney, they increased at 520°C and finished about 20 minutes after the start. After 2 hours at 580°C heating has been stopped and the pyrolizer has been left cooling. Nitrogen flow in the heating chamber has been stopped once room temperature has been reached. The paper filters was almost clean as result of lower amount of fumes. The pyrolyzed residue was scraped from the crucible and weighted: 0.2614 g have been recovered (11.50% of initial weight).

The black solid residue was analyzed through ESEM, EDX, IR.

The chimney has been washed using acetone to recover liquid residue condensed, the liquid was evaporates in fume hood and the residue has been analyzed through IR, NMR, and mass spectrometry.

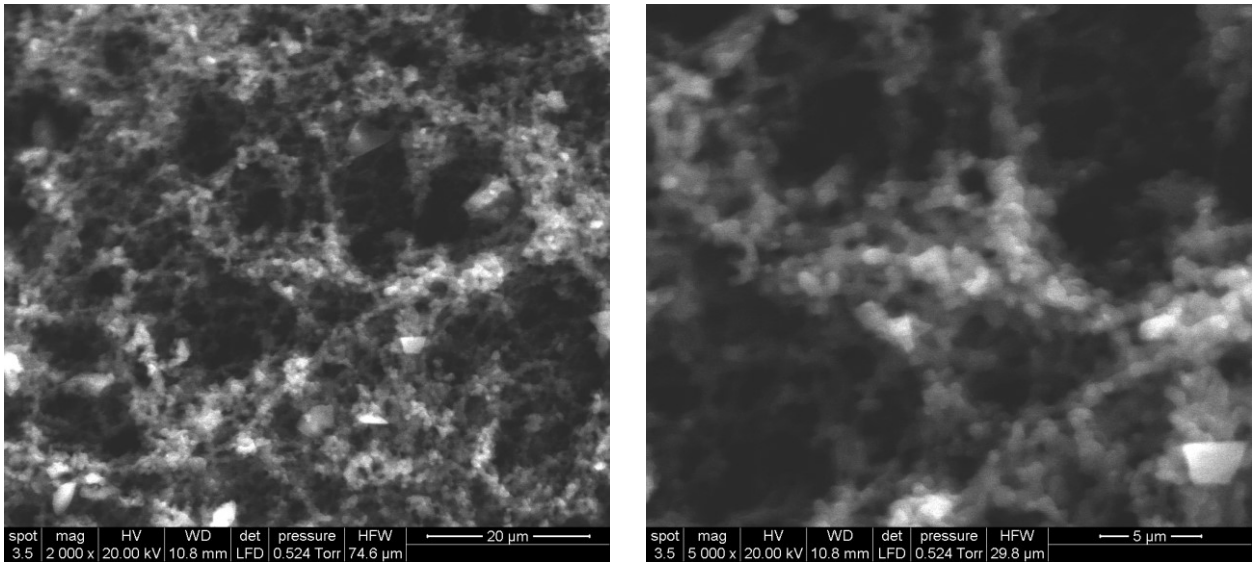

Figure 73: ESEM of solid residue from pyrolysis at 580°C

ESEM photos of the solid residue outline still the presence of a backbone structure which could also in this case be directly derived from the original PU and the presence of spheres of approximately 0.5 µm of diameter. No differences have been noticed respect to the previous experiment performed at 600°C.

EDX

Spectrum	% C	% N	% O
Area 2nd	89.5	7.5	3.1

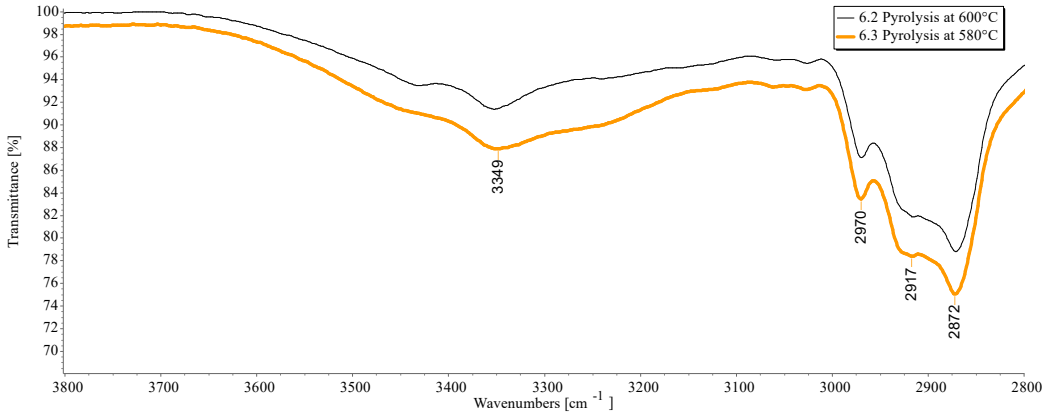

Figure 74: Liquid condensed in the chimney at 580°C (orange thick line) and 600°C. FTIR in range 3800-2800 cm^{-1}

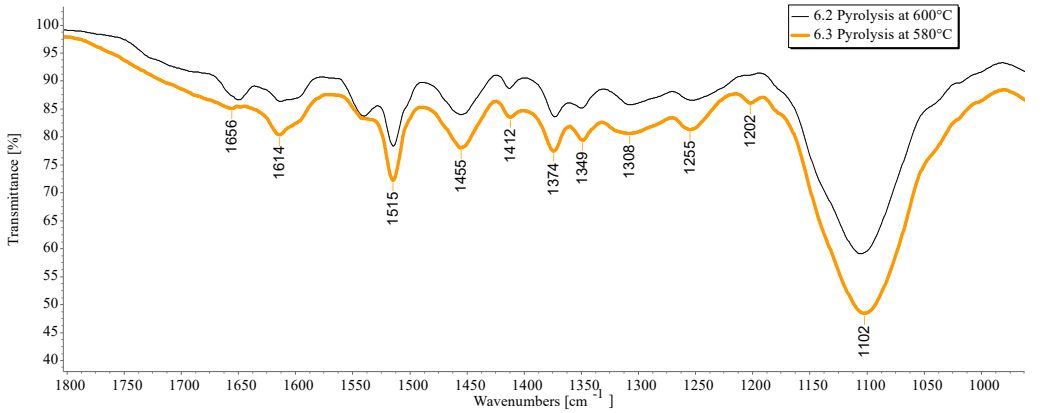

Figure 75: Liquid condensed in the chimney at 580°C (orange thick line) and 600°C. FTIR in range 1800-1000 cm^{-1}

The IR spectra of recovered fumes from the chimney at 580°C (thick line) present the same IR peaks of the experiment at 600°C (thin line).

6.4 Polyurethane pyrolysis at 400°C for 2h with configuration B of pyrolizer

2.2622 g of clean polyurethane of known composition has been pyrolyzed at 400°C for 2 hours. The pyrolizer reported in Figure 9 has been used. The heating ramp was of 42°C/min. After 9 minutes at 400°C white/gray fumes have been observed exiting from the chimney. White fumes flowrate reached a maximum 4 minutes later still at 400°C and ended 16 minutes later. After 2 hours at 400°C heating has been stopped and the pyrolizer has been left cooling. Nitrogen flow in the heating chamber has been stopped once room temperature has been reached. The Schlenk flask presented a small amount of yellowish liquid condensed. The pyrolyzed residue was scraped from the crucible and weighted: 0.3157 g were recovered (13.96% of initial weight).

The black solid residue is analyzed through ESEM, EDX, IR.

The chimney has been washed using acetone to recover liquid residue condensed, the liquid was evaporated in fume hood and the residue has been analyzed through IR, NMR, and mass spectrometry. The Schlenk flask have been washed using deuterated acetone and analyzed through IR and NMR.

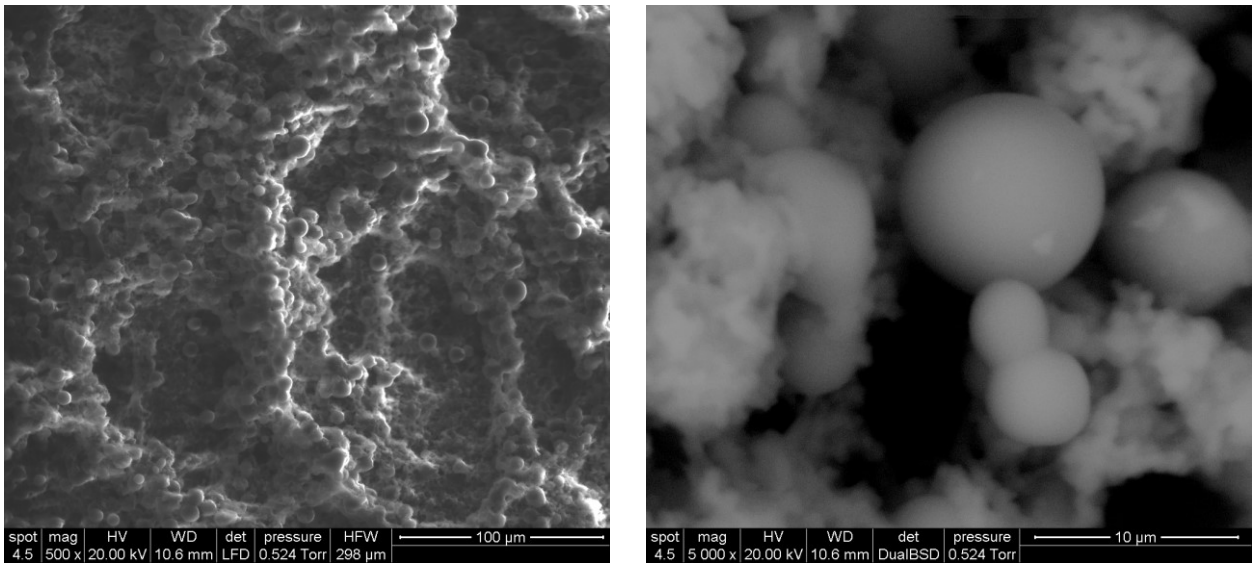

Figure 76: ESEM of solid residue from pyrolysis at 400°C

ESEM photos of the solid residue outline the presence of a backbone structure directly derived from the original PU and the formation of spheres with a diameter approximately of 5 µm correlated to a highly porous structure. No differences have been noted respect to the previous experiment at 400°C.

Spectrum	% C	% N	% O
Area 2nd image	86.9	10.5	2.6
Point sphere 6th image	87.5	7.8	4.7

Compared to original PU, for which EDX analysis showed a concentration of N of 3.5-4.1%, the pyrolyzed PU contain un higher concentration of N. The value are compatible with the previous experiment at 400°C.

As for or the liquid recovered from the chimney the IR spectra of recovered fumes from the chimney at 580°C (thick line) presents the same IR peaks observed in the experiment at 600°C (thin line).

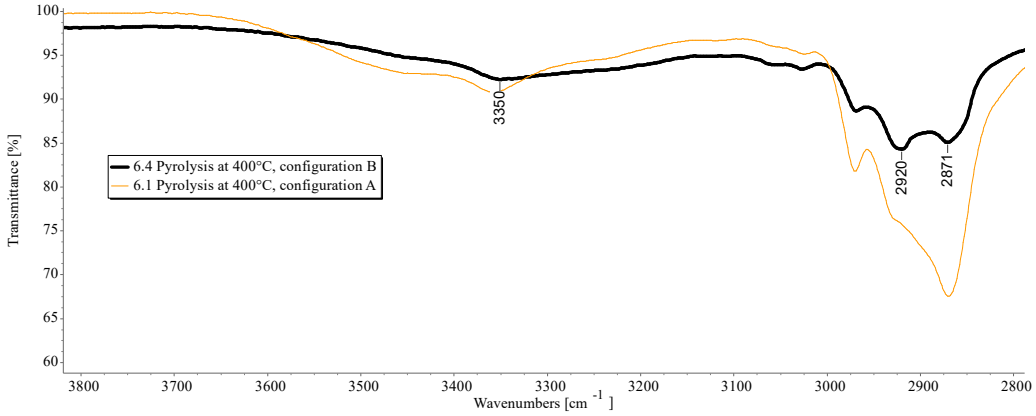

Figure 77: Liquid condensed in the chimney at 400°C conf.B (black line) and 400°C conf.A (orange line). FTIR in range 3800-2800 cm^{-1}

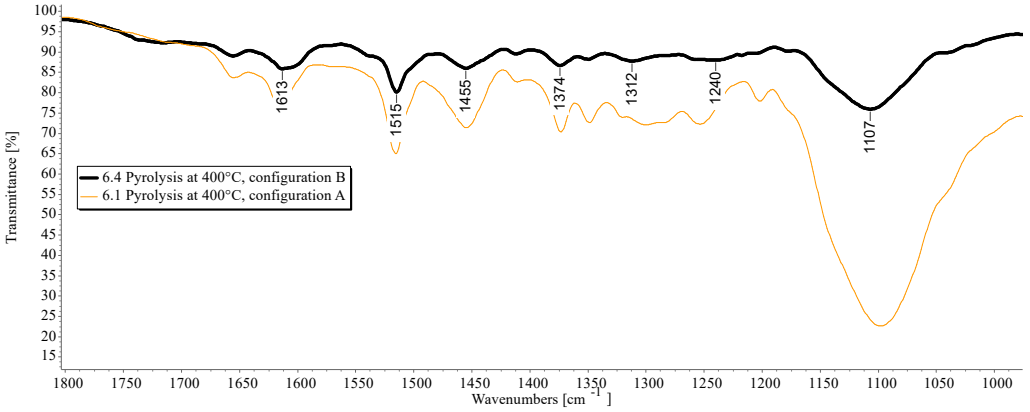

Figure 78: Liquid condensed in the chimney at 400°C conf.B (black line) and 400°C conf.A (orange line). FTIR in range 1800-1000 cm^{-1}

The IR spectra of recovered fumes from the chimney at 400°C with configuration B of pyrolizer (thick line) present the same IR peaks observed in the experiment at 400°C with configuration A of pyrolizer (thin line). A slightly difference in peaks intensity is present, meaning there is a different ratio between the products. This effect can be due to slightly differences in pyrolysis conditions due to the artisanal nature of the pyrolizer.
As for the products collected with the Schlenk flask:

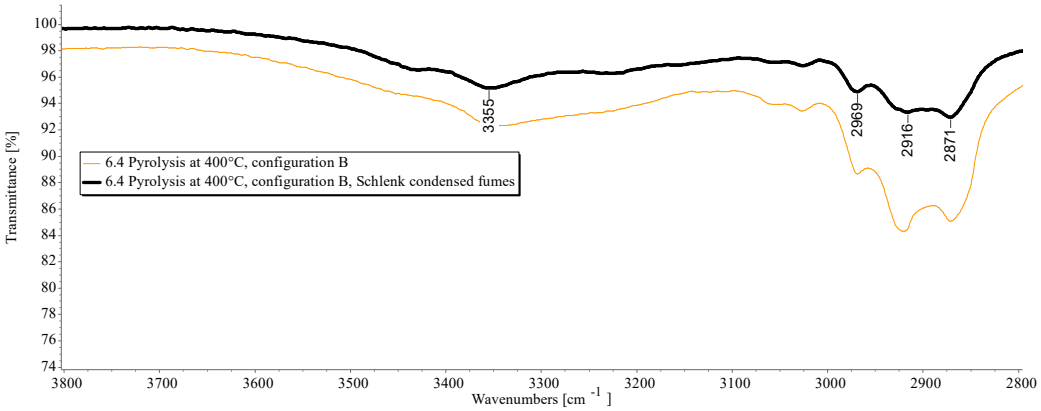

Figure 79A: Condensed in chimney (orange) vs condensed in Schlenk (black). FTIR in range 3800-2800 cm^{-1}

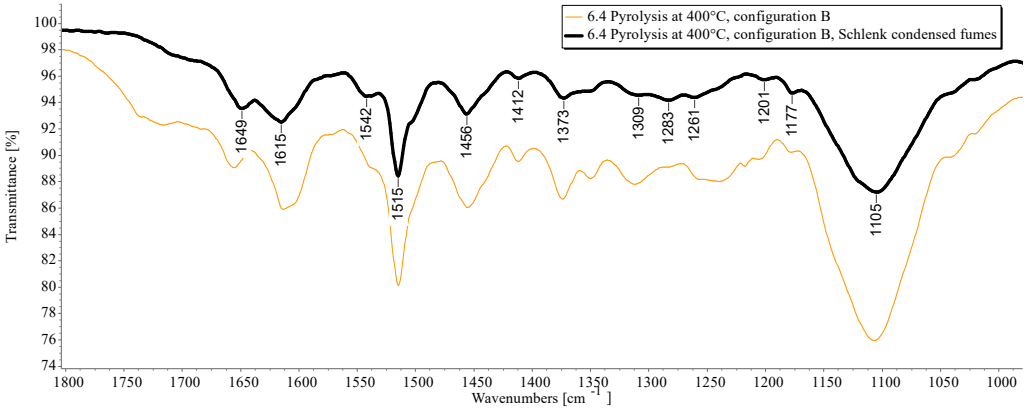

Figure 79B: Condensed in chimney (orange) vs condensed in Schlenk (black). FTIR in range 1800-1000 cm^{-1}

the IR spectra of recovered fumes from the Schlenk (thick line) present similar IR peaks observed from the experiment where the fumes condensed in the chimney (thin line). A slightly difference in peaks intensity is present, meaning there is a different ratio between the products.

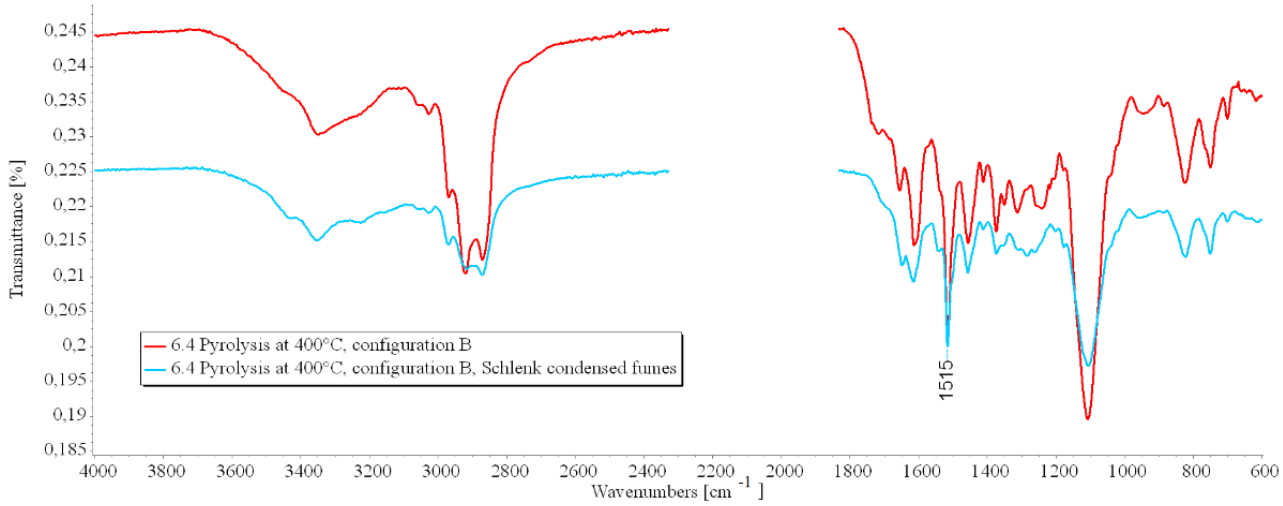

Figure 80: FTIR spectra of condensed in chimney vs condensed in Schlenk

The two spectra, both normalized imposing Transmittance (1515 cm^{-1}) = 0.2, highlight the difference in ratio between peaks. This is ascribable to the difference of volatility between the two mixtures, meaning that the sample collected in the Schlenk tube has similar nature in terms of functional groups but cleaner and more abundant.

6.5 Polyurethane from CF3 pyrolysis at 400°C for 2h with configuration B of pyrolizer

2.2521 g of a sample of polyurethane taken from the car fluff (CF3) has been pyrolyzed at 400°C for 2 hours. The pyrolizer reported in Figure 9B has been used. Heating ramp was of 54°C/min. After 8 minutes from the start at 400°C white/gray fumes have been observed exiting from the chimney. Fumes flowrate reached a maximum 5 minutes later still at 400°C and ended 20 minutes from the fumes begin. After 2 hours at 400°C heating has been stopped and the pyrolizer has been left cooling. Nitrogen flow in the heating chamber has been stopped once room temperature has been reached. The Schlenk flask presented a small amount of white solid condensed. The pyrolyzed residue was scraped from the crucible and weighted: 0.3596 g are recovered (15.97% of initial weight).

The black solid residue was analyzed through ESEM, EDX, IR.

The chimney has been washed using acetone to recover liquid residue condensed, the liquid was evaporated in fume hood and the residue has been analyzed through IR, NMR and mass spectroscopy. The Schlenk flask has been washed using deuterated acetone and the product analyzed through IR, NMR.

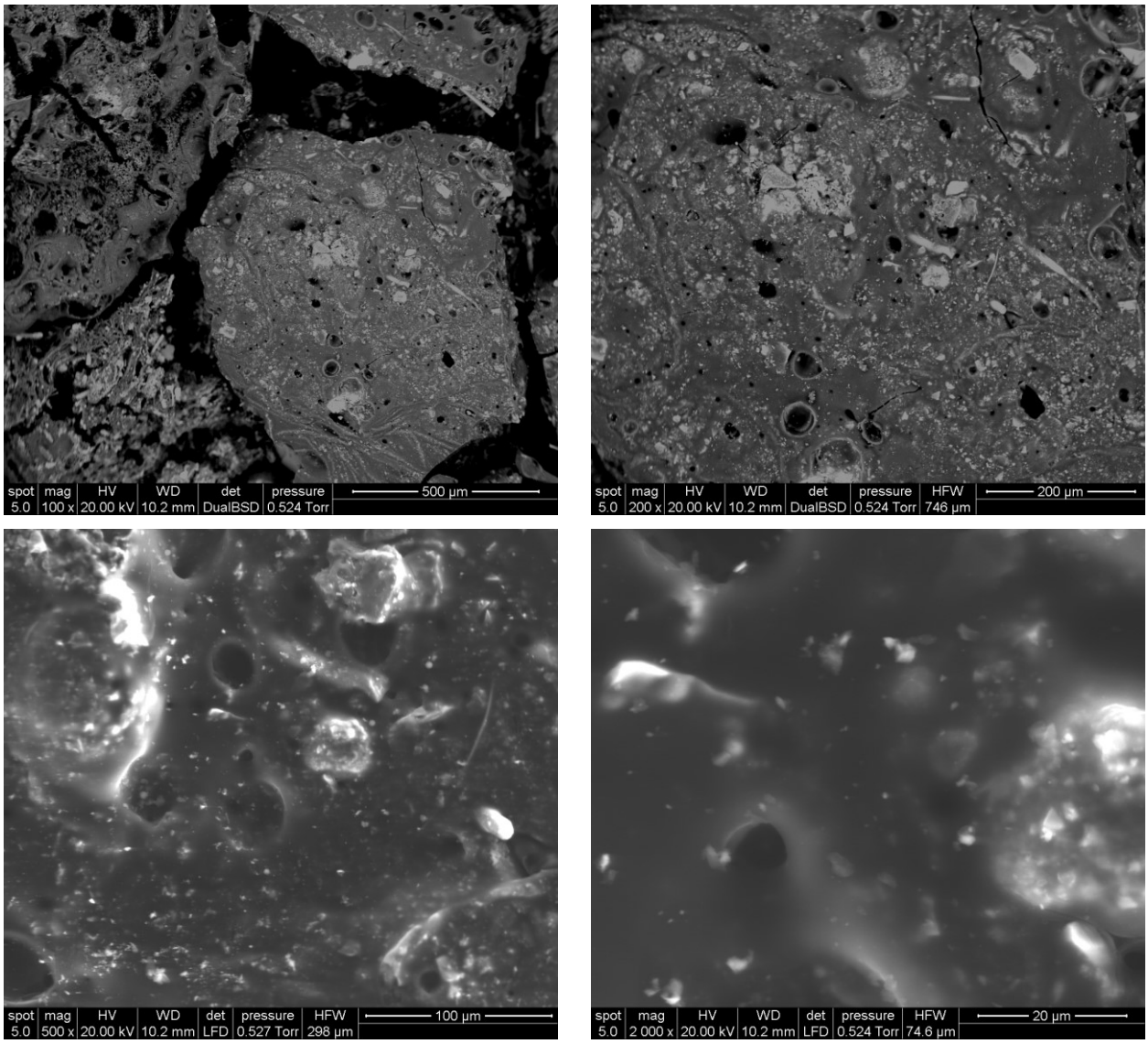

Figure 81: ESEM of solid residue from pyrolysis at 400°C for a sample from batch CF3

ESEM photos of the solid residue outline a structure strongly different from the other sample of PU pyrolyzed. The sample seems melted, there is not any spherical particle meaning low superficial area.

Spectrum	% C	% N	% O	% Fe	% Ca	% Zn	% Si	% Al
Area 2nd image	74.4	8.3	7.5	2.2	2.2	1.8	1.5	0.7

Content of N is of 8.3%, higher comparable with the nitrogen concentration of the other PU pyrolyzed. Pyrolysis, at least on this two sample, is an effective method for increasing nitrogen concentration in the sample.

No liquid has been recovered from the chimney.

This result can be due to the different chemical nature of the unknown polyurethane present in the car fluff.

For the liquid recovered from the Schlenk:

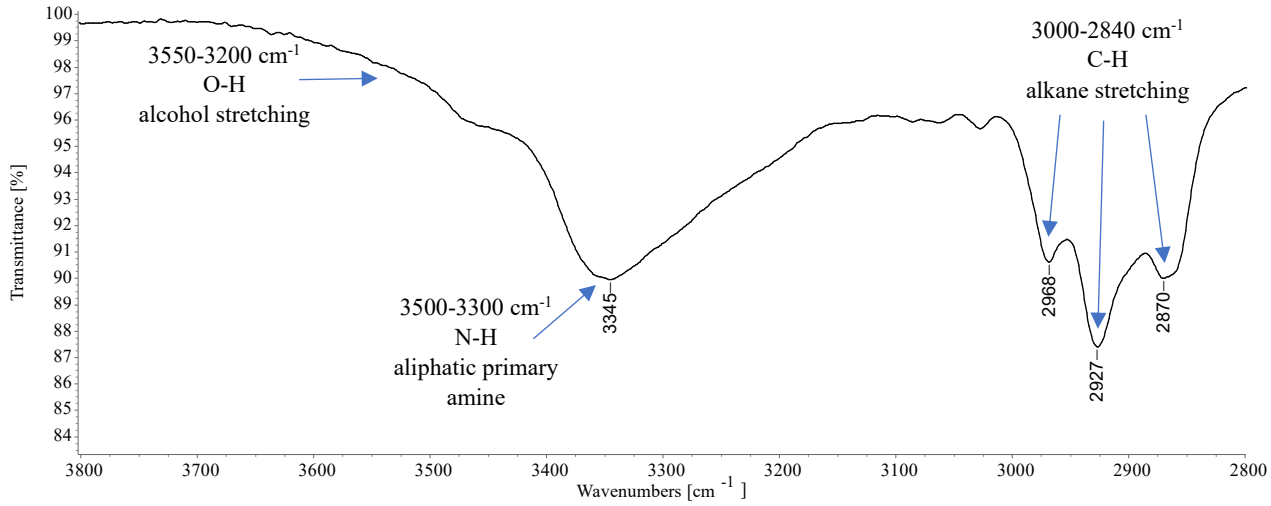

Figure 82:Fumes condensed in Schlenk using liquid nitrogen for a sample from batch CF3 . FTIR in range 3800-2800 cm-1

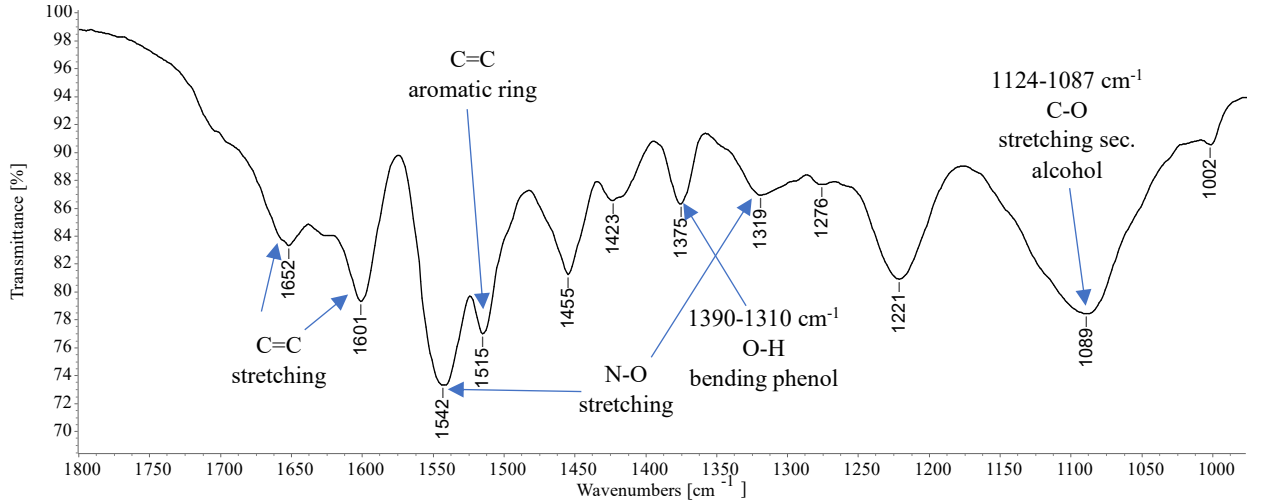

Figure 83:Fumes condensed in Schlenk using liquid nitrogen for a sample from batch CF3 . FTIR in range 1800-1000 cm-1

FTIR spectra highlight the presence of the same functional group but in different concentrations respect to experiments carried out with a different type of polyurethane.

6.6 Pyrolysis conclusions

The first 4 experiments were performed on a PU obtained following a reaction like the following:

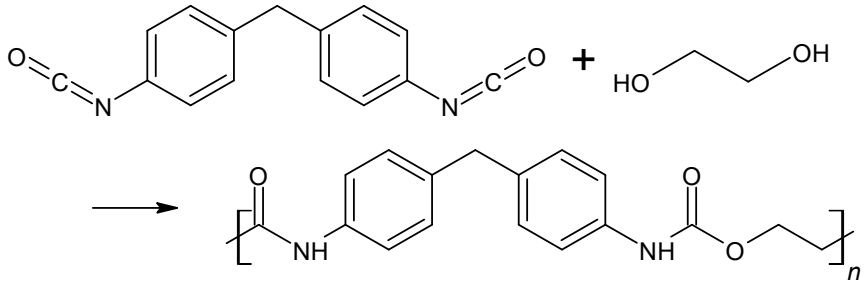

Based on the product identified we could hypothesize the following reaction occurring:

- Release of N-products: NH_3, HCN, N_2, NO_2, NO
- Release of CO_2 leading to formation of secondary amines
- Cleavage to primary ammine, olefin, CO_2
- Dissociation into isocyanate and alcohols
- Formation of products of the type:

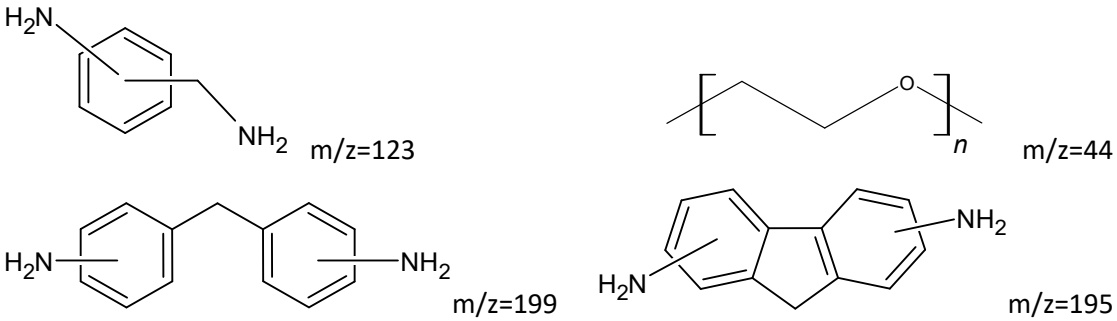

The variety of product is however huge as we can see from the MS/MS in fig.84 where subsequent losses of m/z 44 (corresponding to -OCH2CH2- units) have been observed

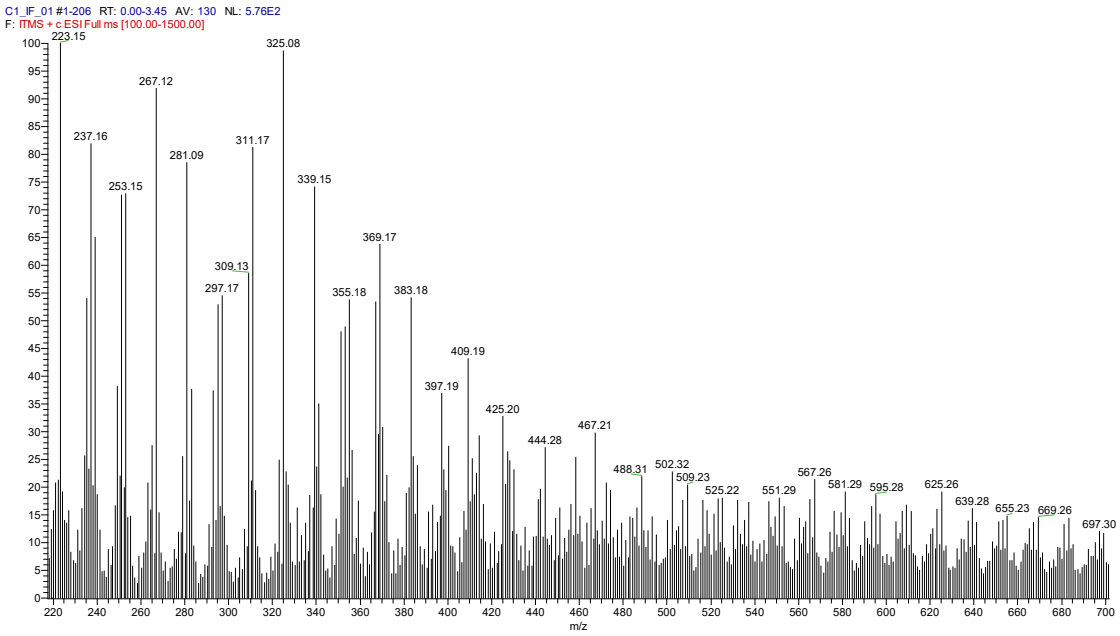

Figure 84: MS/MS of fumes condensed in chimney, experiment 6.1

Here we can propose some other species for which we can suggest the following structures

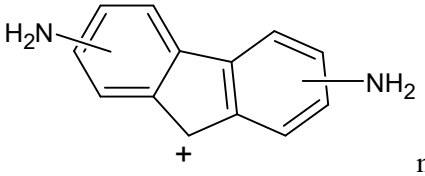

+ m/z=195

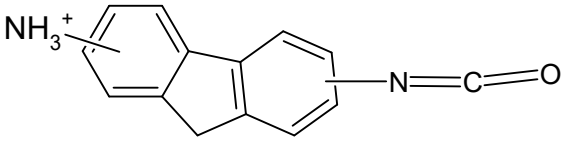

$+ CO \rightarrow$ m/z=223

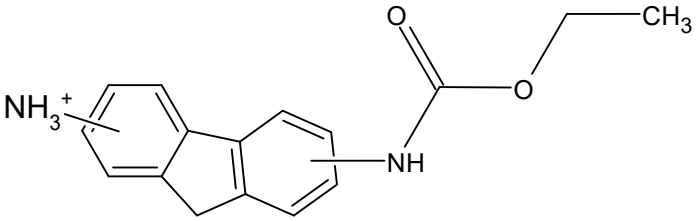

$\rightarrow$ m/z=267

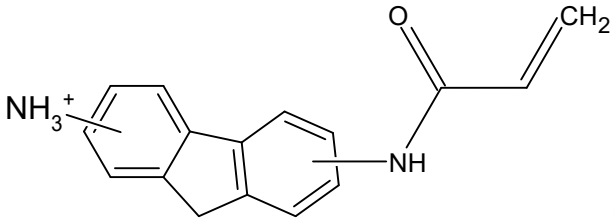

$-H_2O \rightarrow$ m/z=249

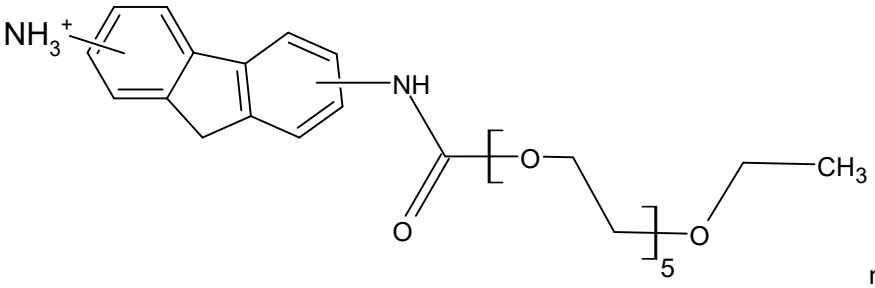

m/z=448

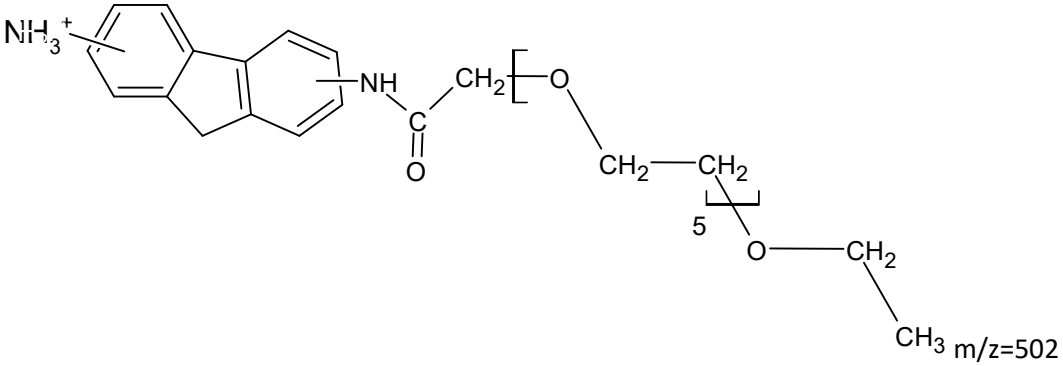

m/z=502

7. CHEMICAL RECYCLE

Using polyurethane from batch CF3 four experiments of chemical recycle have been done in order to identify if the process is feasible also with a dirty sample of polyurethane. A brief introduction to the topic has been reported in chapter 1.6.2.

7.1 Glycolysis: PU from CF3 using 10 g of glycerol and NaOH as catalyst

1 g of polyurethane (CF3) was cut in pieces using scissors, then 10 g of glycerol are added together with 0.5 g of NaOH water concentrated solution (corresponding to 0.03 g of NaOH). The sample was put in a 30 mL vial and treated using Anton Paar microwave reactor. The program followed was: ramp to 180°C in 2 min, hold at 180°C for 5 min, cold down.

To decrease the viscosity EtOH was added. The mixture was centrifuged to separate small particles of contaminants such as metals powder and unreacted polyurethane. An extraction using CH_2Cl_2 was performed searching for non-polar components. Dichloromethane was then evaporated in fume hood. ^{1}HNMR and 2D NMR (^{1}HNMR and ^{13}CNMR) determinations were performed using deuterated acetone as solvent.

An IR analysis of the fraction CH_2Cl_2 extracted was performed:

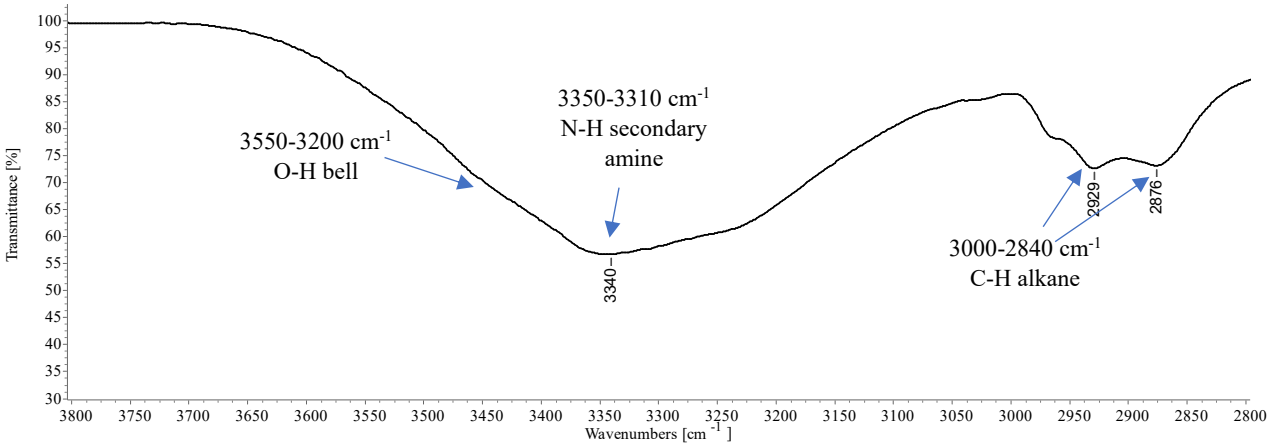

Figure 85: FTIR of glycolysis product obtained using glycerol and extracted using CH_2Cl_2. Range 3800-2800 cm^{-1}

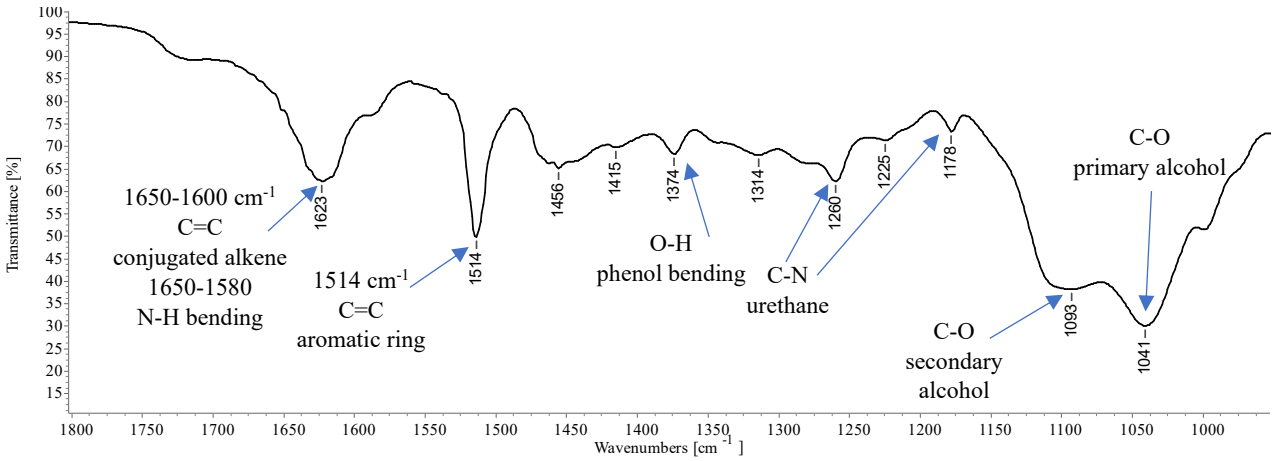

Figure 86: FTIR of glycolysis product obtained using glycerol and extracted using CH_2Cl_2. Range 1800-1000 cm^{-1}

The HPLC analysis of the mixture extracted using CH_2Cl_2 has been reported in fig.87:

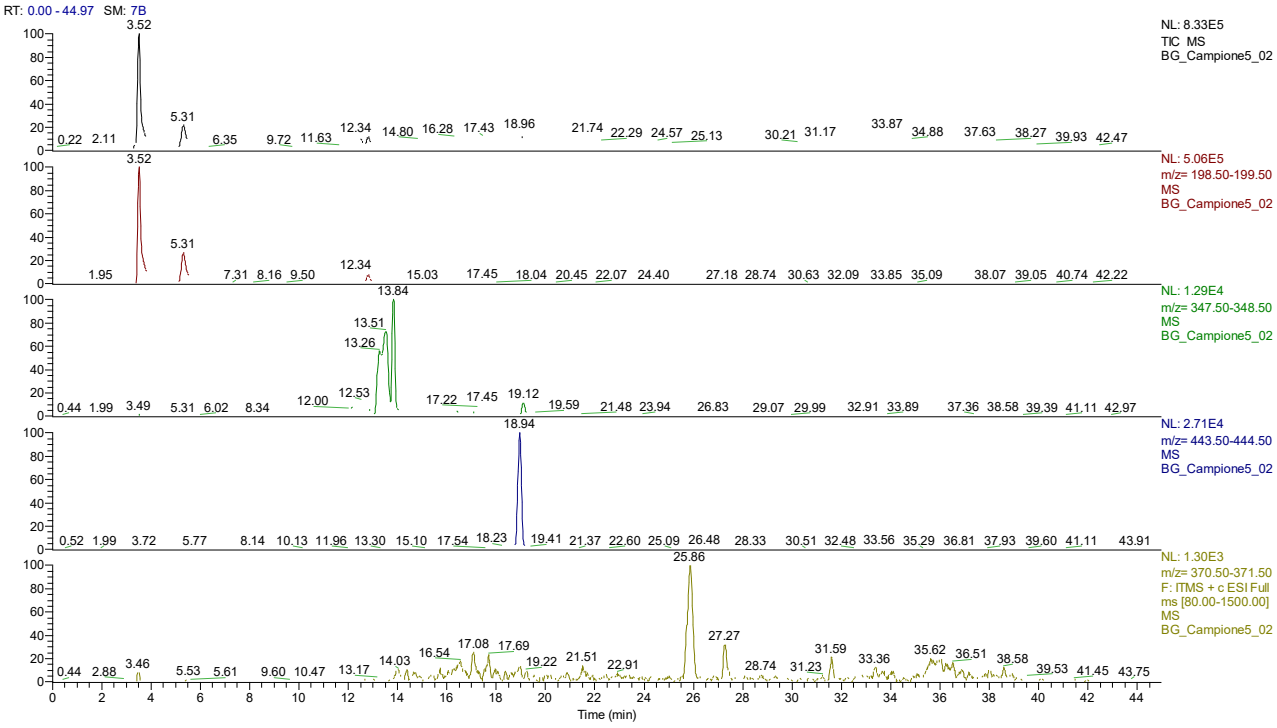

Figure 87: HPLC analysis of glycolysis product obtained using glycerol and extracted using CH_2Cl_2

Some species corresponding to m/z 199, 347, 371 and 444 have been selected, and for which on the basis of the MS/MS experiments and spectroscopic data some structures can be proposed:

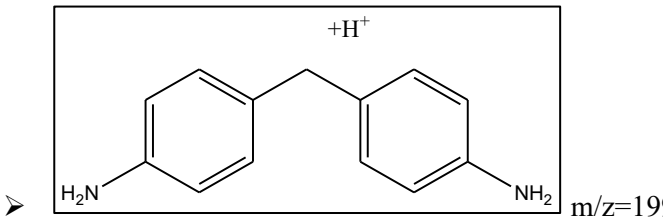

m/z=199

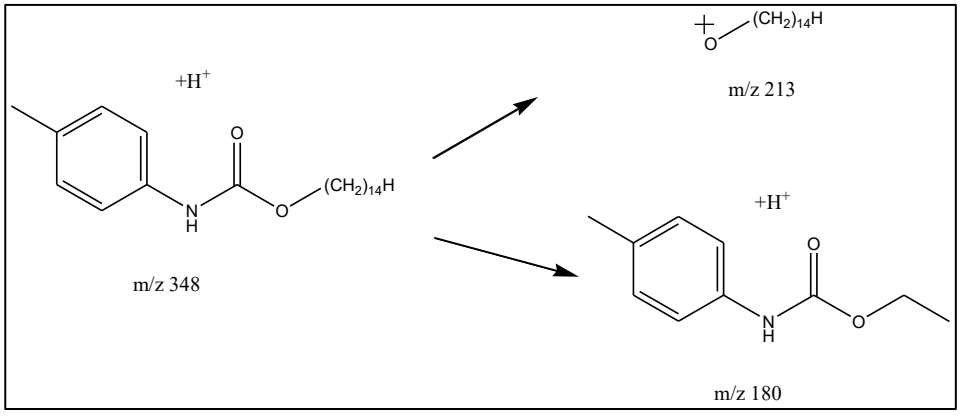

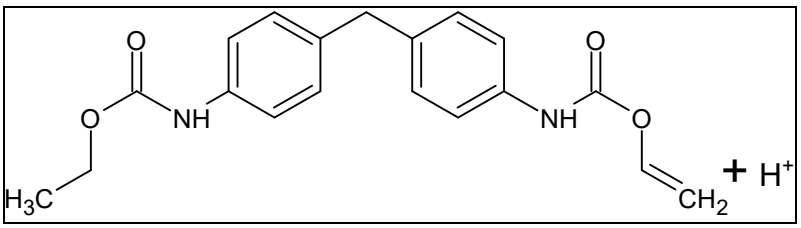

m/z=371

➢ 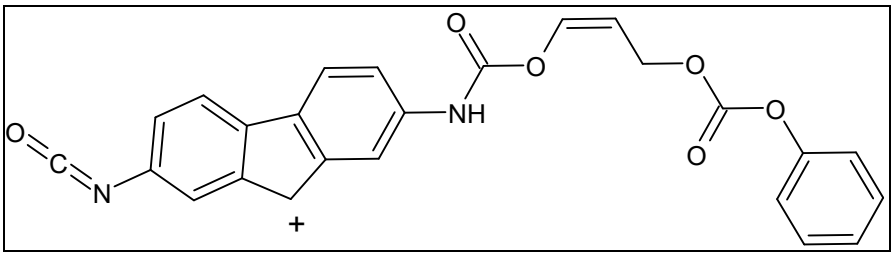

m/z=444

It is also interesting to observe that in the ^{1}HNMR spectrum reported in fig.88 in the aromatic region the signals of isomers of the substituted diphenyl skeleton are visible:

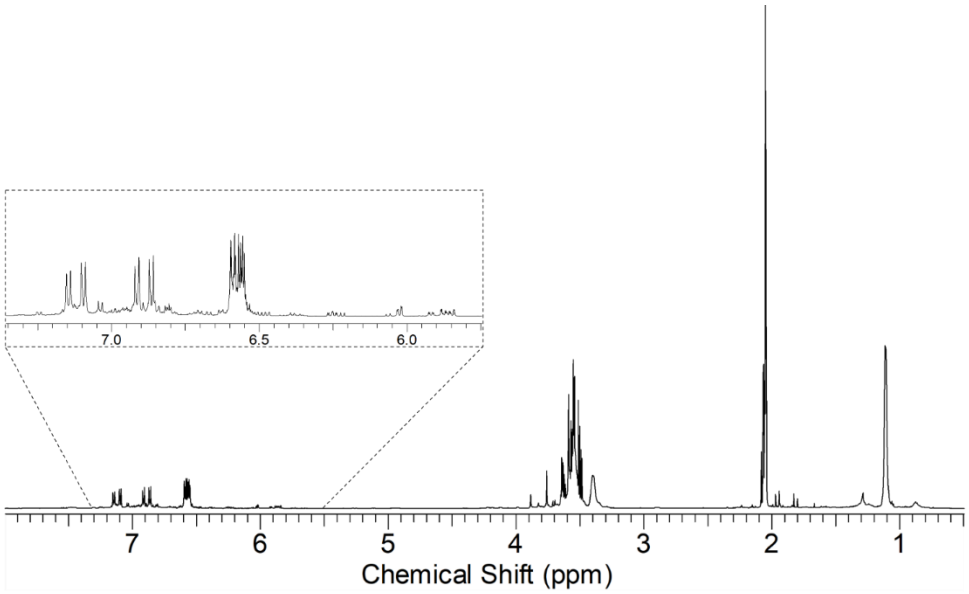

Figure 88: ^{1}HNMR of glycolysis product obtained using glycerol and extracted using CH_2Cl_2

7.2 Hydroglicolysis: PU from CF3 using 2 g of glycerol, 8 g of H_2O and NaOH as catalyst

0.50 g of polyurethane (CF3) was added to 8 mL of H_2O, 2 g of glycerol and 0.50 g of NaOH water concentrated solution (corresponding to 0.12 g of NaOH). The sample was put in a 30 mL vial and treated using Anton Paar microwave reactor. The program followed was: ramp to 180°C in 5 min, hold at 180°C for 15 min, cold down.

This treatment led to an incomplete degradation of the polyurethane. The mixture was centrifuged to separate solid particles from the liquid. The precipitate was analyzed through ESEM and EDX. The liquid surnatant was analyzed using IR.

Analysis of the precipitate:

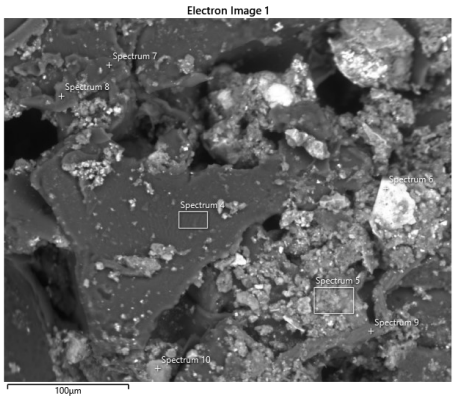

Figure 89: ESEM of solid residue from experiment 7.2

Spectrum	% C	% O	% N	% Na	% Fe	% Si	% Ca	% Zn	% Al
Area 4	67.2	26.8	3.5	1.0	0.4	0.3	0.2	-	-
Area 5	42.8	38.9	6.6	-	1.3	4.8	1.3	2.8	0.9
Point 6	36.2	39.9	-	4.7	11.6	3.0	1.0	2.3	0.9
Point 10	46.0	31.3	-	3.5	1.1	11.3	3.4	1.5	-

Analysis of the surnatant fraction:

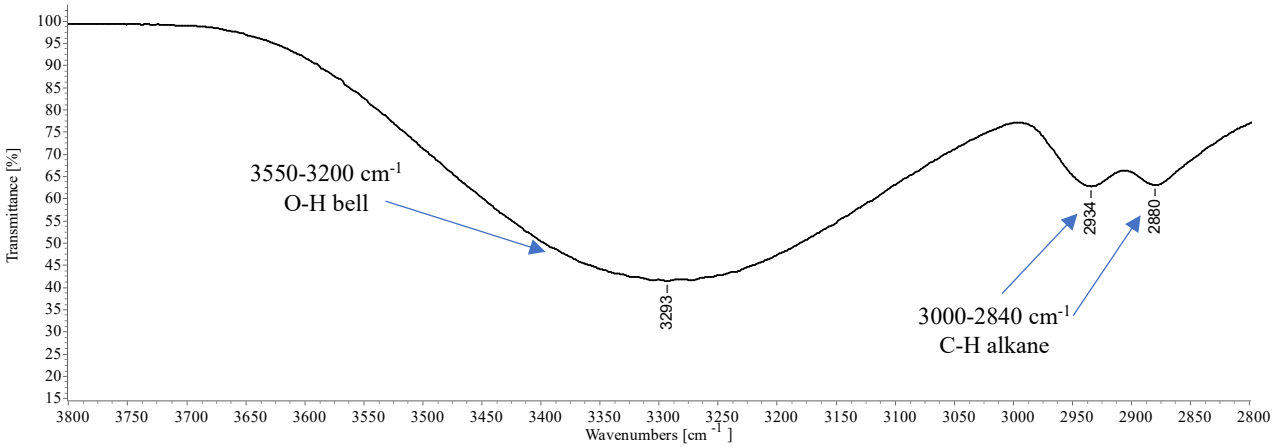

Figure 90: FTIR of hydroglycolysis products obtained using glycerol. Range 3800-2800 cm^{-1}

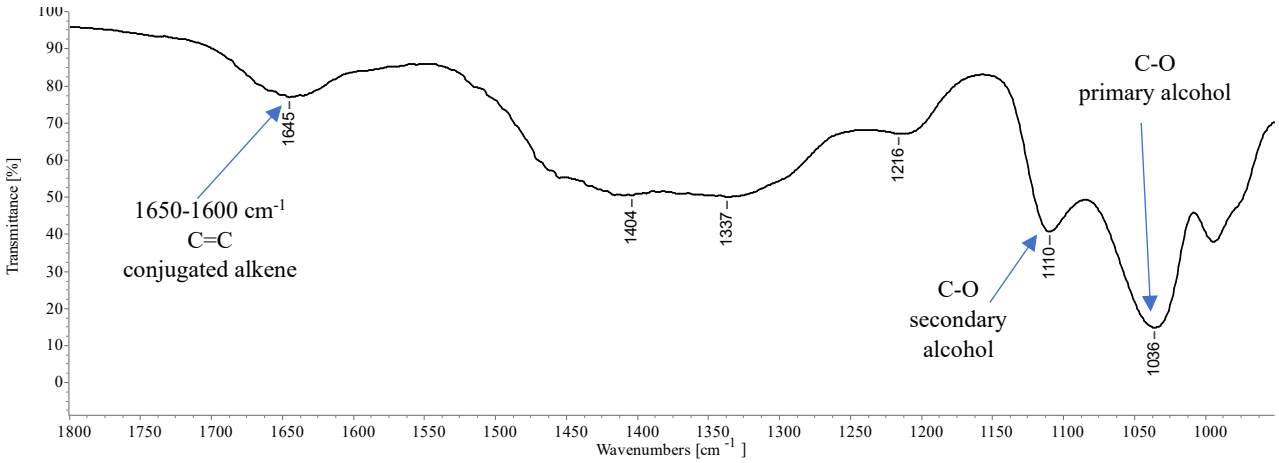

Figure 91: FTIR of hydroglycolysis products obtained using glycerol. Range 1800-1000 cm^{-1}

Glycerol in the sample was abundant due to its low volatility: IR spectrum of the sample is confronted with IR of pure glycerol in fig.92, observing small differences:

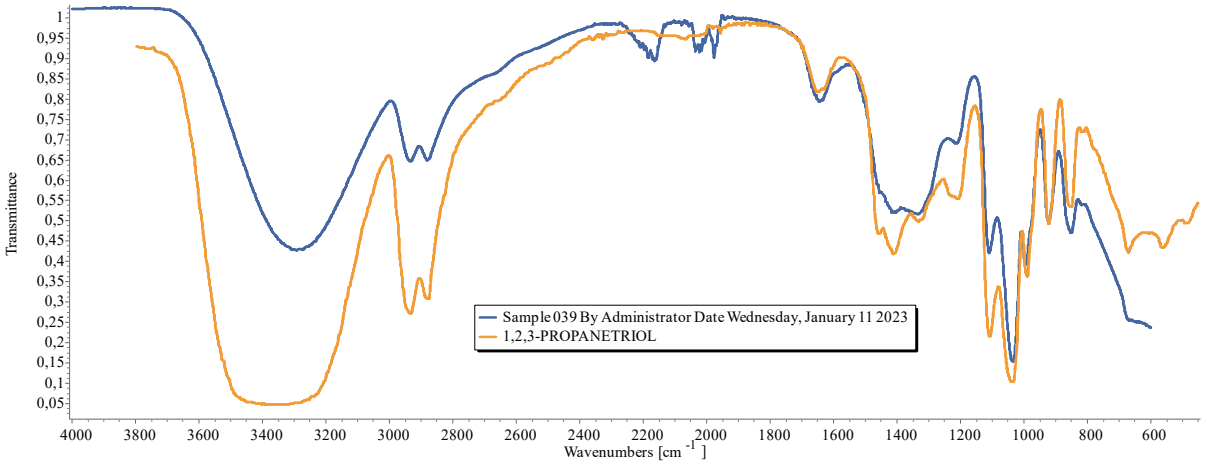

Figure 92: FTIR of liquid products from experiment 7.2 vs pure glycerol

7.3 Glicolysis: PU from CF3 using 10 g of DEG and NaOH as catalyst

0.50 g of polyurethane (CF3) was added to 10 mL of diethylene glycol (DEG) and 0.50 g of NaOH water concentrated solution (corresponding to 0.10 g of NaOH). The sample was put in a 30 mL vial and treated using Anton Paar microwave reactor. The program followed was: ramp to 180°C in 5 min, hold at 180°C for 15 min, cold down.

This treatment led to an incomplete degradation of the polyurethane. The mixture was centrifuged to separate solid particles from the liquid. The crystallized supernatant was left evaporate in fume hood and was analyzed using ESEM, EDX and IR.

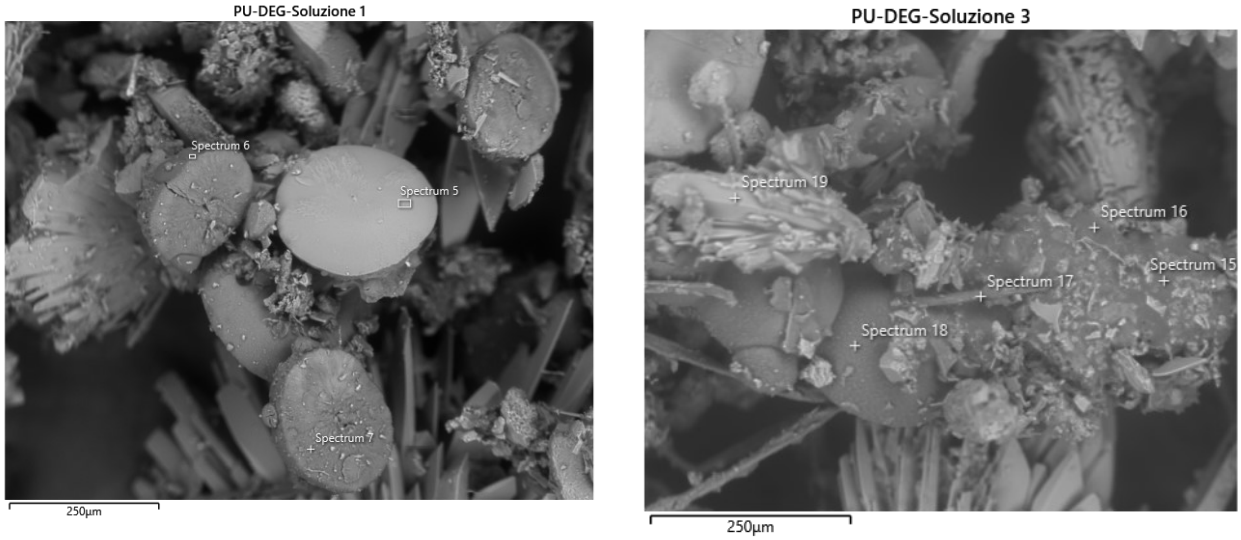

Figure 93: ESEM of solid residue and crystals obtained in experiment 7.3

Spectrum	% C	% O	% N	% Na
Area 5	22.8	52.2	-	24.8
Area 6	52.6	26.9	12.1	7.9
Point 7	50.6	28.2	9.9	11.0
Point 15	66.2	22.7	7.7	3.1
Point 16	53.5	29.7	10.6	6.0
Point 17	61.5	18.2	17.8	2.2
Point 18	57.4	24.6	7.7	9.9
Point 19	21.9	52.9	-	25.0

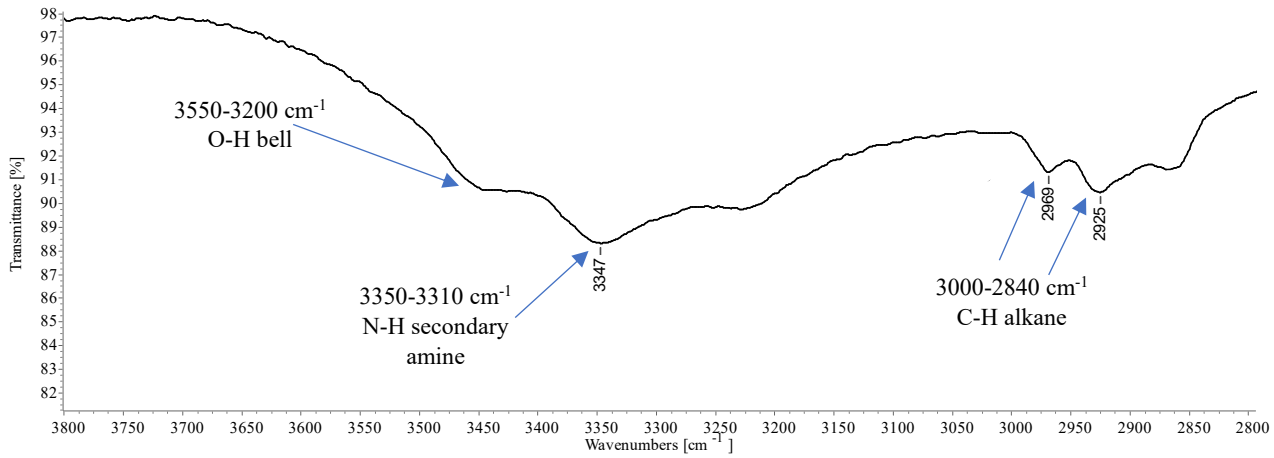

Figure 94: FTIR of glycolysis products obtained using DEG. Range 3800-2800 cm-1

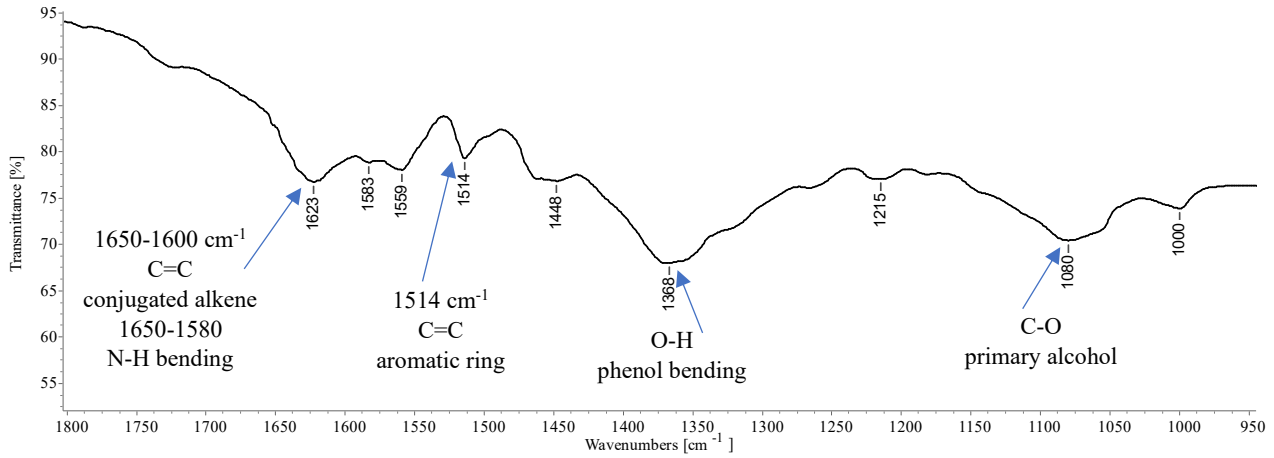

Figure 95: FTIR of glycolysis products obtained using DEG. Range 1800-1000 cm-1

It is noteworthy that in this case the formation of Na_2CO_3 has been detected: reasonably formed by the reaction of NaOH, present as catalyst and CO_2 released during the reaction.

The HPLC analysis of the mixture is reported in fig.96, where some species corresponding to m/z 199, 255, 293 and 389 have been selected, and for which on the basis of the MS/MS experiments and spectroscopic data some structures can be proposed:

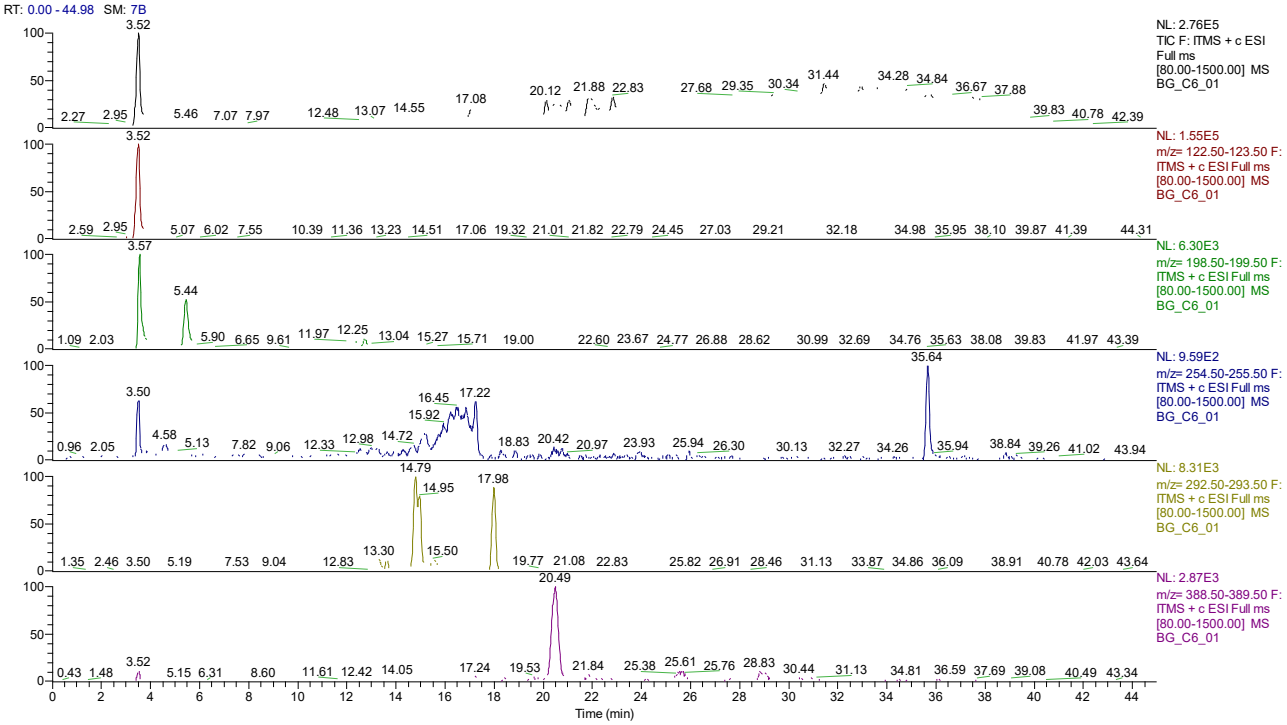

Figure 96: MS/MS of products obtained using DEG as glycolysis agent and NaOH as catalyst

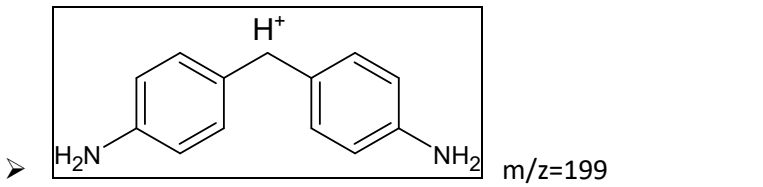

m/z=199

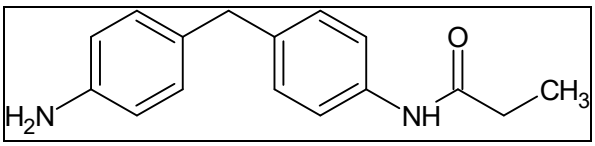

m/z=255

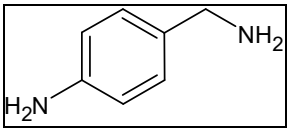

m/z=123

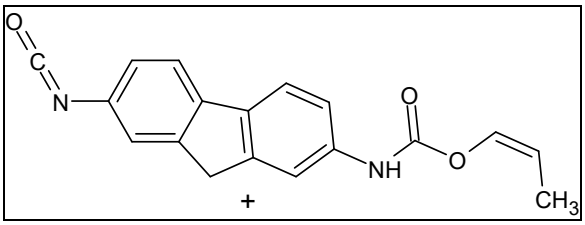

m/z=293

The [1]HNMR spectrum reported in fig.97 shows the presence of a complex mixture, containing either aromatic and aliphatic compounds:

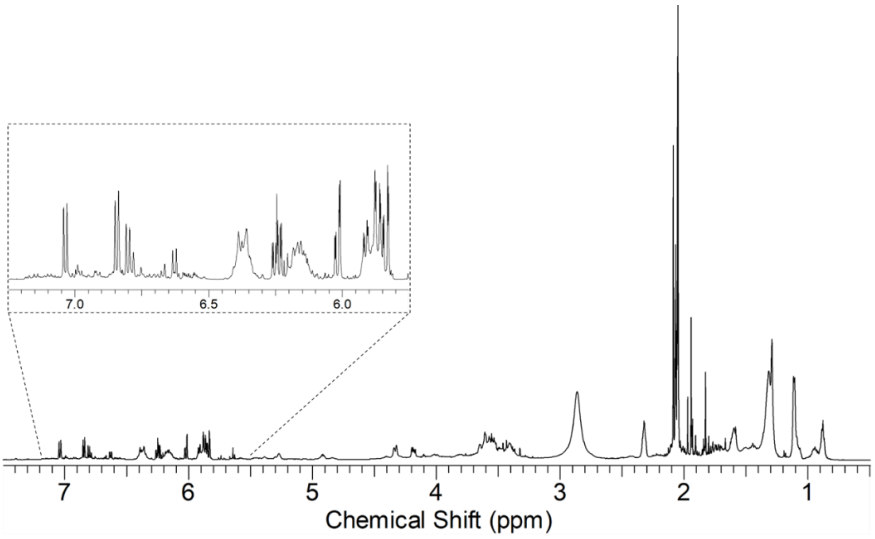

Figure 97: [1]HNMR of products obtained using DEG as glycolysis agent and NaOH as catalyst

7.4 Ethanolysis: PU from CF3 using 10 g of EtOH and NaOH as catalyst

0.26 g of polyurethane (CF3) was added to 10 mL of ethanol 96% are added together with 0.42 g of NaOH water concentrated solution (corresponding to 0.10 g of NaOH). The sample was put in a 30 mL vial and treated using Anton Paar microwave reactor. The program followed was: ramp to 180°C in 5 min, hold at 180°C for 15 min, cold down.

This treatment led to a complete degradation of the polyurethane. The mixture was centrifuged to separate heavy particles from the liquid. The precipitate was constituted by metal powders and crystal of sodium carbonate produced from reaction with CO_2. The liquid supernatant was analyzed using IR, NMR and MS/MS.

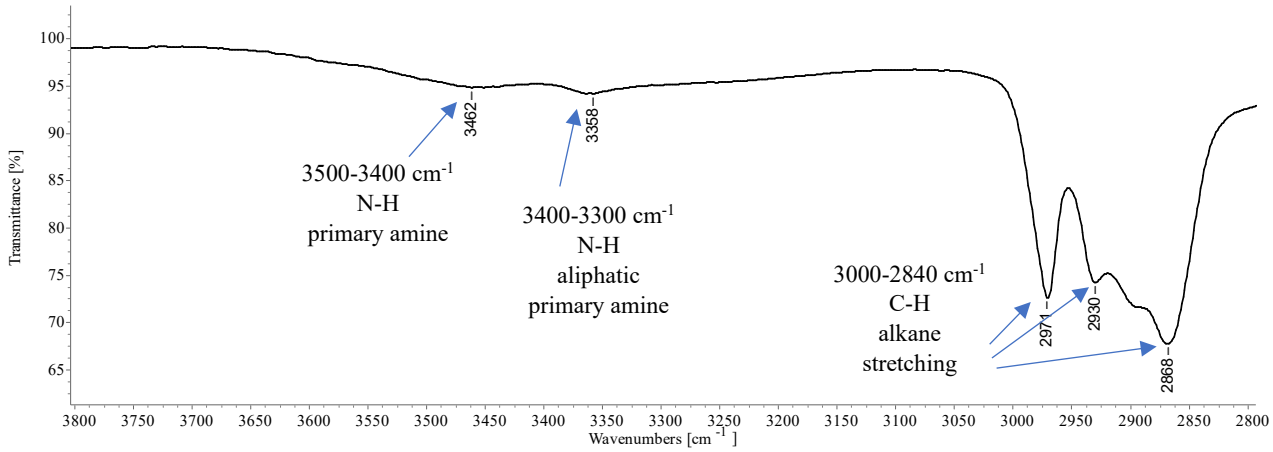

Figure 98: FTIR of glycolysis products obtained using EtOH. Range 3800-2800 cm^{-1}

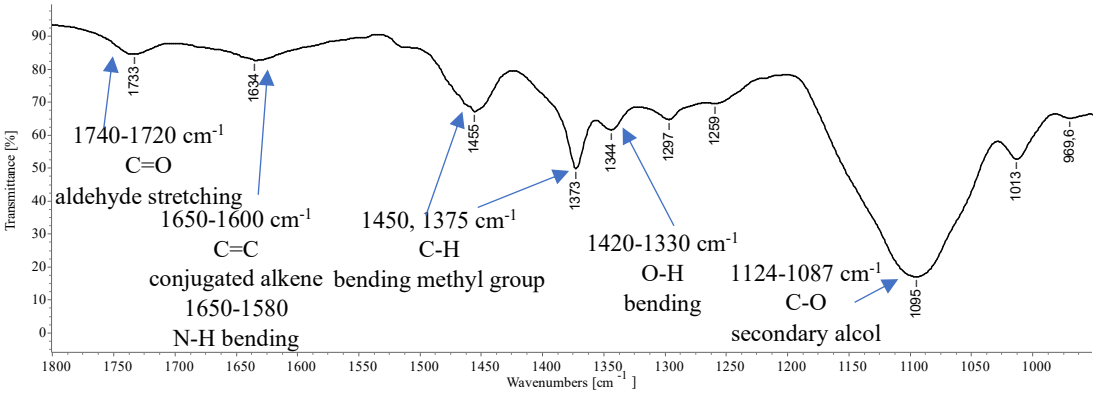

Figure 99: FTIR of glycolysis products obtained using EtOH. Range 1800-1000 cm^{-1}

The HPLC analysis of the mixture has been reported in fig.100, where some species corresponding to m/z 123, 199, 254, 268, 294, 334 and 348 have been selected, some of which are similar to the previously detected species.

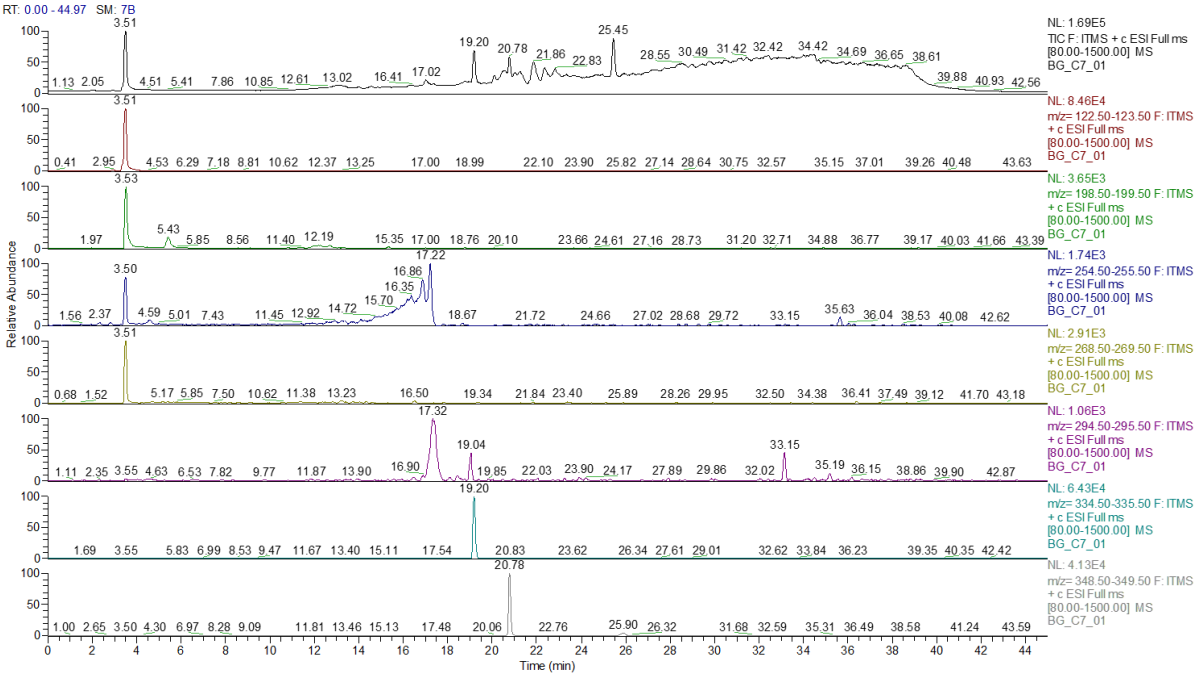

Figure 100: HPLC analysis of glycolysis products obtained using EtOH and NaOH as catalyst

The 1H NMR spectrum shows again in the aromatic region the presence of many species with substituents in different positions.

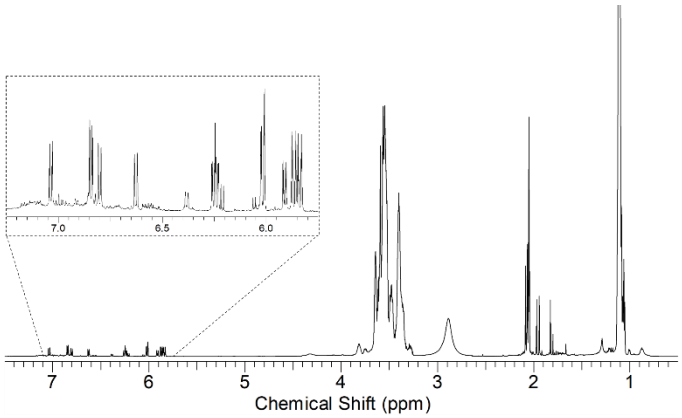

Figure 101: [1]HNMR of glycolysis products obtained using EtOH and NaOH as catalyst

7.5 Chemical recycle conclusions

Chemical recycle could be operated using different chemical reagents. The products identified using EtOH, DEG and glycerol using NaOH as catalyst are similar in all the experiment without great differences. We however expect a different ratios of products obtained as function of the catalyst and reagent used. Glycerol is the cheapest reagent used but however its performance are lower than DEG and EtOH since at the end of our experiments there was still an amount of unreacted PU. Viscosity of glycerol also makes the process more difficult, and a more expensive separation unit is expected to decrease the cost-effectiveness of the process. On the contrary EtOH appear to be extremely reactive and the products could be recovered in an easier and less expensive way.

8 HTC: HYDROTHERMAL CARBONIZATION

Several experiments were made using polyurethane from batch CF3 and mixed powder from CF15.

HTC reaction under advanced oxidation conditions has also been investigated.

8.1 PU from CF3 at 180° for 15 min using microwave reactor

A sample of polyurethane (CF3) of 0.17g was put in 10 mL of water. The mixture was put in a temperature-controlled microwave reactor where the temperature of 180°C was reached in 10 min through a ramp heating, then the temperature of 180°C was hold for 15 min. The maximum pressure registered by the control system was of 7.2 bar. Ultimately the sample was rapidly cooled through the vent system of the reactor.

Note that at 180°C vapor pressure of water is around 10 bar, suggesting there may be an error in the pressure or in the temperature (or, both) measuring system of the system in this experiment.

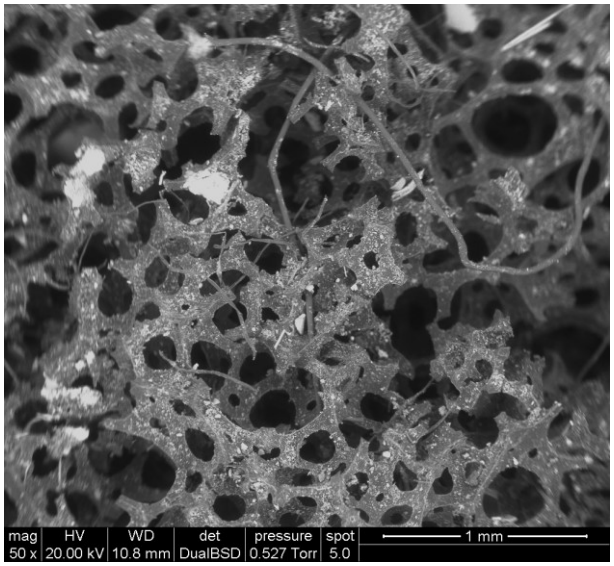

Figure 102: ESEM after experiment

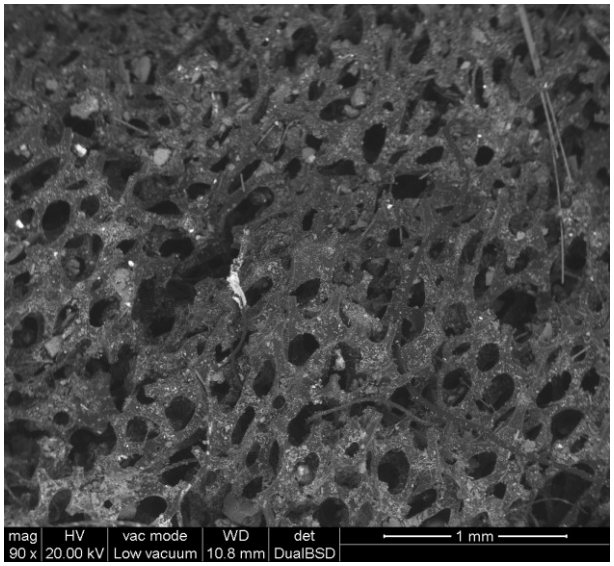

Figure 103: ESEM of a sample untreated

In fig.102, ESEM photo of the material after the experiment 8.1 has been reported to compare with fig 103, where the same scale ESEM analysis of an untreated sample of polyurethane (CF3) is shown. It is to note that every sample collected from CF3 is slightly different so an uncertainty in the comparison is inevitable. The sample on the left shows larger holes in the porous structure, also more breaks are present in the filaments. A possible explanation of this phenomenon is that boiling water forms pressure gradients in the fluid phase stretching the polyurethane structure leading to larger holes and breaks. Although no chemical reaction is evident at these conditions, the experiment suggests that at these temperature/pressure conditions the mass transfer is enhanced.

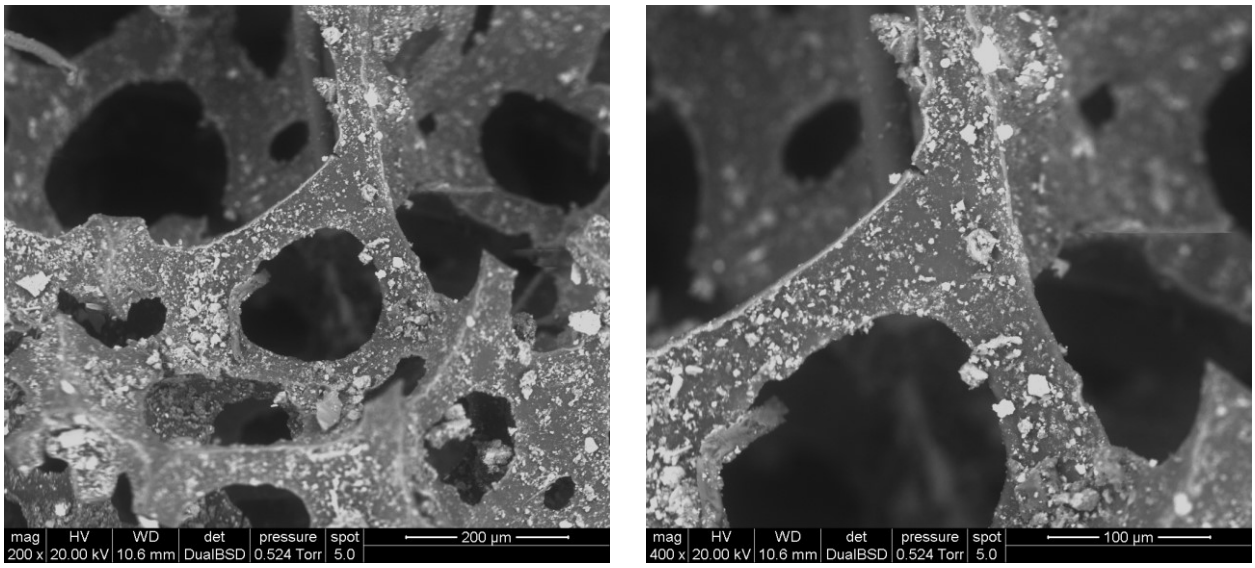

Figure 104: two ESEM of the sample after experiment 8.1

The surface of the polymer is still dirty and full of contaminants meaning that these physical conditions do not lead to high fluid speed on the surface of the polymer, meaning that mass transfer could be increased.

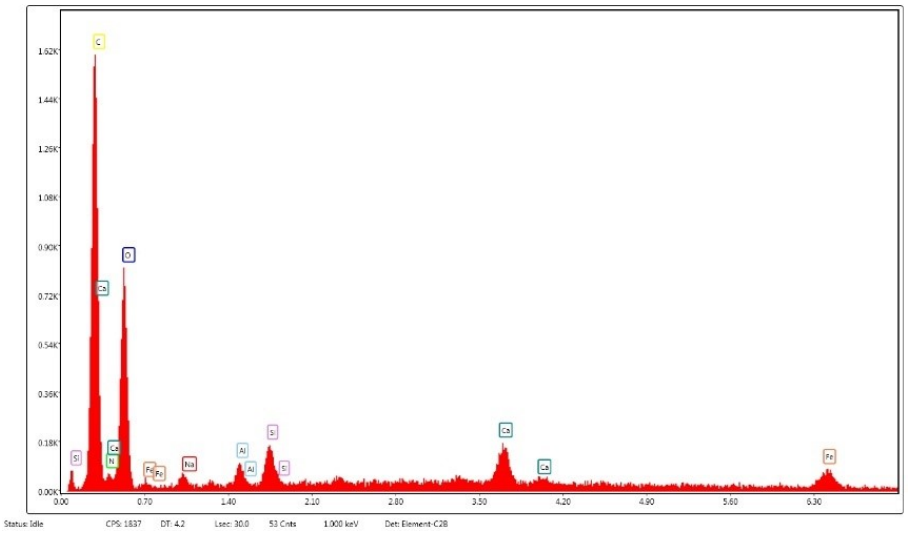

Figure 105: EDX analysis of sample after experiment 8.1

EDX analysis performed on a large area highlights the presence of contaminants such as Fe, Ca, Si and Al, similarly to the EDX analysis performed on the CF3 sample previously analyzed. Different element abundance is expected since each sample is slightly different, however the presence of many elements confirms that the surface of the polymer is still contaminated.

8.2 PU from CF3 and mix from CF15 performing personalized program using microwave ETHOS reactor

A sample of polyurethane (CF3) of 0.50 g was added to 10 mL of water. A sample of small size sieved particles (CF15) of 0.50g was added to 10 mL of water. Both were put in the Ethos microwave reactor with power control. No pressure/temperature information are present. The following program, chosen from one of the preset, was performed:

Time [min]	Power [W]
1	250
1	0
5	250
5	400
5	650
5	Vent

Analysis of polyurethane

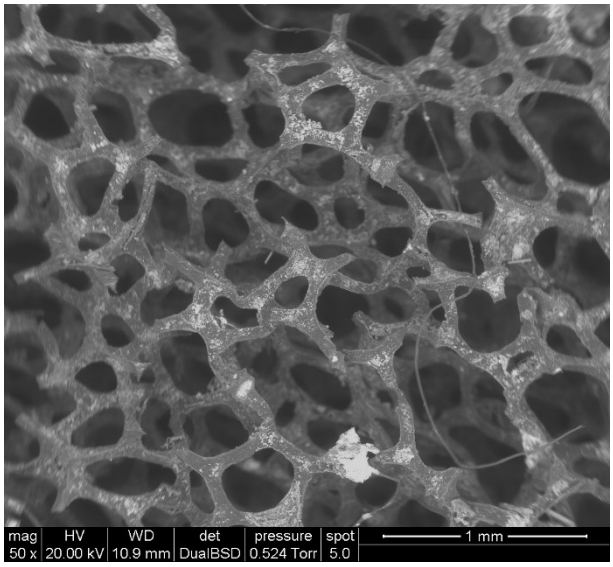

Figure 106: ESEM after experiment

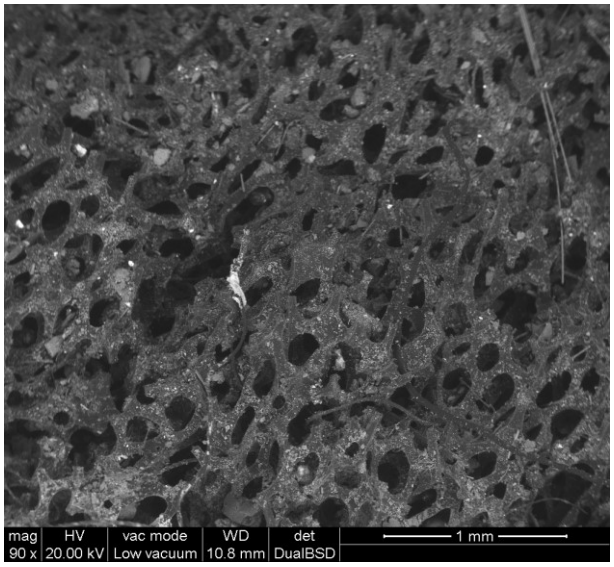

Figure 107: ESEM of a sample untreated

In fig.106, ESEM analysis after the product from the experiment #2 has been reported to compare with fig.107, where the same scale ESEM analysis of an untreated sample of polyurethane (CF3) has been shown. It is to note that each sample collected from CF3 is slightly different so an uncertainty in the comparison can be expected. The sample on the left shows much larger holes in the reticular structure and more breaks. Also, compared to the experiment 8.1 performed at 180°C the stretching effect is higher, meaning that although no temperature control is available, it is reasonable to assume that similar temperature pressure conditions were reached.

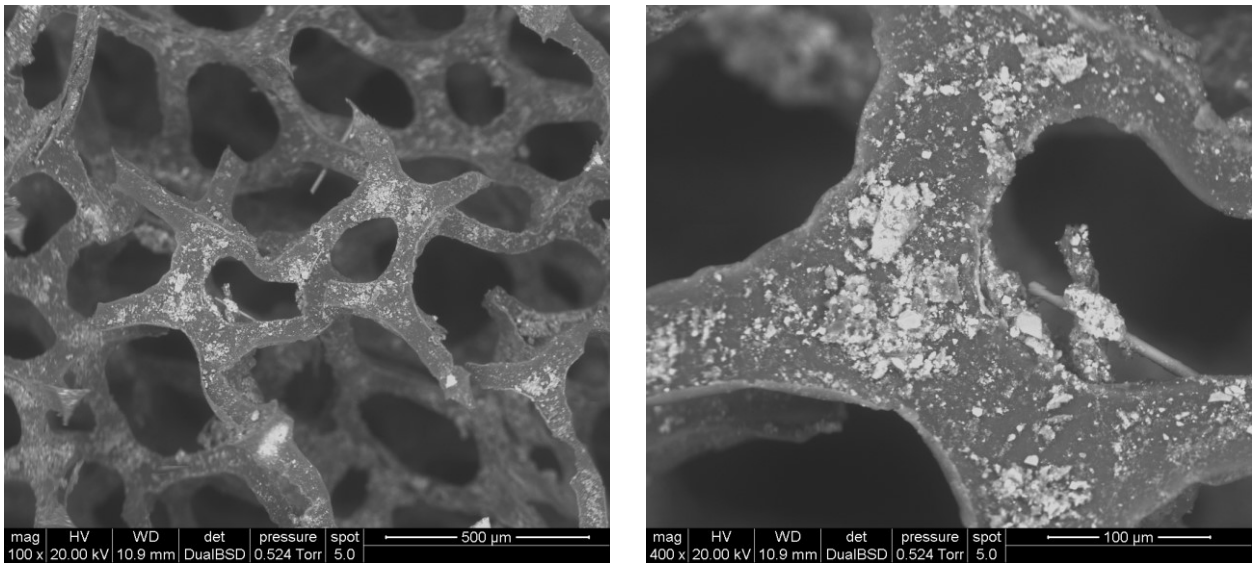

Figure 108: two ESEM of sample after experiment 8.2

The surface of the polymer is, compared to experiment 8.1, much cleaner but some residue is still present on the polymer surface. EDX analysis shows that the nature of this residue is heterogenous since Si, Ca, Fe, K, Zn and Mg are present. The cleaner surface suggests the presence of high fluid speed near the surface, condition which enhance the mass transfer.

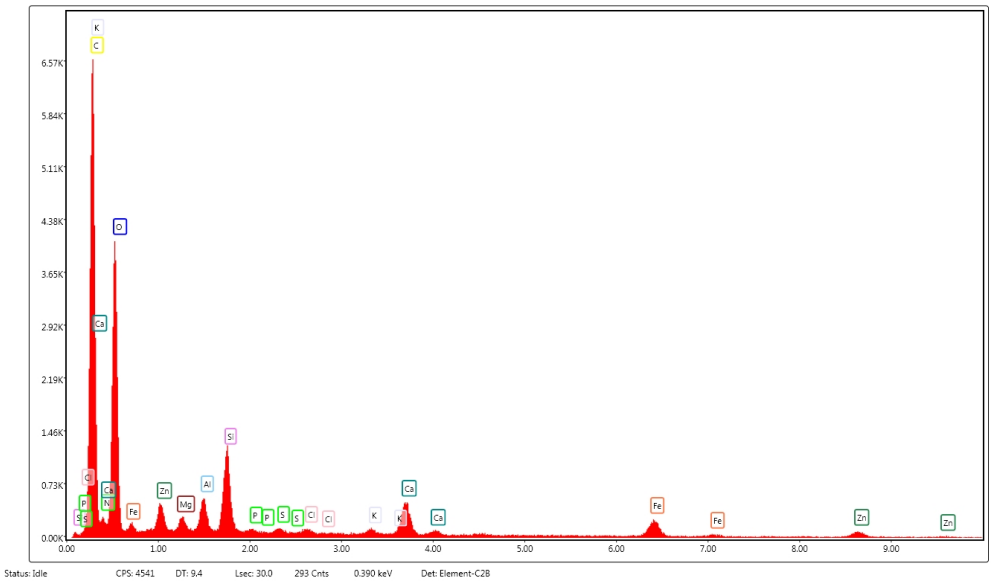

Figure 109: EDX of the sample after experiment 8.2

Finally, the powder present was analyzed. Since the polymer surface is much cleaner, it is reasonable to expect that this powder contains the small particle of contaminants removed from the surface. If any hydrochar has been formed, it should be present here.

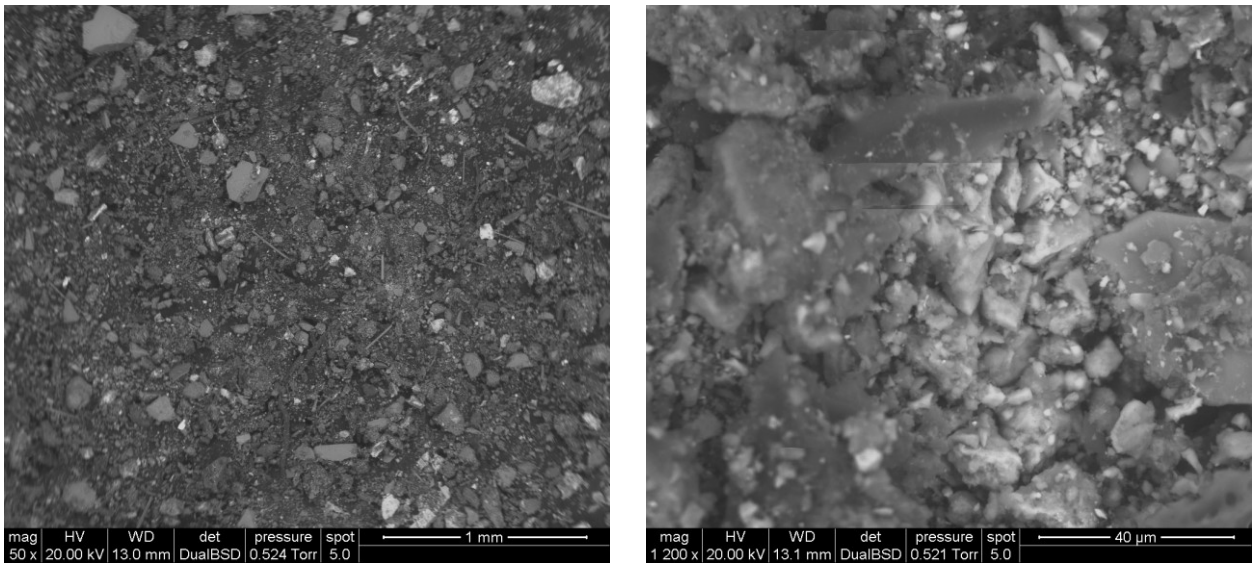

Figure 110: Two ESEM of untreated fine sieved particles from batch CF15

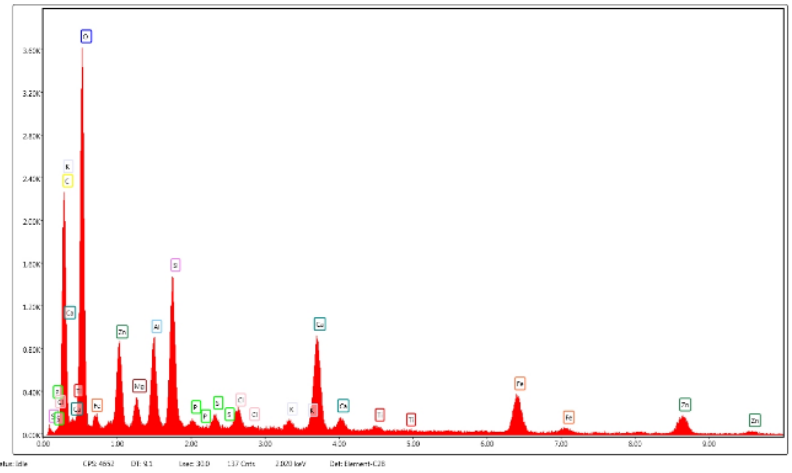

ESEM and ESX analysis highlight the presence of many elements such as Si, Al, Zn, Fe, Mg, O and also C. No spherical particles have been identified meaning that the hydrothermal carbonization HTC reaction has not happened in these conditions.

Figure 111: EDX of powder after experiment

Analysis of small size sieved particles:

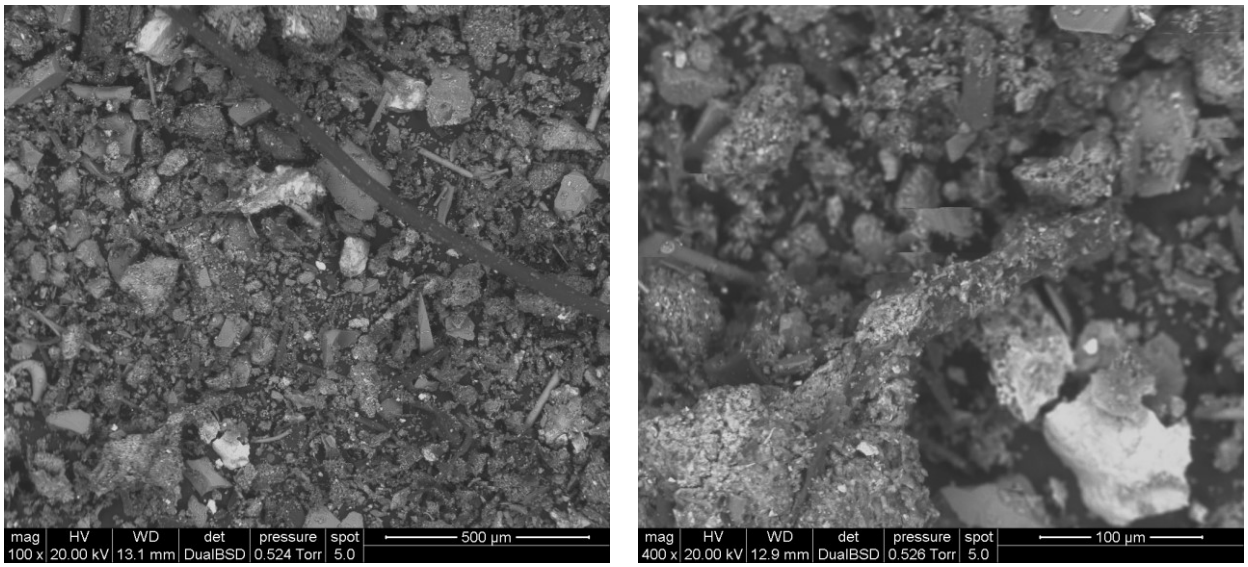

Figure 112: Two ESEM of the powder after experiment 8.2

As before, no spherically shaped particle has been founded. HTC reaction has not occurred.

8.3 PU from CF3 performing personalized program using microwave ETHOS reactor

This experiment is similar to experiment 4.2 but the time at power 650 W was increased to 10 min.

A sample of polyurethane (CF3) of 0.50g was added to 10 mL of water. The mixture was in a microwave reactor with power control. No pressure/temperature information are present. The following program was performed:

Time [min]	Power [W]
1	250
1	0
5	250
5	400
10	650
5	Vent

The pH of the solution at the end of the program was equal to 7.

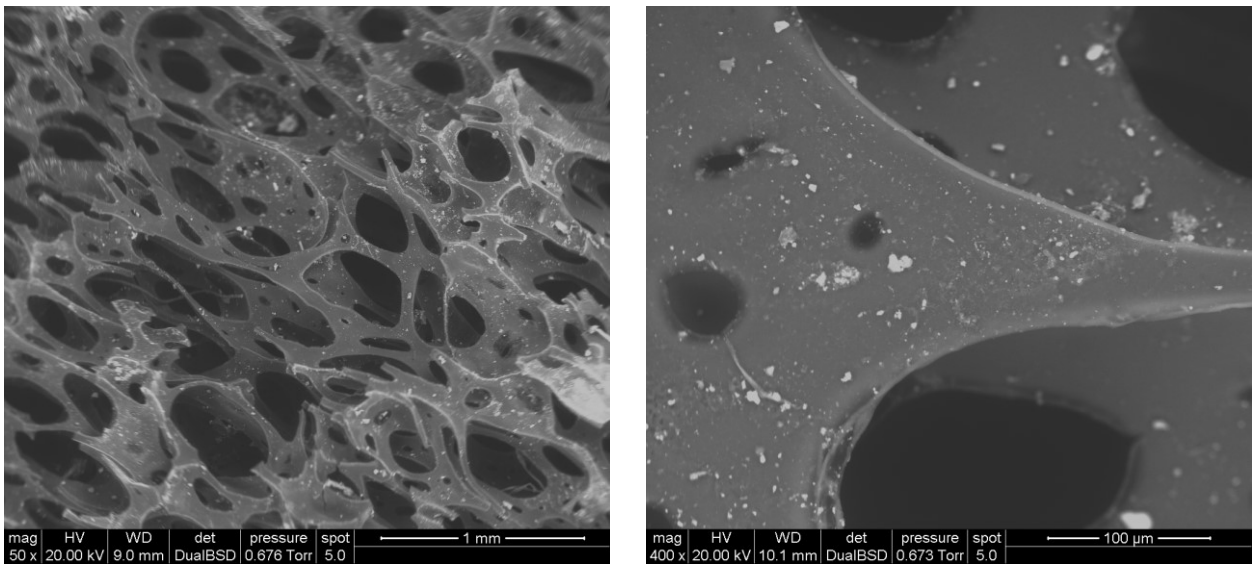

Figure 113: Two ESEM of the sample after experiment 8.3

The polyurethane structure appears to be more stretched according to the physical effect of pressure previously described. The edges of the polymer are well defined and do not show the presence of any reaction occurring. Based on that, we could exclude the hypothesis of HTC reaction occurring in this condition also on this polyurethane sample.

8.4 PU from sample "CF3 TQ1" at 200° for 15 min using microwave reactor

Experiment 8.4, 8.9, 7.2, 7.3 and 4.4 were performed on the same sample of polyurethane called "CF3 TQ1" in order to be able to make comparison between them.

0.24 g of polyurethane (CF3 TQ1) is added to 10 g of H_2O. The sample is put in a 30 mL vial and treated using Anton Paar microwave reactor. The program followed was: ramp to 200°C in 5 min, hold at 200°C for 15 min, cold down. The pressure registered from the instrument was of 15 bar, in accordance with the water vapor pressure at 200°C.

In order to make comparison before-after, firstly the ESEM picture about the untreated polyurethane are reported:

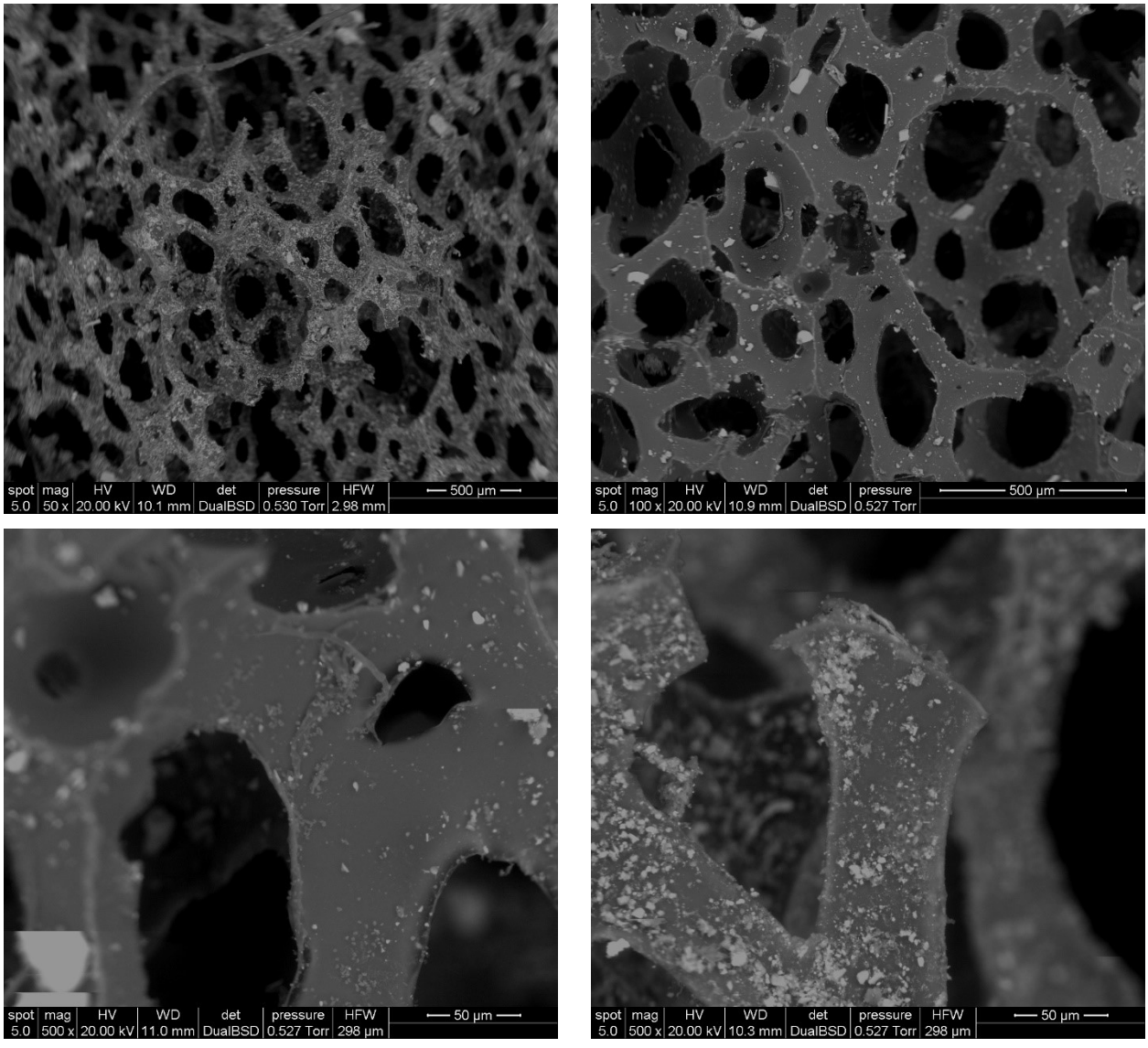

Figure 114: Four ESEM of untreated sample "CF3 TQ1"

The inner part (picture 2-3) are present visible less dirty respect the outer part (1-4) as expectable. The lattice already presents some breakage.

For the treated sample:

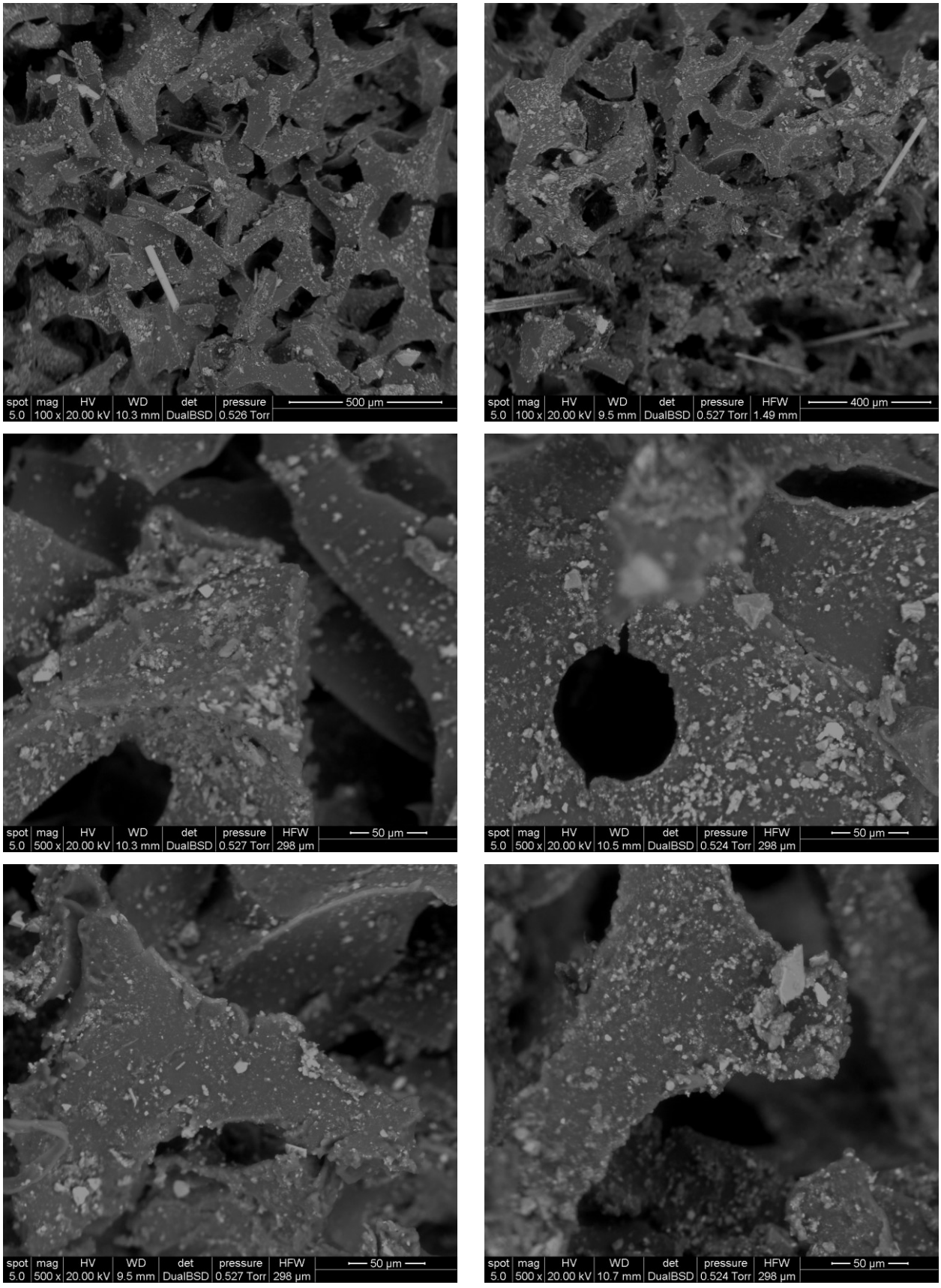

Figure 115: Six ESEM of the sample after experiment 8.4

The overall lattice structure is almost destroyed and surface of the polymer presents sign of degradation. Subcritical condition tested are however not enough to reach the desired HTC reaction as far as we can observe.

8.5 PU from CF3 using Ethos microwave reactor and H_2O_2-water in ratio 1:9

A sample of polyurethane (CF3) of 0.47 g was added to 9 mL of water and 1 mL of H_2O_2 30%. The mixture was put in a microwave reactor with power control. No pressure/temperature information are present. The following program, chosen from one of the presets, was performed:

Time [min]	1	1	5	5	5	5
Power [W]	250	0	250	400	650	Vent

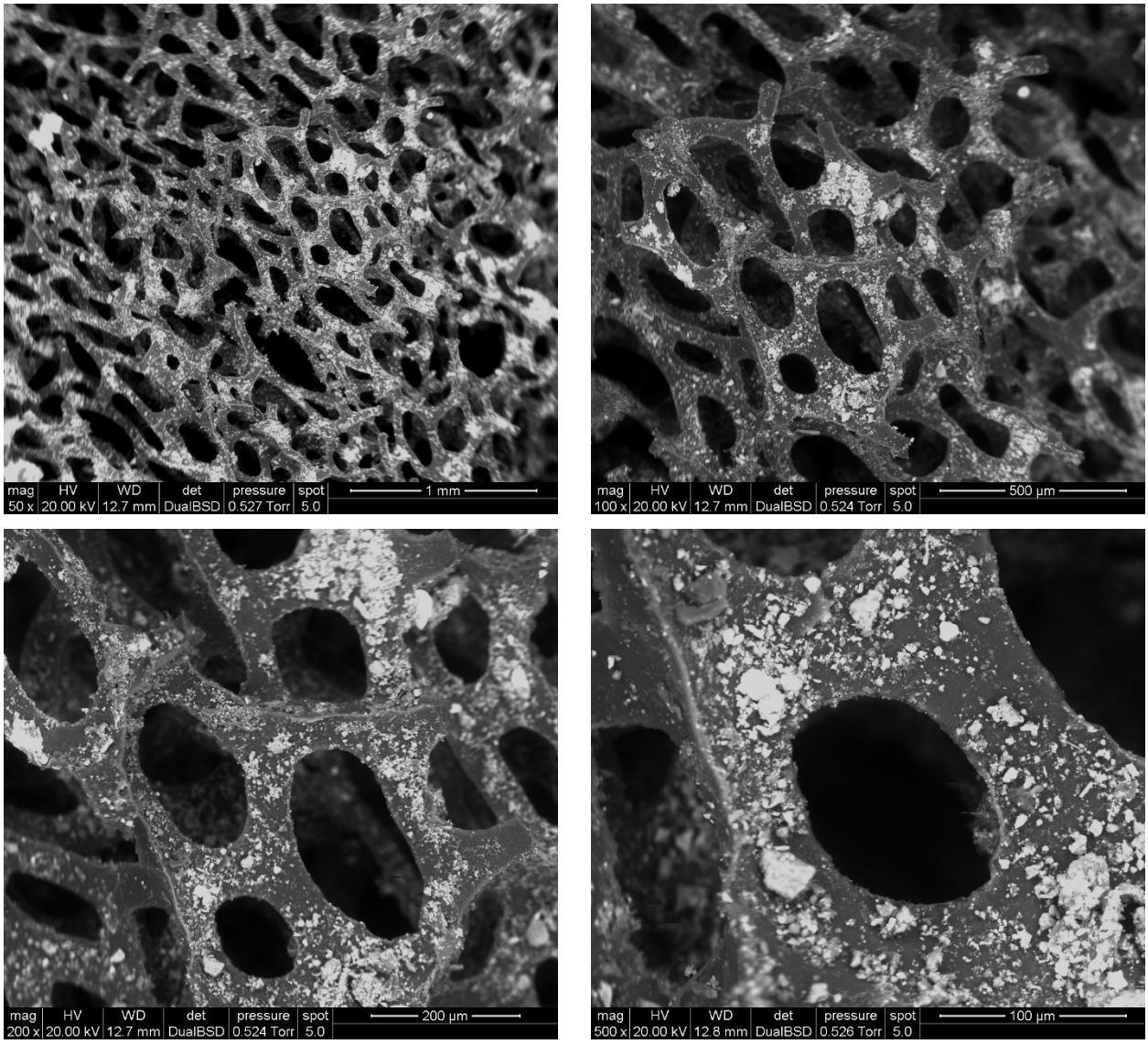

Figure 116: Four ESEM of the sample after experiment 8.5

Compared to experiment 8.2, the surface of the polyurethane is slightly dirtier while holes size is almost the same. As before, each sample has its own story and his peculiarities so the higher presence of contaminants on

the surface is probably due to a higher presence of contaminants at the beginning. Since no evident effect is visible, we discard the hypothesis that in this condition HTC or any other chemical reaction occurs.

Spectrum	% C	% O	% Fe	% Ca	% N	% Zn	% Si	% Al
Area	53.4	28.6	5.7	2.9	2.7	2.4	1.7	0.8

The performed EDX analysis found also on this sample the presence of metals such as Fe, Ca, Zn. The presence of metal elements is checked every time since they may catalyze some chemical reaction and if they already present in the sample, it could be an interesting feature from an economical point of view.

8.6 PU from CF3 using Ethos microwave reactor and H_2O_2-water in ratio 2:9

This experiment is similar to experiment 4.5 with the only difference that 2 mL of H_2O_2 30% instead of 1 was used.

A sample of polyurethane (CF3) of 0.47 g was added to 8 mL of water and 2 mL of H_2O_2 30%. The mixture was put in a microwave reactor with power control. No pressure/temperature information are present. The following program, chosen from one of the preset, was performed:

Time [min]	Power [W]
1	250
1	0
5	250
5	400
5	650
5	Vent

The pH of the solution at the end of the program was equal to 7.

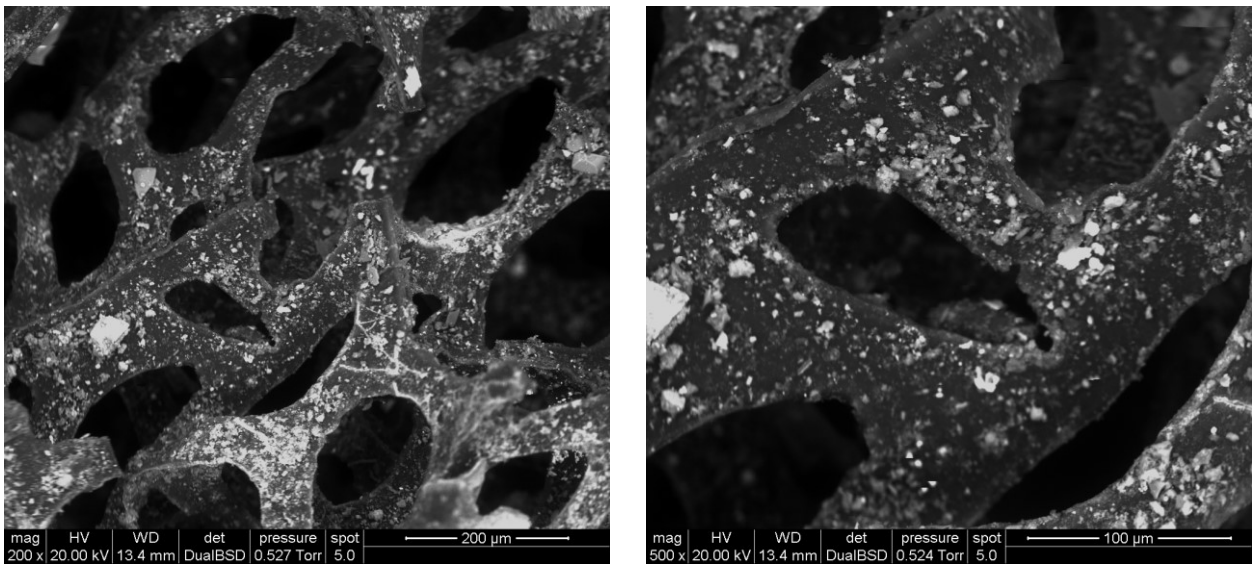

Figure 117: Two ESEM of the sample after experiment 8.6

Compared to experiment 8.4, no evident difference is noticed. No effect is present increasing the H_2O_2 concentration, in accordance with the previous consideration for which no chemical reactions affecting polyurethane was occurring. As far as, polyurethane does not appear to have bonds oxidable by H_2O_2 in this conditions.

Spectrum	% C	% O	% Fe	% Ca	% Zn	% Si	% Pb	% Al	% N
Area	54.3	30.7	4.7	2.4	2.3	1.6	1.5	0.6	0.4

The performed EDX analysis found also on this sample the presence Fe, Ca, Zn and even the presence of Pb. Nitrogen is present in very low concentration; we attribute this value to the instrumental error.

8.7 Mix from CF15 using ETHOS microwave reactor and H_2O_2-water in ratio 1:9

0.50 g of fine sieved particles (CF15) are treated as in experiment #4 with 1 mL of H_2O_2 30% and 9 mL of water. The mixture was put in the microwave reactor and the following program was performed:

Time [min]	Power [W]
1	250
1	0
5	250
5	400
5	650
5	Vent

The pH of the solution at the end of the program was equal to 7.

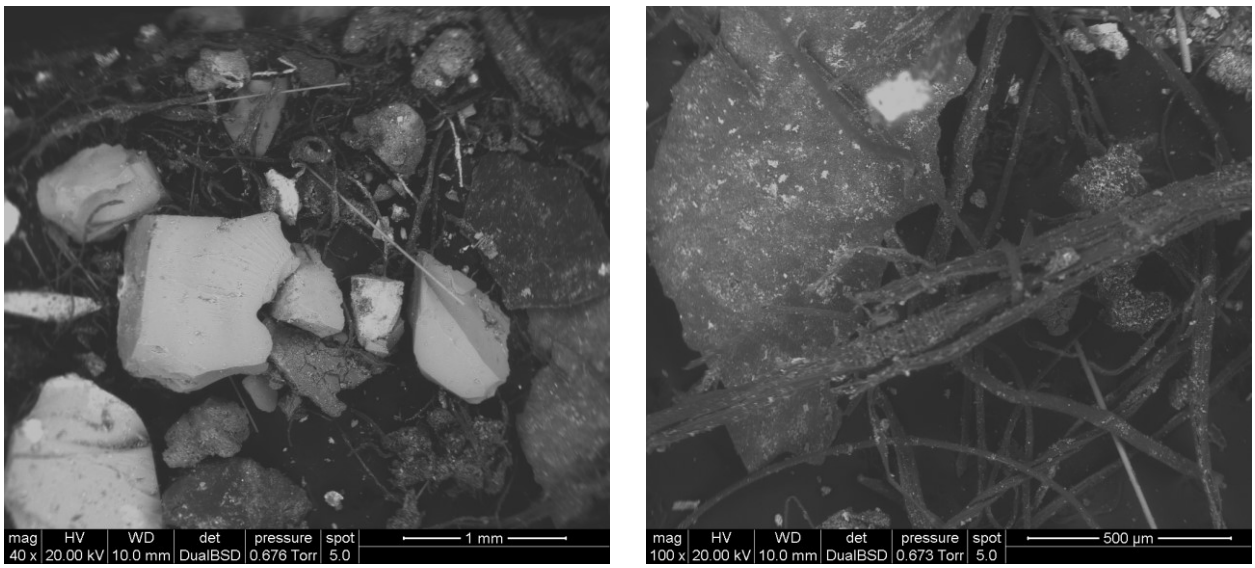

Figure 118: Two ESEM of the sample after experiment 8.7 at 40x and 100x

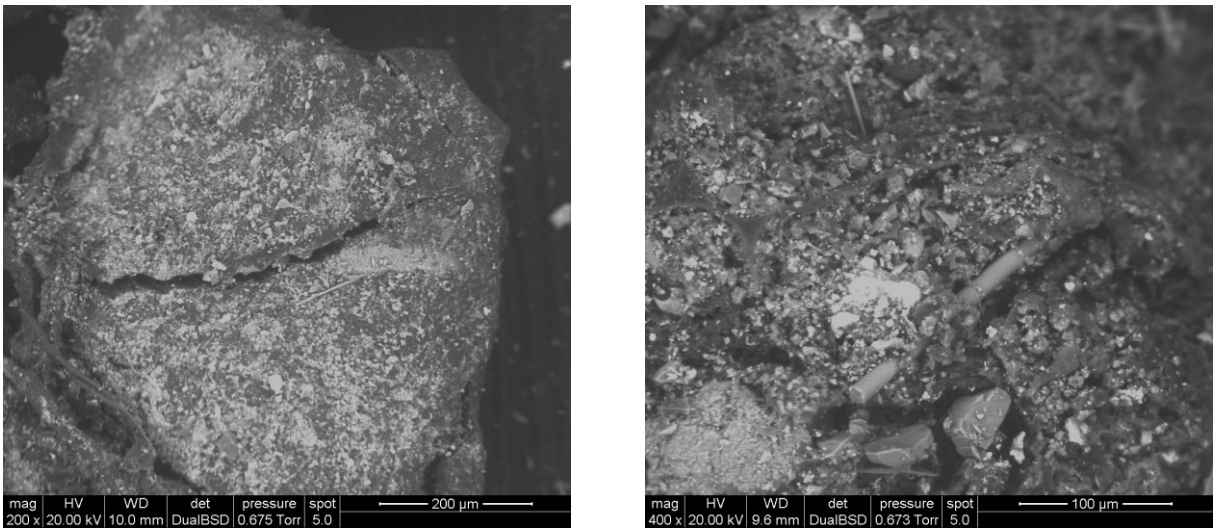

Figure 119: Two ESEM of the sample after experiment 8.7 at 200x and 400x

The ESEM photos taken on the sample after treatment do not show evident difference compared to the untreated sample analyzed in the previous chapter. No evident sign of reaction occurring is found. Since particle in this sample are already of small size, the physical effect of pressure does not modify the shape of particles.

8.8 PU from CF3 using Ethos microwave reactor and H2O2-water in ratio 1:9 with more time

This experiment is similar to experiment 4.3 and 4.5.

A sample of polyurethane (CF3) of 0.50g was added to 9 mL of water and 1 mL of H_2O_2 30%. The mixture was in a microwave reactor with power control. No pressure/temperature information are present. The following program was performed:

Time [min]	1	1	5	5	10	5
Power [W]	250	0	250	400	650	Vent

The pH of the solution at the end of the program was equal to 7.

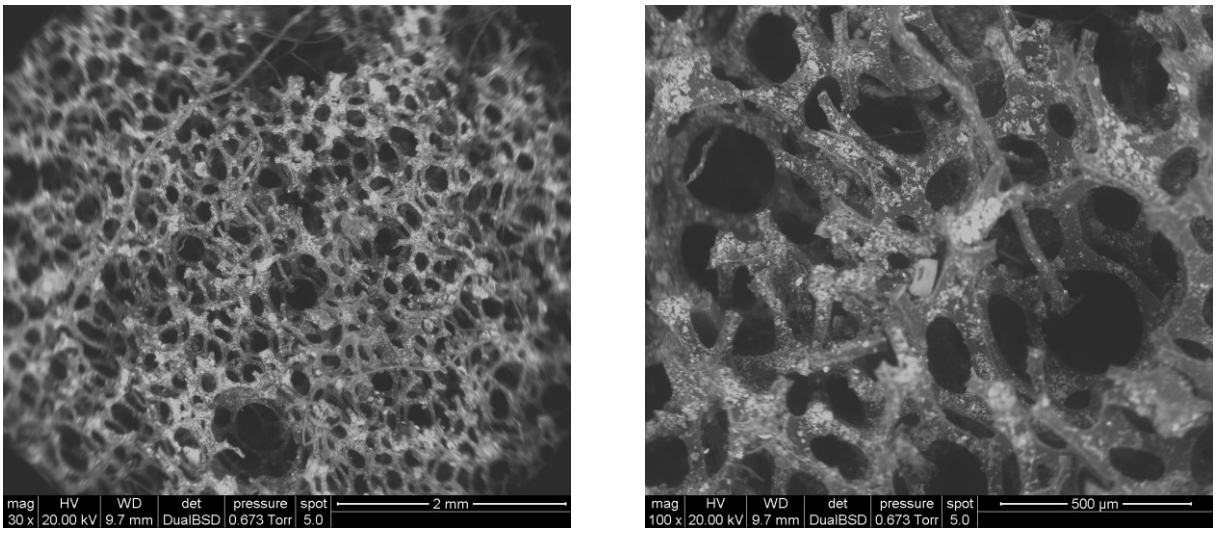

Figure 120: Two ESEM of the sample after experiment 8.8 at 30x and 100x

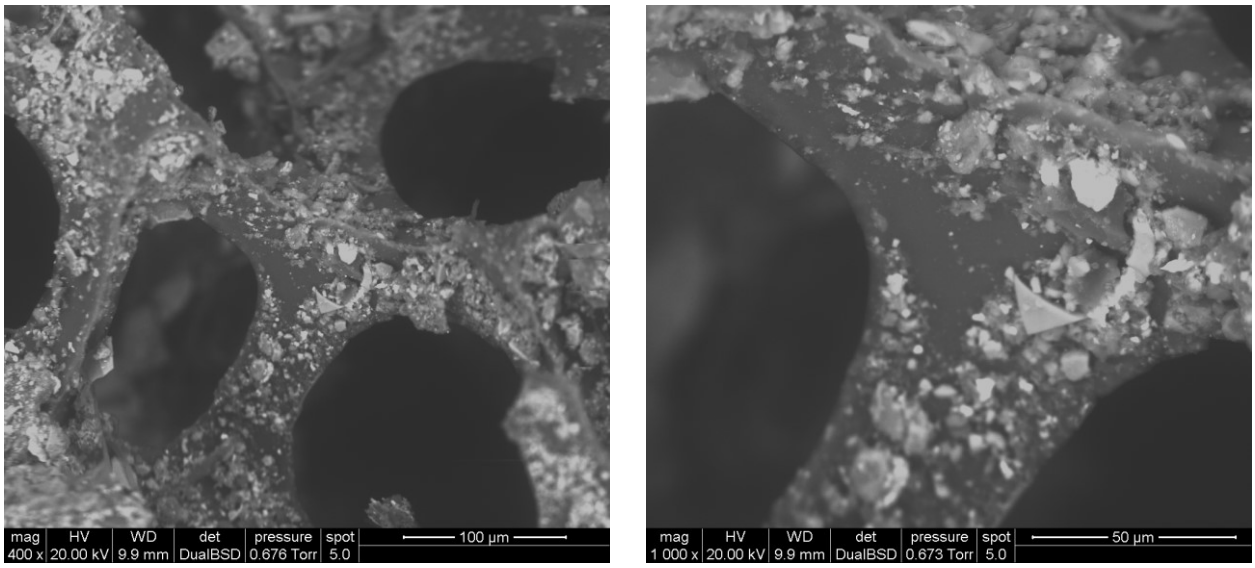

Figure 121: Two ESEM of the sample after experiment 8.8 at 400x and 1000x

Compared to experiment 4.5, the polyurethane structure appears to be slightly more stretched according to the physical effect of pressure previously described. No other evident difference can be noticed. The edges of the polymer are well defined and not show the presence of any reaction occurring. Based on that, we could exclude the hypothesis of any chemical reaction occurring also on this polyurethane sample.

8.9 PU from "CF3 TQ1" at 180°C for 15 min using microwave reactor and H_2O_2-water in ratio 1:9

0.31 g of polyurethane (CF3) is added to 9 g of H_2O and 1 mL of H_2O_2 30%. The sample was put in a 30 mL vial and treated using Anton Paar microwave reactor. The program followed was: ramp to 180°C in 5 min, hold at 180°C for 15 min, cold down. The pressure registered from the instrument was of 15 bar.

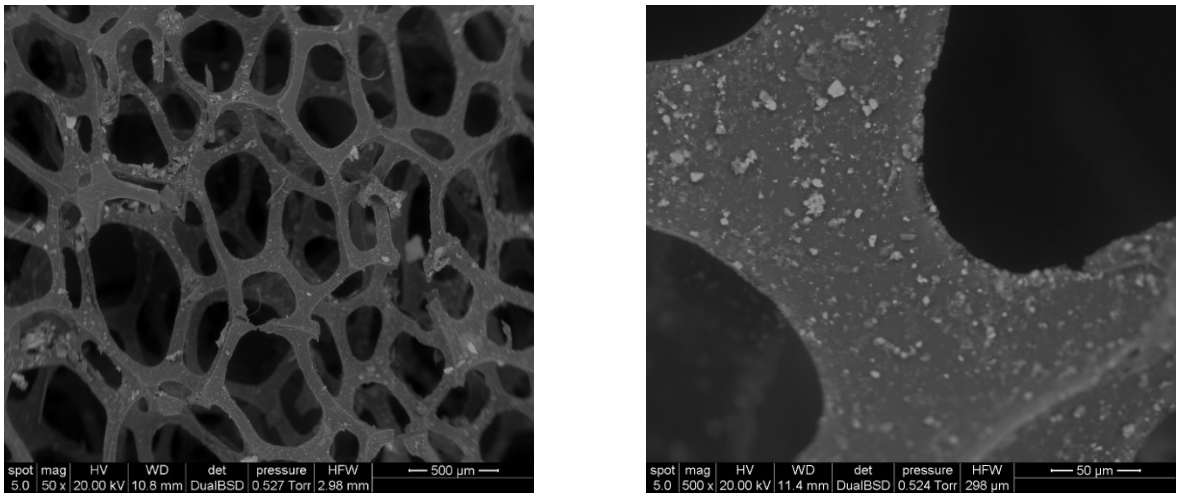

Figure 122: Two ESEM of the sample after experiment 8.9 at 50x and 500x

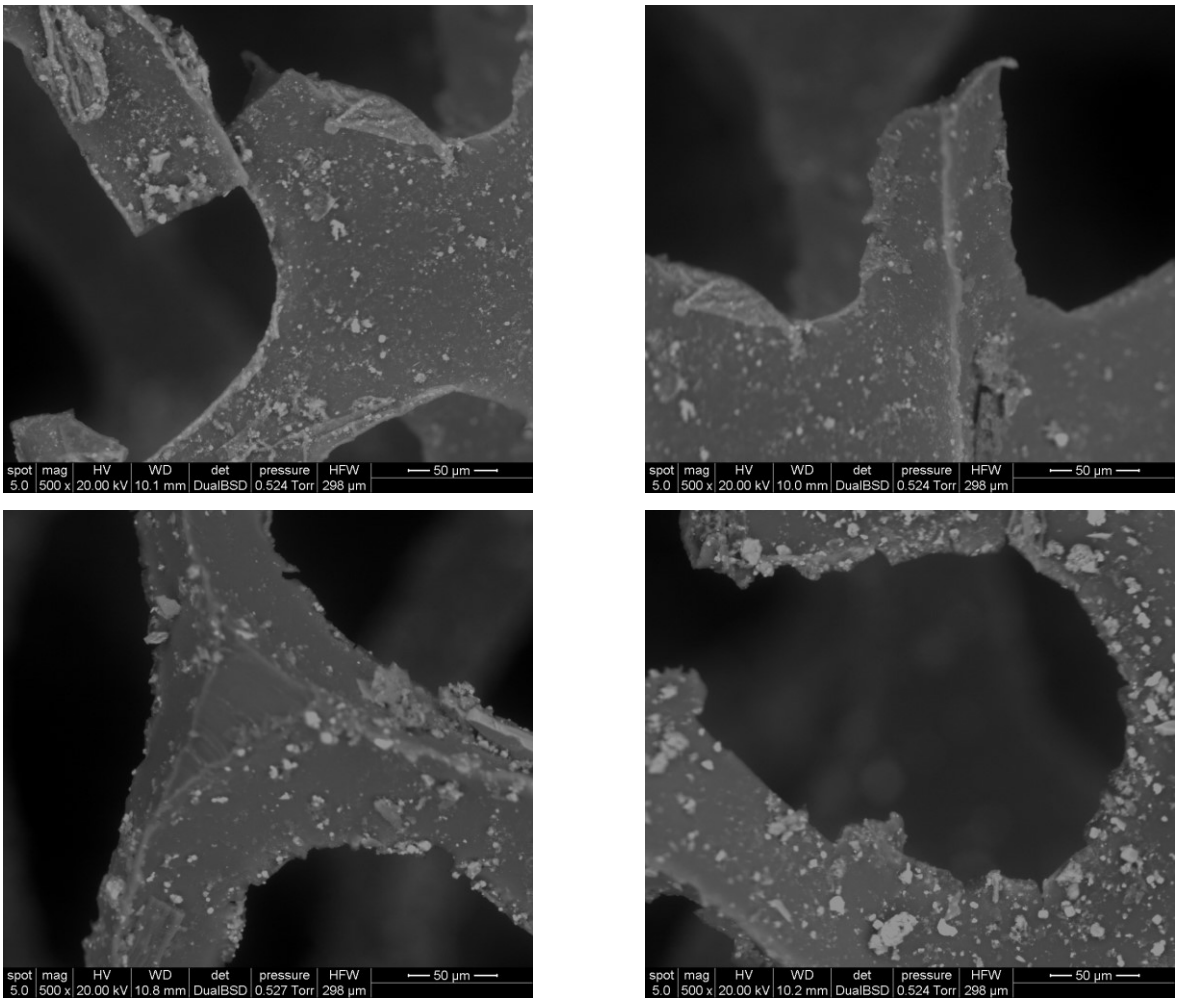

Figure 123: Four ESEM of the sample after experiment 8.9 at 500x

The lattice presents no new breakages but, as reported before, the effect of hydrogen peroxide in this condition lead to an enlargement of the structure. Since the edges present a shape comparable to the untreated polymer the enlargement of the structure could be explained as a physical effect of H_2O_2 decomposition leading to local overpressures.

8.10 PU from CF3 using Ethos microwave reactor and Fe^{2+} Fenton

In this experiment polyurethane (CF3) is treated using Fenton and microwave reactor.

A sample of polyurethane (CF3) of 0.52 g is taken and 0.2790 g of $FeSO_4*7H_2O$ (1.00 mmol) is added. 9 mL of water and 1 mL of H_2O_2 30% (9.7 mmol) are added. Finally, in order to achieve an acid pH, 3 drops of HCl 1M are added. The mixture was the put in a microwave reactor with power control. No pressure/temperature information are present. The following program, chosen from one of the preset, was performed:

The following program was performed:

Time [min]	1	1	5	5	5	5
Power [W]	250	0	250	400	650	Vent

The pH of the solution at the end of the program was equal to 3.

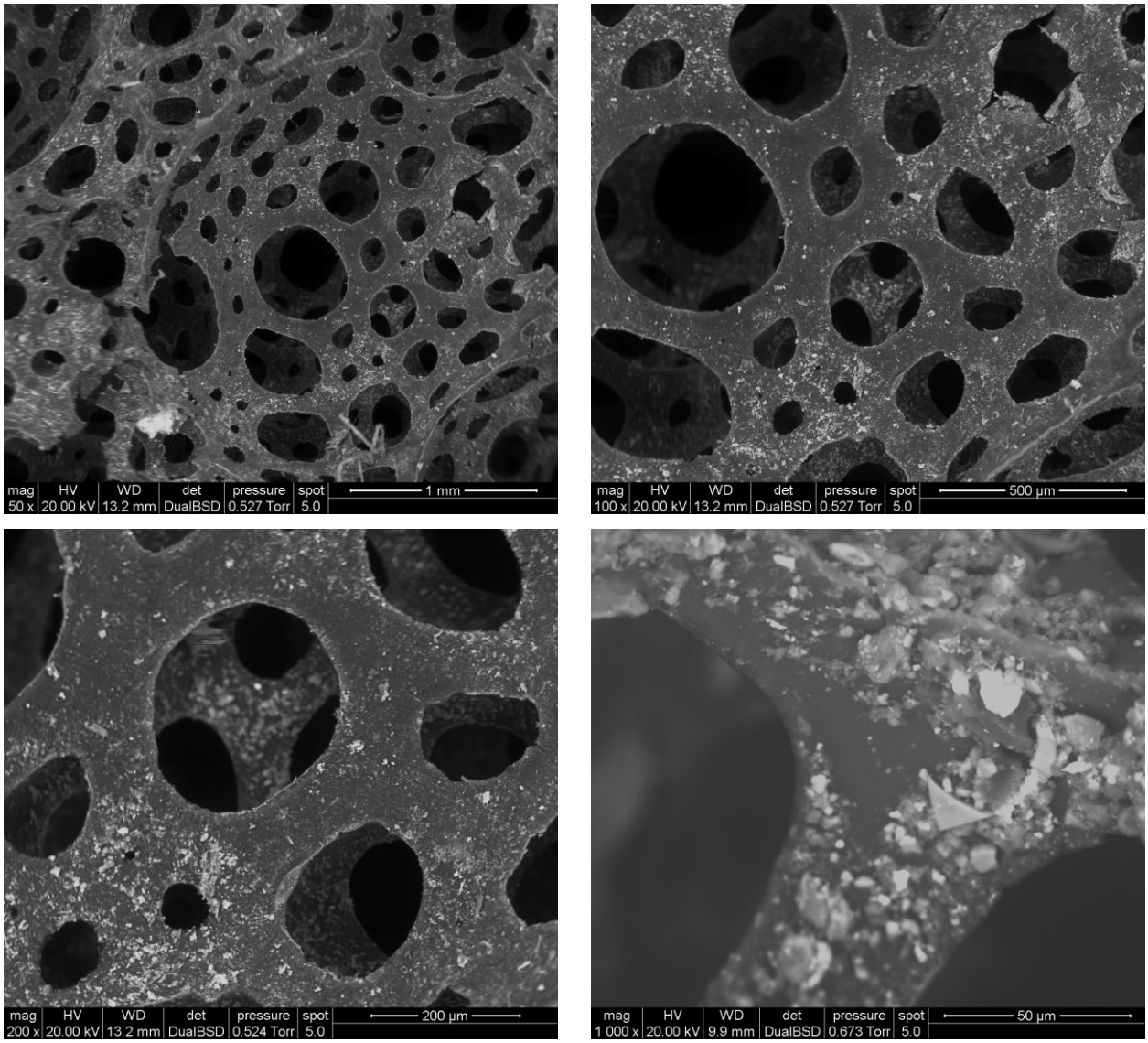

Figure 124: Four ESEM of the sample after experiment 8.10

The polymer structure and surface does not show any evident difference respect to other polyurethane sample seen previously. Although the surface is clean, the Fenton reagent (which produces hydroxyl radicals) does not attack the polyurethane bonds.

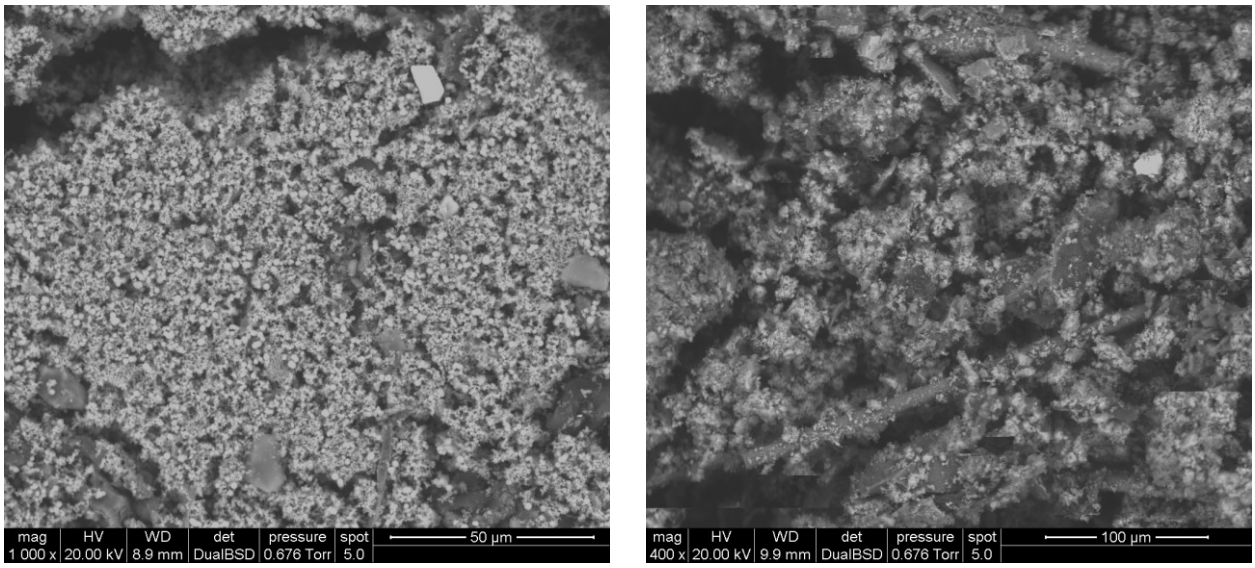

Figure 125: Two ESEM of the crystals and small particles after experiment 8.10

The liquid phase containing small floating particle is centrifugated and the sediment is dried out in fume hood. The resulting solid phase is made of iron oxide, iron sulfate, some small plastic particle that was entrained in the foam and other molecules base principally on Si, Al, Zn and Ca, as confirmed by the following EDX analysis:

Spectrum	% O	% Fe	% C	% S	% Si	% Al	% Ca	% Zn
Area 1	41.3	41.0	9.5	5.3	1.5	0.6	0.4	-
Area 2	35.4	35.3	19.9	1.1	3.2	2.1	1.3	0.9

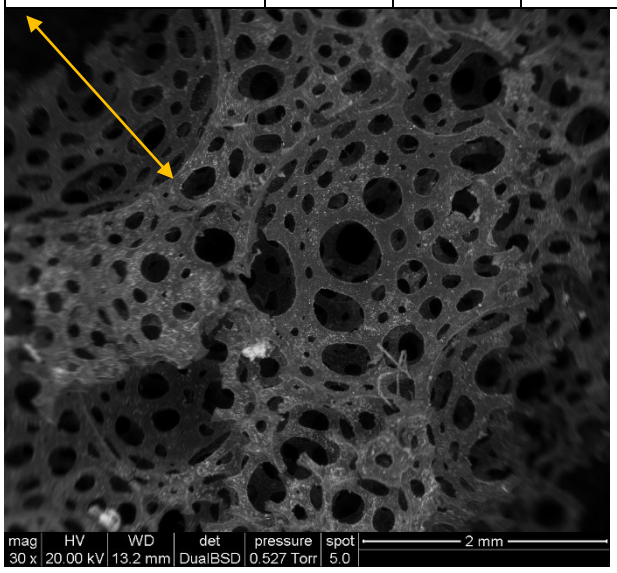

At a first visual analysis, high size holes (yellow arrow) in the structure were identified, suggesting that some chemical reaction was occurring but, looking at the structure in proximity of this holes, it appears to be well arranged. This suggest that these holes were probably present at the beginning, produced by the manufacture in the foam molding, but their presence was not seen initially because the sample, as a waste, was tangled up on itself.

Figure 126: ESEM after experiment 8.10

8.11 PU from CF3 using Ethos microwave reactor and Cu^+ Fenton

A sample of polyurethane (CF3) of 0.48 g is taken and 0.1484 g of CuBr (1.04 mmol) is added. 9 mL of water and 1 mL of H_2O_2 30% (9.7 mmol) are added. Finally, in order to achieve an acid pH, 3 drops of HCl 1M are added. The mixture was put in a microwave reactor with power control. No pressure/temperature information are present. The following program, chosen from one of the preset, was performed:

The following program was performed:

Time [min]	Power [W]
1	250
1	0
5	250
5	400
5	650
5	Vent

The pH of the solution at the end of the program was equal to 4.

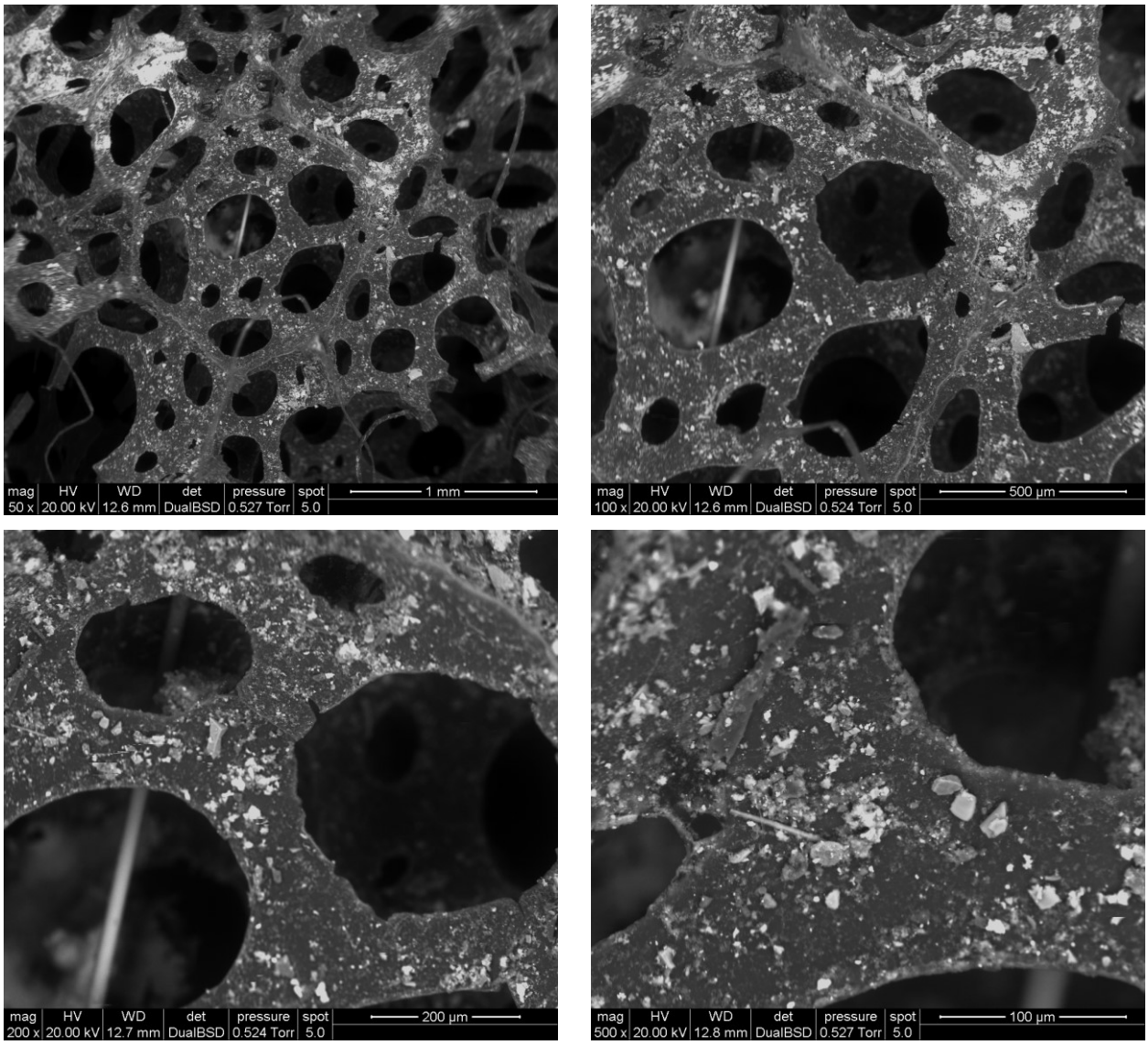

Figure 127: Four ESEM of the sample after experiment 8.11

Compared to experiment 4.10 (where Fe^{2+} Fenton reagent was used), only minor differences are present. The polymer surface is slightly dirtier, but the reason is that it was probably dirtier at the beginning. The polymer edges are once again well-defined and don't present evident sign of chemical reaction occurring.

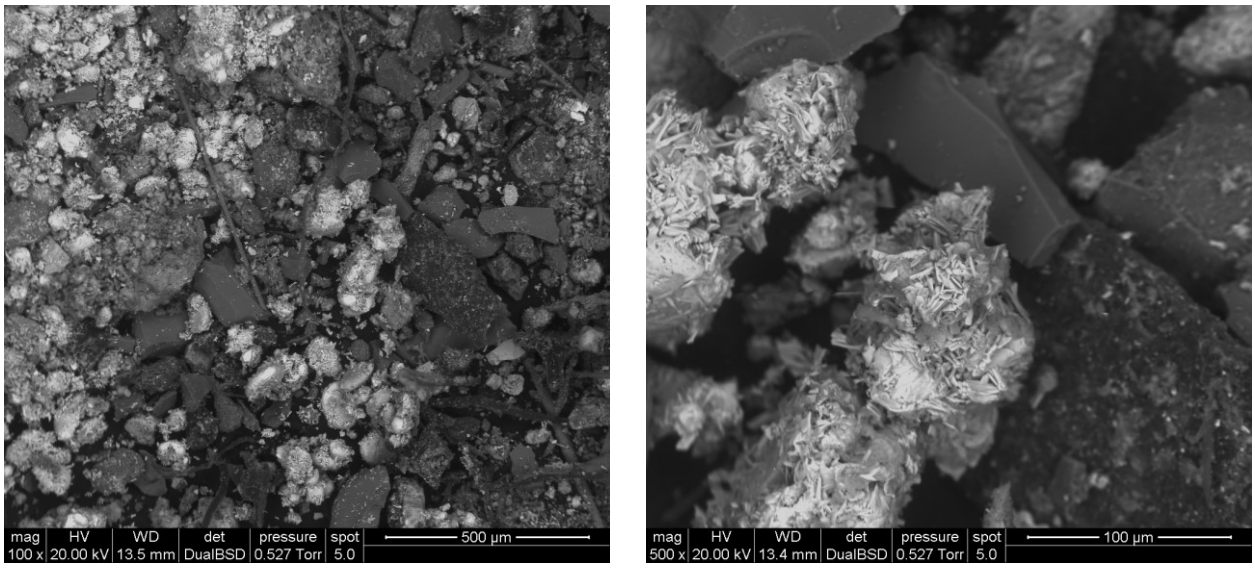

Figure 128: Two ESEM of the crystals and small particles after experiment 8.11

The liquid phase containing small floating particle was centrifugated and the sediment was dried out in fume hood. The resulting solid phase contains small particles entrained in the foam and copper crystal (either CuO_2 or CuBr).

Spectrum	% C	% O	% Cu	% Br	% Si	% Fe	% Ca	% Zn
Area	30.2	26.8	23.2	6.9	5.0	3.9	1.3	1.0

8.12 Hydrothermal treatment conclusions

Most important results from experiments concerning polyurethane are summarized in table:

Experiment	Result
Liquid water at 180°C or below (8.1, 8.2, 8.3)	Pores enlargement, stretching of the PU structure
Liquid water at 200°C (8.4)	Breaks in the PU structure, sign of degradation in the surface of the PU
Liquid water at 180°C or below with H_2O_2 (8.5, 8.6, 8.8, 8.9)	Pores enlargement, high stretching of the PU structure, minor signs of degradation of PU surface
Fenton conditions at 180°C or below	Pores enlargement, stretching of the PU structure

From these experiments we can state that HTC reactions for PU needs higher temperature than the ones we were able to achieve using the two microwave reactors available for us. Ethos 1600 reactor is claimed to be able to reach 300°C and 100 bar, since the effect on PU was equal or lower than the effect reached using Anton Paar Monowave 400 at 180°C, we can affirm that the actual temperature reached is lower than 180°C.

Anyway, the result obtained at 200°C suggest that it may be possible to obtain degradation reactions in subcritical/supercritical water increasing temperature in pressure: we than suggest to try those conditions but with suitable equipments.

9. CONCLUSIONS

The activity carried out in this thesis can be summarized as follows:

a) Characterization of a real sample of car fluff from a scrapyard in Bologna:

A detailed analysis has been carried out by FTIR and ESEM. Determinations gave out the following result:

Component	Amount w/w
Polymeric filaments	12.0%
Rigid polymers	25.9%
Polyurethane foam	18.4%
Wood	0.2%
Glass	0.1%
Rigid PU foam	0.2%
Other polymers	11.4%
Electric wire	2.7%
Textile material	10.1%
Electronic material	0.2%
Fragments diameter > 2 mm	5.8%
Fragments diameter < 2 mm	13.1%

As it can be observed, the previous processes of separation of glass, metals, oil and fuel are efficient, thus the most abundant components are polymers, and from a volumetric point of view the most relevant problem is represented by polyurethane of different morphologies. For this reason our attention has been devoted for the subsequent processes suitable for PU.

b) Energy recovery: one of the possible approaches to face the problem of a large amount of plastic residues is combustion for energy recovery. The gross calorific value of our sample, which has been grinded in order to have a suitable sample for the determinations according to ISO 1928:2020, resulted to be 18'000 kJ/kg. The value is in agreement with the value reported in the literature where a value of 14'000 kJ/kg was indicated by Mancini et al. [19]. A relevant aspect is represented by the nature of the final residue: the ESEM analysis showed that only inorganic products are present with no environmental hazardous. Exhaust gases produced by combustion have not been analyzed.

c) Pyrolytic processes: pyrolysis is actually extensively investigated aiming to the possibly to modulate the nature of the products depending on reaction conditions. We performed the pyrolytic process under two conditions: with a home-made pyrolizer and in a N_2-oven. Our interest was in particular devoted to the formation of N-doped activated carbon which can have interesting industrial applications as catalyst or as material for supercapacitors. In the activated carbon achieved from our processes at least 6-7 $\%^{w}/_{w}$ of nitrogen is still present. The characterization of the materials obtained at 600°C has been carried out using FTIR, Raman, NMR, HPLC and MS. Further characterization (by BET, XRD and XPS) is undergoing.

It was observed that performing the pyrolysis at 400°C some spherical particles of diameter 5 μm are formed, containing a high level of nitrogen, representing reasonably an intermediate situation during

thermal decomposition of PU. Spherical particles have been observed also performing pyrolysis at 600°C with a lower diameter of 0.5 μm. This aspect will be further investigated.

d) Chemical recycling: we carried out the glycolysis process on a PU sample from car fluff under microwave activation using EtOH, glycerol and DEG with NaOH as catalyst. It is observed that the starting material is completely destroyed using a viscous liquid mixture in the case of EtOH and DEG while for the reaction carried out in glycerol part of the starting PU was present at the end of the experiment.

   The reaction mixtures have been analyzed using FTIR, NMR and liquid MS. The MS spectra of the methanol solutions of the samples are quite similar each other. In particular the sample obtained by reaction with glycerol has been purified by extraction with CH_2Cl_2 and the MS spectra show the presence of fragments based on the methyl diphenyl group bonded to different carbamate moieties, in agreement with literature.

e) The hydrothermal process: with the objective to carry on oxidation reactions in supercritical water on PU, we studied the effect of high temperature/high pressure on PU under microwave activation. It was observed that hot water (200°C) under pressure (15 atm) induced an increase in the hole dimensions of PU, and when also H_2O_2 is present an initial degradation of the structure can be observed, even if it results to be more stable than other polymeric materials such as PC, ABS, PP and PA6. The experiments carried out under Fenton conditions (Fe and Cu catalyzed) do not show further level of degradation.

   Anyway, the partial deformation and the initial degradation observed in water and water/H_2O_2 can represent an intriguing result suggesting that the advanced and peculiar oxidation conditions represented by SCW (with O_2) can be effective in PU degradation which on the basis of preliminary calculations resulted to be self-sustainable.

Bibliography

[1] https://ec.europa.eu/commission/presscorner/detail/en/ip_19_6691

[2] https://environment.ec.europa.eu/strategy/circular-economy-action-plan_en

[3]https://app.dimensions.ai/discover/publication?search_mode=content&search_text=circular+economy&search_type=kws&search_field=text_search

[4] Lazarevic, D., & Valve, H. (2017). Narrating expectations for the circular economy: Towards a common and contested European transition. Energy Research & Social Science, 31, 60–69. https://doi.org/10.1016/j.erss.2017.05.006

[5] Corvellec, H., Stowell, A. F., & Johansson, N. (2022). Critiques of the circular economy. Journal of Industrial Ecology, 26(2), 421–432. https://doi.org/10.1111/jiec.13187

[6] Cullen, J. M. (2017). Circular economy: Theoretical benchmark or perpetual motion machine?: CE: Theoretical benchmark or perpetual motion machine? Journal of Industrial Ecology, 21(3), 483–486. https://doi.org/10.1111/jiec.12599

[7] Velis, C. A., & Vrancken, K. C. (2015). Which material ownership and responsibility in a circular economy? Waste Management & Research: The Journal of the International Solid Wastes and Public Cleansing Association, ISWA, 33(9), 773–774. https://doi.org/10.1177/0734242X15599305

[8] Bali Swain, R., & Sweet, S. (Eds.). (2021). Sustainable consumption and production, volume II: Circular economy and beyond. Springer International Publishing.

[9] Johansson, N., & Krook, J. (2021). How to handle the policy conflict between resource circulation and hazardous substances in the use of waste? Journal of Industrial Ecology, 25(4), 994–1008. https://doi.org/10.1111/jiec.13103

[10] Völker, T., Kovacic, Z., & Strand, R. (2020). Indicator development as a site of collective imagination? The case of European Commission policies on the circular economy. Culture and Organization, 26(2), 103–120. https://doi.org/10.1080/14759551.2019.1699092

[11] https://ec.europa.eu/eurostat/statistics-explained/index.php?title=End-of-life_vehicle_statistics#Number_of_end-of-life_vehicles

[12] Directive 2000/53/EC of the European Parliament and of the Council

[13] https://aic.camera.it/aic/scheda.html?core=aic&numero=5/05991&ramo=C&leg=18

[14] https://www.isprambiente.gov.it/files/pubblicazioni/manuali-lineeguida/Linee_guida_Veicoli_fuori_Uso_Fonte_APAT_20051.pdf

[15] Colangelo, F., Messina, F., Di Palma, L., & Cioffi, R. (2017). Recycling of non-metallic automotive shredder residues and coal fly-ash in cold-bonded aggregates for sustainable concrete. Composites. Part B, Engineering, 116, 46–52. https://doi.org/10.1016/j.compositesb.2017.02.004

[16] https://www.borsarifiuti.com/documenti/carfluff/ebara_IARC03_TwinRec_manuscript.pdf

[17] https://ec.europa.eu/environment/green-growth/waste-prevention-and-management/index_en.htm

[18] https://docs.european-bioplastics.org/publications/bp/EUBP_BP_Energy_recovery.pdf

[19] Mancini, G., Tamma, R., & Viotti, P. (2010). Thermal process of fluff: preliminary tests on a full-scale treatment plant. Waste Management (New York, N.Y.), 30(8–9), 1670–1682. https://doi.org/10.1016/j.wasman.2010.01.037

[20] Brereton, G., Emanuel, R. M., Jr, Lomax, R., Pennington, K., Ryan, T., Tebbe, H., Timm, M., Ware, P., Winkler, K., Yuan, T., Zhu, Z., Adam, N., Avar, G., Blankenheim, H., Friederichs, W., Giersig, M., Weigand,

E., Halfmann, M., Wittbecker, F.-W., … Wussow, H.-G. (2019). Polyurethanes. In Ullmann's Encyclopedia of Industrial Chemistry (pp. 1–76). Wiley-VCH Verlag GmbH & Co. KGaA.

[21] Kruse, A., & Dahmen, N. (2018). Hydrothermal biomass conversion: Quo vadis? The Journal of Supercritical Fluids, 134, 114–123. https://doi.org/10.1016/j.supflu.2017.12.035

[22] Poerschmann, J., Weiner, B., Woszidlo, S., Koehler, R., & Kopinke, F.-D. (2015). Hydrothermal carbonization of poly(vinyl chloride). Chemosphere, 119, 682–689. https://doi.org/10.1016/j.chemosphere.2014.07.058

[23] Brebu, M., Bhaskar, T., Muto, A., & Sakata, Y. (2006). Alkaline hydrothermal treatment of brominated high impact polystyrene (HIPS-Br) for bromine and bromine-free plastic recovery. Chemosphere, 64(6), 1021–1025. https://doi.org/10.1016/j.chemosphere.2006.02.036

[24] Zhao, X., Zhan, L., Xie, B., & Gao, B. (2018). Products derived from waste plastics (PC, HIPS, ABS, PP and PA6) via hydrothermal treatment: Characterization and potential applications. Chemosphere, 207, 742–752. https://doi.org/10.1016/j.chemosphere.2018.05.156

[25] Zhao, X., Xia, Y., Zhan, L., Xie, B., Gao, B., & Wang, J. (2019). Hydrothermal treatment of E-waste plastics for tertiary recycling: Product slate and decomposition mechanisms. ACS Sustainable Chemistry & Engineering, 7(1), 1464–1473. https://doi.org/10.1021/acssuschemeng.8b05147

[26] Uddin, M. A., Bhaskar, T., Kusaba, T., Hamano, K., Muto, A., & Sakata, Y. (2003). Debromination of flame retardant high impact polystyrene (HIPS-Br) by hydrothermal treatment and recovery of bromine free plastics. Green Chemistry: An International Journal and Green Chemistry Resource: GC, 5(2), 260–263. https://doi.org/10.1039/b206704h

[27] Mishra, S., Zope, V. S., & Kulkarni, R. D. (2004). Kinetics and thermodynamics of hydrolytic depolymerization of polyurethane foam at higher temperature and pressure. Polymer-Plastics Technology and Engineering, 43(4), 1001–1011. https://doi.org/10.1081/ppt-200030008

[28] Dai, Z., Hatano, B., Kadokawa, J.-I., & Tagaya, H. (2002). Effect of diaminotoluene on the decomposition of polyurethane foam waste in superheated water. Polymer Degradation and Stability, 76(2), 179–184. https://doi.org/10.1016/s0141-3910(02)00010-1

[29] Asahi, N., Sakai, K., Kumagai, N., Nakanishi, T., Hata, K., Katoh, S., & Moriyoshi, T. (2004). Methanolysis investigation of commercially available polyurethane foam. Polymer Degradation and Stability, 86(1), 147–151. https://doi.org/10.1016/j.polymdegradstab.2004.04.002

[30] Heiran, R., Ghaderian, A., Reghunadhan, A., Sedaghati, F., Thomas, S., & Haghighi, A. H. (2021). Glycolysis: an efficient route for recycling of end of life polyurethane foams. Journal of Polymer Research, 28(1). https://doi.org/10.1007/s10965-020-02383-z

[31] Costantini, F., (2017). Riciclo chimico via glicolisi di espansi rigidi poliuretanici e poliisocianurici. Tesi, Università degli studi di Padova

[32] Yin, F., Lu, K.-L., Wei, X.-Y., Fan, Z.-C., Li, J.-H., Kong, Q.-Q., Zong, Z.-M., & Bai, H.-C. (2022). Fabrication of N/O self-doped hierarchical porous carbons derived from modified coal tar pitch for high-performance supercapacitors. Fuel (London, England), 310(122418), 122418. https://doi.org/10.1016/j.fuel.2021.122418

[33] Wang, C., Kang, J., Sun, H., Ang, H. M., Tadé, M. O., & Wang, S. (2016). One-pot synthesis of N-doped graphene for metal-free advanced oxidation processes. Carbon, 102, 279–287. https://doi.org/10.1016/j.carbon.2016.02.048

[34] Venderbosch, R. H., & Prins, W. (2010). Fast pyrolysis technology development. Biofuels, Bioproducts & Biorefining : Biofpr, 4(2), 178–208. https://doi.org/10.1002/bbb.205

[35] https://advanced-microscopy.utah.edu/education/electron-micro/#:~:text=Thus%20the%20resolution%20of%20an,lens%20system%20in%20electron%20microscopes

[36] https://www.researchgate.net/figure/Schematic-drawing-of-a-the-typical-Scanning-Electron-Microscope-SEM-column-170_fig5_281184428

[37]: Krammer, P., Mittelstädt, S., Vogel, H., (1999). Investigating the Synthesis Potential in Supercritical Water. *Chemical Engineering & Technology*, 22(2), 126-130. https://doi.org/10.1002/(SICI)1521-4125(199902)22:2%3C126::AID-CEAT126%3E3.0.CO;2-4

[38]: Jiang, Z., Li, Y., Wang, S., Cui, C., Yang, C., & Li, J. (2020). Review on mechanisms and kinetics for supercritical water oxidation processes. Applied Sciences (Basel, Switzerland), 10(14), 4937. https://doi.org/10.3390/app10144937

[39]: Directive 2000/76/EC of the European Parliament and of the Council of 4 December 2000 on the incineration of waste

[40]: Zhang, F., Chen, J., Su, C., & Ma, C. (2018). Energy consumption and economic analyses of a supercritical water oxidation system with oxygen recovery. Processes (Basel, Switzerland), 6(11), 224. https://doi.org/10.3390/pr6110224

[41]: Chen, Z., Zhang, X., Han, W., Gao, L., & Li, S. (2018). A power generation system with integrated supercritical water gasification of coal and CO2 capture. Energy (Oxford, England), 142, 723–730. https://doi.org/10.1016/j.energy.2017.10.077

[42]: Ketata, N., Sanglar, C., Waton, H., Alamercery, S., Delolme, F., Raffin, G., & Grenier-Loustalot, M. F. (2005). Thermal degradation of polyurethane bicomponent systems in controlled atmospheres. Polymers and Polymer Composites, 13(1), 1–26. https://doi.org/10.1177/096739110501300101

[43]: Allan, D., Daly, J., & Liggat, J. J. (2013). Thermal volatilisation analysis of TDI-based flexible polyurethane foam. Polymer Degradation and Stability, 98(2), 535–541. https://doi.org/10.1016/j.polymdegradstab.2012.12.002

[44]: Donadini, R., Boaretti, C., Lorenzetti, A., Roso, M., Penzo, D., Dal Lago, E., & Modesti, M. (2023). Chemical recycling of polyurethane waste via a microwave-assisted glycolysis process. ACS Omega, 8(5), 4655–4666. https://doi.org/10.1021/acsomega.2c06297

[45] Molero, C., de Lucas, A., & Rodríguez, J. F. (2006). Recovery of polyols from flexible polyurethane foam by "split-phase" glycolysis with new catalysts. Polymer Degradation and Stability, 91(4), 894–901. https://doi.org/10.1016/j.polymdegradstab.2005.06.023

Ringraziamenti

Desidero ricordare tutti coloro che mi hanno assistito ed aiutato nello svolgimento della tesi.

Ringrazio il professor Renato Bonora per essere stato il mio relatore e per i preziosi consigli.

Ringrazio la professoressa Roberta Bertani per avermi accolto nel suo laboratorio, per il fondamentale sostegno datomi nell'arco di questi mesi e per tutti gli insegnamenti trasmessi.

Ringrazio la dottoressa Anna Scettri per l'assistenza ed i momenti di leggerezza.

Ringrazio i colleghi ed amici di corso, che mi hanno aiutato nei momenti di difficoltà e che hanno saputo arricchire la mia esperienza universitaria.

Non per ultimi, ringrazio specialmente la mia famiglia.

Ringrazio i miei genitori che mi hanno permesso di studiare e che mi hanno supportato nel mio percorso.

Ringrazio mia sorella Giada per l'aiuto in questi anni.